The energy levels of muonic atoms

E. Borie

*Kernforschungszentrum Karlsruhe GmbH, Institut für Kernphysik and Institut für Experimentelle Kernphysik der Universität Karlsruhe, 7500 Karlsruhe 1, Federal Republic of Germany**

G. A. Rinker

Theoretical Division, Los Alamos National Laboratory, Los Alamos, New Mexico 87545

The theory of muonic atoms is a complex and highly developed combination of nuclear physics, atomic physics, and quantum electrodynamics. Perhaps nowhere else in microscopic physics are such diverse branches so intimately intertwined and yet readily available for precise experimental verification or rejection. In the present review we summarize and discuss all of the most important components of muonic atom theory, and show in selected cases how this theory meets experimental measurements.

CONTENTS

I. Introduction 67
A. General description of a muonic atom 68
B. Principal kinematics and interactions 69
C. Notation and numerical values 69
II. Classical Interactions and Kinematics 69
A. Dirac equation 69
B. Zero-order approximations 70
C. Decomposition in spherical coordinates 70
D. Numerical methods 71
1. Eigenvalues 71
2. Solution of the radial Dirac equations 72
E. "Model-independent" interpretation 72
F. Corrections for static nuclear moments 73
1. Electric multipole interactions 74
2. Magnetic dipole interactions 74
G. Intrinsic nuclear dynamics 75
1. Formal description 75
2. Explicit formulas 77
3. Radiative transition rates 78
4. Examples 78
a. General case of nuclear polarization 78
b. Helium 80
c. Lead 81
d. Deformed nuclei 82
e. Transitional nuclei 82
H. Translational nuclear motion 83
1. Nonrelativistic corrections 83
2. Relativistic corrections 83
I. Electron screening 86
III. Quantum Electrodynamic (QED) Corrections 87
A. Vacuum polarization 87
1. Order $\alpha Z\alpha$ 87
a. e^+e^- pairs 87
b. $\mu^+\mu^-$ pairs 89
c. Effect on higher nuclear multipoles 89
d. Effect on the recoil correction 89
e. Hadronic vacuum polarization 89
2. Order $\alpha^2 Z\alpha$ 90
a. e^+e^- pairs 90
b. Mixed $\mu - e$ vacuum polarization 90
3. Orders $\alpha(Z\alpha)^n$, $n = 3,5,7\ldots$ 91
4. Order $\alpha^2 (Z\alpha)^2$ 94
B. Self-energy 99
1. Orders $\alpha(Z\alpha)^n$, $n \geqslant 1$ 99
2. Orders $\alpha^2 (Z\alpha)^n$, $n \geqslant 1$ 101
C. Anomalous interactions 101
D. Experimental tests of QED with muonic atoms 102
1. Heavy elements 103
2. Experiments using crystal spectrometers 109
3. Very light elements ($Z = 1,2$) 110
IV. Acknowledgments 113
Appendix 113
References 114

I. INTRODUCTION

Perhaps the most interesting theoretical aspect of muonic atoms is that their study provides one of the most highly developed and complete theories of a complex physical system which is amenable to both accurate calculation and accurate experimental verification. There are few serious outstanding difficulties in our present understanding. This has not always been so. Each advance in experimental technique has opened new questions which were met with increasingly refined and complicated theoretical calculations. Old effects have had to be recalculated repeatedly to higher precision, and new effects have been added periodically to the list of known contributions. Meaningful calculations require that some of these effects be recalculated every time comparison is made with experiment. For other effects, such recalculation is impractical, owing to the complexity of the calculations, and in experimental comparisons one resorts either to published numbers or to semiempirical approximations to the more laboriously calculated values.

The main intent of the present review is to collect in one place in logical order all currently available methods, formulas, and results which are necessary for the accurate calculation of muonic atom energy levels throughout the periodic table. Where possible, we either derive or motivate the relevant expressions. Naturally, some omissions must be made. We hope and believe that these omissions will be unimportant for most cases of interest. In selected cases we present experimental results which bear directly upon the validity of the calculations, but we do not attempt an exhaustive review of the present experimental situation. For this the reader is referred to the review by Engfer *et al.* (1974).

A number of excellent books and review articles have appeared on this subject in the last 15 years (Devons and Duerdoth, 1968; Wu and Wilets, 1969; Kim, 1971; Barrett, 1974; Hüfner *et al.*, 1977; Scheck, 1977; Hughes and Wu, 1975), in which a wealth of information is contained. An additional source of information, insight, and inspiration is the classic paper of Wheeler (1949), which marked the beginning of the theory of muonic atoms and

set forth numerous physical ideas which are still important today. The reader is urged to consult these references for alternate discussions from different points of view, as well as for further historical details.

A. General description of a muonic atom

When a negative muon is stopped in matter, it passes through a variety of environments before finally ending its life in the vicinity of an atomic nucleus. In the early stages it scatters from atom to atom as does a free electron, but gradually it loses energy until it is captured into a high atomic orbit of a particular atom. The probability for capture into various orbits is known to depend upon the chemical composition and crystalline structure of the material (Fermi and Teller, 1947; Ponomarev, 1973; Leon and Seki, 1977; Kunselman *et al.*, 1976; Gershtein and Ponomarev, 1975; Daniel *et al.*, 1977, 1978, 1979; Schneuwly, *et al.*, 1978; Leon, 1978; Bergmann, *et al.*, 1979; Schneuwly, 1977; Daniel, 1979; Dubler *et al.*, 1979; Leisi, 1980). Information about the initial distribution of orbits persists as the muon cascades through the electron cloud, ejecting Auger electrons and emitting electromagnetic radiation, until it arrives in a region inside the innermost electron orbit. Then it traverses a zone of relative quiet, being perturbed from its stationary states only by its interaction with the photon field, which permits it to make transitions of energy determined by essentially static interactions with the atomic electrons and the nucleus, and by a variety of quantum electrodynamical (QED) effects (see Fig. 1). The measured energies of these transitions provide stringent tests of our understanding of QED. As the muon moves into lower orbits, it is affected more strongly by the size and shape of the nucleus and its possibility for excitation. For all but the lightest nuclei, muon orbits can be comparable to the nuclear size, and muon transition energies comparable to nuclear excitation energies (see Fig. 2). The capture and cascade processes take place in a time of the order $10^{-12}-10^{-9}$ sec, so by the time the muon reaches the 1*s* state, it has barely begun its life. There it sits for another $10^{-7}-2\times10^{-6}$ sec, waiting for the weak interaction to destroy it. For light nuclei this happens most of the time via decay into an electron and two neutrinos. In heavy nuclei the muon is usually captured by the nucleus via the elementary reaction $\mu^- + p \rightarrow n + \nu_\mu$. Its mass appears as nuclear excitation energy or as neutrino kinetic energy.

Because of the variety of physical effects which occur between the formation and the destruction of a muonic atom, its study involves a number of distinct physical theories and types of measurement. Those effects concerned with the capture and cascade through the electron cloud are called chemical effects. Theories of these are relatively primitive at present, owing to the complexity of the physical situation; we shall not discuss them here except as they relate to other topics. Measurements in the "quiet" zone, however, have stimulated a great deal of theoretical work over the last ten years. Discussion of these calculations (primarily QED) and how they relate to experiments forms a substantial part of the present review. In the same context we discuss how the muon can be viewed not as a known probe but as a particle whose assumed properties can be tested. Interaction with the extended nucleus is the oldest use of the muon as a probe [muonic atoms provided the first accurate measurements of nuclear size (Fitch and Rainwater, 1953)]. We also discuss the calculation of these nuclear effects, both static and dynamic, in detail and relate these to some selected experimental measurements. Finally, one can, in principle, study the weak interaction and nuclear excitation spectra through the destruction of the muonic atom by muon capture. In practice, details of the weak interaction are lost in the details of nuclear structure, and although considerable work has been done on the subject,

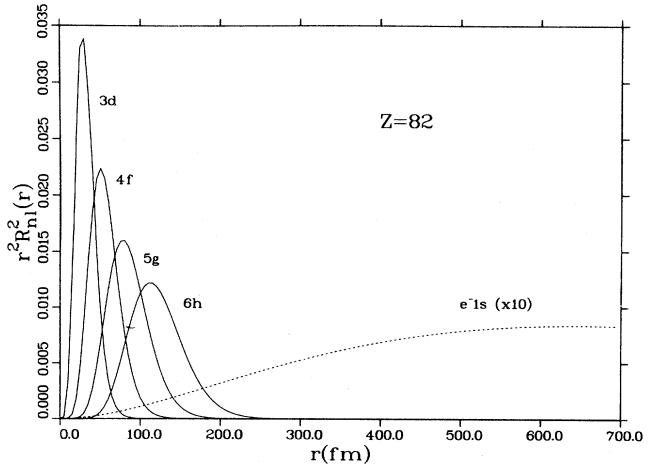

FIG. 1. Muon wave functions (solid lines) for relatively high-lying states, compared to the electron 1*s* wave function (dashed line).

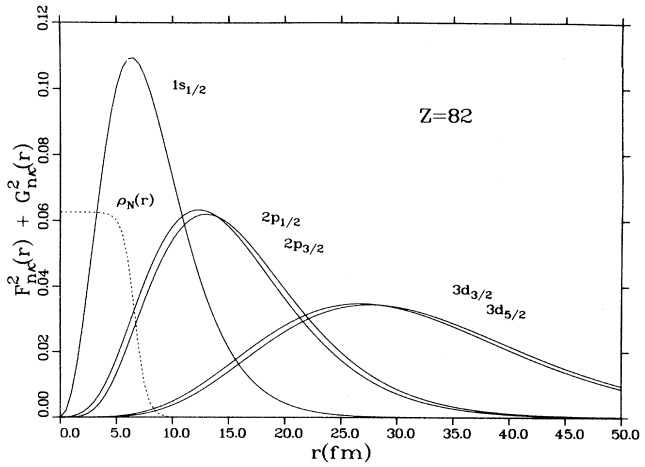

FIG. 2. Muon wave functions (solid lines) for relatively low-lying states, compared to the nuclear charge distribution $\rho_N(r)$ (dashed line).

we shall not discuss it here. For more information, see the reviews by Mukhopadhyay (1977, 1980).

The principal quantities to be calculated for a muonic atom are the energies and relative rates for various radiative transitions. To our knowledge, no quantitative measurements of Auger transitions exist. In view of the known difficulties associated with the solution of the relativistic bound-state problem, we depend in practice upon a Hamiltonian formalism in which each physical effect is represented by an effective potential, to be included as desired in the Dirac equation or in a perturbative treatment. The fact that this can be carried out to sufficient accuracy in a systematic step-by-step manner is due to a fortuitous combination of coupling constants and masses. Otherwise one would be faced with solving an extremely complicated many-body problem with many degrees of freedom. For example, the fact that the electromagnetic interaction is much weaker than the strong interaction implies that the muon will not normally perturb the nucleus to any significant degree, so that the nuclear degrees of freedom may be neglected as a first approximation. The fact that the muon mass is much smaller than the nuclear mass permits us to regard the nucleus as a nearly static source of the Coulomb interaction, and to treat the recoil correction as a perturbation.

B. Principal kinematics and interactions

We shall begin the construction of our effective Hamiltonian with the three primary constituents of a muonic atom: the muon, the nucleus, and the atomic electrons, each of which is assumed to obey a "free" Hamiltonian in the absence of interactions with the others. Other objects, such as neighboring atoms, are either of negligible importance or can be included as minor modifications to this Hamiltonian. The muon Hamiltonian is the free Dirac Hamiltonian $\boldsymbol{\alpha}\cdot\boldsymbol{p}+\beta m$, appropriate for a point particle of spin $\frac{1}{2}$. The nuclear Hamiltonian H_N appears in a primarily formal way; although one could imagine it to be an approximate Hartree-Fock Hamiltonian, for example, we regard it here as an operator which produces the nuclear mass, charge (including electric and magnetic multipole) distributions, and excitation spectra. We thereby avoid building into our calculation from the start the uncertainties associated with any particular nuclear theory. The Hamiltonian for the atomic electrons could be treated similarly. However, the confidence with which present-day atomic Hartree-Fock calculations are carried out makes it practical to use this approximation explicitly.

Interactions among these constituents of the system will be taken in three classes: time-averaged (i.e., static) classical electromagnetic interactions; kinematic and dynamic corrections to these; and quantum (including weak interaction) corrections to both. The fact that this particular decomposition is useful arises, as mentioned above, from the combinations of masses and coupling constants which reduce the dynamic and quantum interactions among the different constituents to small perturbations and allow the approximate isolation of many degrees of freedom. The time-averaged classical static interactions determine nearly all of the basic structure of a muonic atom, as well as a number of less important effects. This subject will be treated in detail in Sec. II. Kinematic and dynamic corrections arise both from translational nuclear (and electronic) motion and from excitation of the internal degrees of freedom of the nucleus and the atom. These will be treated in Sec. II.G and II.H. Quantum corrections fall into three classes: the vacuum polarization, which is the self-energy of the electromagnetic field due to its coupling to all pairs of charged particles; the muon self-energy, which arises from its self-interaction with the electromagnetic field; and the weak (or anomalous) interactions which couple the various components of the system. These will be treated in Sec. III. Naturally, such effects also appear internally in the nuclear and atomic electron systems, but we assume that they have been either included phenomenologically or lost among the other uncertainties therein.

C. Notation and numerical values

In general, muon coordinates will be unsubscripted, nuclear coordinates will carry a first subscript N, and electron coordinates a first subscript e. Other quantities, such as energies and quantum numbers, will be distinguished in the same way if there is any possibility of confusion.

All formulas will be written in natural units such that $\hbar=c=1$. Conventional units may be resurrected with the aid of the following table of definitions and numerical values (Kelly *et al.*, 1980):

$Z=$ nuclear charge
$A=$ nuclear mass number
mc^2 = muon rest mass = 105.65946 ± 0.00024 MeV
$\hbar c/mc^2$ = muon Compton wavelength = 1.867 5903 ± 0.000 0064 fm
$m_e c^2$ = electron rest mass = 0.511 0034 ± 0.000 0014 MeV
$\hbar c/m_e c^2$ = electron Compton wavelength = 386.15905 ± 0.0015 fm
$M_N c^2$ = nuclear rest mass = (931.5016 ± 0.0026) A MeV
$\alpha=$ fine-structure constant = 1/(137.036 04 ± 0.000 11)
$e^2=$ square of electron charge $=4\pi\alpha$
$\hbar c$ = 197.32858 ± 0.000 51 MeV fm

II. CLASSICAL INTERACTIONS AND KINEMATICS

A. Dirac equation

The Dirac equation for a muon moving in an external classical electromagnetic field is (Schiff, 1968)

$$[\boldsymbol{\alpha}\cdot(\mathbf{p}+e\mathbf{A})+\beta m-E-e\phi]\psi=0\ . \tag{1}$$

The use of fully relativistic muon kinematics is dictated by the required computational accuracy. Even in helium, the muon velocity near the nucleus is $\simeq(2Z\alpha/mR_N)^{1/2}\simeq 0.2c$, while it can be several times this in heavy nuclei. The electromagnetic potentials $\mathbf{A}$ and ϕ, which are in principle time dependent, are generated both by the nucleus and by the atomic electrons. The former source dominates due to its relative compactness and hence determines the essential structure of any muonic atom. The electrons are much less important for most interesting muonic transitions because their orbits are much larger than those of the muon, and we shall neglect them until Sec. II.I (except for noting some obvious parallels to topics under discussion). The muon mass m appearing in Eq. (1) is formally the mass of the free muon. We shall make extensive use of static approximations for $\mathbf{A}$ and ϕ, in which they are replaced by effective time-independent potentials and m is replaced by the nonrelativistic reduced mass m_r. These approximations are justified in Sec. II.H.

For computational convenience we shall work almost entirely in the Coulomb gauge. Although it leads to a noncovariant formulation, this gauge is useful because it allows simplifying approximations which are quantitatively less severe than similar approximations made in the Lorentz gauge (Breit and Brown, 1948; Grotch and Yennie, 1969; Friar, 1977). The main reasons for this are that the dominant scalar potential ϕ is given in terms of the instantaneous nuclear (and electron) charge distributions and thus may be formulated simply; and that the vector potential $\mathbf{A}$, which will be neglected or only approximated, is "smaller" in the sense that it depends only upon the external transverse current. Although treating these potentials unequally can lead to spurious effects in the completely relativistic regime (Brown and Ravenhall, 1951), such effects are unimportant for many applications because the sources (nucleus and electrons) are largely nonrelativistic in the laboratory frame of reference. We shall generally refer to the scalar potential ϕ as a Coulomb interaction even though it is generated by a nonpointlike distribution of charge.

B. Zero-order approximations

Since we want to consider the nuclear degrees of freedom as well as those of the muon, we write the total Hamiltonian of the muon-nucleus system as

$$H_{N\mu}=H_N+\boldsymbol{\alpha}\cdot\mathbf{p}+\beta m_r+e\boldsymbol{\alpha}\cdot\mathbf{A}-e\phi\ , \tag{2}$$

where, as indicated above, $\mathbf{A}$ and ϕ represent the potentials generated by the nucleus and contain both muon and nuclear operators. H_N is the nuclear Hamiltonian in the absence of the muon.

As a first approximation, we neglect the term $e\boldsymbol{\alpha}\cdot\mathbf{A}$ and separate the muon and nuclear degrees of freedom in the following manner. We define a static potential $V_0(\mathbf{r})$, which represents a time-averaged electrostatic potential generated by the nucleus and is intended to provide accurate zero-order solutions for the muon wave functions. We are free to construct and to interpret this potential as we wish. In practice, we normally parametrize and adjust it to yield fits to measured transition energies. Precisely what the averaging means is a matter of choice. Writing $|0\rangle$ for the nuclear ground state in the absence of the muon, the customary choice is

$$\begin{aligned}V_0(\mathbf{r})&=-e\langle 0\,|\,\phi\,|\,0\rangle\\&=-Z\alpha\int d^3r_N\frac{\rho_0(\mathbf{r}_N)}{|\,\mathbf{r}-\mathbf{r}_N\,|}\ ,\end{aligned} \tag{3}$$

where $\rho_0(\mathbf{r}_N)=\langle 0\,|\,\rho(\mathbf{r}_N)\,|0\rangle$ is the average nuclear ground-state charge distribution in the absence of the muon, normalized to $\int d^3r_N\,\rho_0(\mathbf{r}_N)=1$. This choice has the advantage of eliminating certain diagonal terms in the dynamic corrections (to be discussed later) and, provided that the remaining corrections are carried out appropriately, it admits to a straightforward interpretation of any fitted function $\rho_0(\mathbf{r})$. It is well known that $\rho_0(\mathbf{r})$ contains the charge distributions of all particles in the nucleus folded over their point distributions. Less widely appreciated is the fact that any *fitted* $\rho_0(\mathbf{r})$ also includes the folded classical muon charge distribution (if it is not pointlike), a result obtained from the convolution theorem and the Dirac equation (1). This is not to be confused with the QED form factor of the muon arising from the vertex corrections, which are well defined and accounted for separately. Equation (2) is then rewritten as

$$H_{N\mu}=H_N+\boldsymbol{\alpha}\cdot\mathbf{p}+\beta m_r+V_0(\mathbf{r})+V_P\ , \tag{4}$$

where $V_P=-e\phi-V_0(\mathbf{r})$ is the residual muon-nucleus interaction, responsible for polarization effects. Neglecting V_P (to be treated later as a perturbation) separates the Hamiltonian into terms containing either muon or nuclear operators but not both, so that the eigenstates are products of muon and nuclear states. Assuming that the latter are given by other considerations, the problem thus reduces in this approximation to finding the eigenfunctions and eigenvalues of

$$H=\boldsymbol{\alpha}\cdot\mathbf{p}+\beta m_r+V_0(\mathbf{r})\ . \tag{5}$$

C. Decomposition in spherical coordinates

Solving Eq. (5) is most conveniently handled in spherical coordinates, by expanding $V_0(\boldsymbol{r})$ in multipoles, and constructing a set of basis states using only the monopole term $V_0(r)$. We use the representation (Schiff, 1968; Merzbacher, 1970)

$$\boldsymbol{\alpha}=\begin{bmatrix}0 & \boldsymbol{\sigma}\\ \boldsymbol{\sigma} & 0\end{bmatrix},\quad \beta=\begin{bmatrix}1 & 0\\ 0 & -1\end{bmatrix}. \tag{6}$$

The muon Dirac spinor is (McKinley, 1969a)

$$\psi_{n\kappa}(\mathbf{r})=\begin{bmatrix}\frac{1}{r}G_{n\kappa}(r) & \langle \mathbf{r}\,|\,\kappa\mu\rangle \\ \frac{i}{r}F_{n\kappa}(r) & \langle \mathbf{r}\,|\,-\kappa\mu\rangle\end{bmatrix},$$

where the angular spinors $|\kappa\mu\rangle$ may be shown to be eigenstates of the operators $\mathbf{l}^2$, $\boldsymbol{\sigma}^2$, $\mathbf{j}^2$, and j_z, with $\mathbf{j}=\mathbf{l}+\boldsymbol{\sigma}/2$, so that

$$\begin{aligned}&\mathbf{l}\cdot\mathbf{l}\,|\,\kappa\mu\rangle=l(l+1)\,|\,\kappa\mu\rangle\,,\quad \boldsymbol{\sigma}\cdot\boldsymbol{\sigma}\,|\,\kappa\mu\rangle=3\,|\,\kappa\mu\rangle\,,\\ &\mathbf{j}\cdot\mathbf{j}\,|\,\kappa\mu\rangle=j(j+1)\,|\,\kappa\mu\rangle\,,\quad j_z\,|\,\kappa\mu\rangle=\mu\,|\,\kappa\mu\rangle\,.\end{aligned}\tag{8}$$

An explicit construction which exhibits these required properties is the Pauli spinor

$$\langle \mathbf{r}\,|\,\kappa\mu\rangle=\begin{bmatrix}C(\frac{1}{2},+\frac{1}{2},l,\mu-\frac{1}{2}\,|\,j,\mu) & Y_{l,\mu-1/2}(\hat{r})\\ C(\frac{1}{2},-\frac{1}{2},l,\mu+\frac{1}{2}\,|\,j,\mu) & Y_{l,\mu+1/2}(\hat{r})\end{bmatrix}.\tag{9}$$

One may also show from Eqs. (5)–(7), with the aid of some commutator algebra and with $V_0(\mathbf{r})\rightarrow V_0(r)$ as already noted, that

$$\begin{aligned}&-(1+\boldsymbol{\sigma}\cdot\mathbf{l}\,|\,\kappa\mu\rangle=\kappa\,|\,\kappa\mu\rangle\,,\\ &\boldsymbol{\sigma}\cdot\hat{r}\,|\,\kappa\mu\rangle=-\,|\,-\kappa\mu\rangle\,.\end{aligned}\tag{10}$$

Since $\mathbf{j}$ commutes with the total muon Hamiltonian, the same value of j is associated with both Pauli spinors in Eq. (7). Two distinct values of l are involved, however. These may be determined by observing from Eqs. (8) and (10) that

$$\kappa=l(l+1)-j(j+1)-\tfrac{1}{4}=\begin{cases}-(l+1), & j=l+\frac{1}{2}\\ l, & j=l-\frac{1}{2}\end{cases}\tag{11}$$

so that $|\kappa|=j+\frac{1}{2}=1,2\ldots$ Thus the lower component of Eq. (7) has associated orbital angular momentum $l-1$ if $\kappa>0$ and $l+1$ if $\kappa<0$. Even though the states $|\kappa\mu\rangle,|-\kappa\mu\rangle$ thus have opposite parities, the four-component spinor $\psi_{n\kappa}$ is an eigenstate of the relativistic parity operator constructed by combining space inversion with multiplication by the Dirac matrix β. The parity is thus determined by the l value associated with the large component. Note the choice of phase for the Pauli spinors (9). Use of Clebsch-Gordan coefficients $C(l,\mu\pm\frac{1}{2},\frac{1}{2},\mp\frac{1}{2}|j,\mu)$ results in no observable differences, but would lead to different phase factors and coupling coefficients later. Another useful identity is

$$\boldsymbol{\sigma}\cdot\mathbf{p}=-i\frac{\boldsymbol{\sigma}\cdot\mathbf{r}}{r^2}\left[\frac{\partial}{\partial r}r-(1+\boldsymbol{\sigma}\cdot\mathbf{l})\right].\tag{12}$$

Assembling the above results gives in the usual way the radial equations which are to be solved

$$\begin{aligned}\frac{d}{dr}G_{n\kappa}(r)&=-\frac{\kappa}{r}G_{n\kappa}(r)+[m_r+E_{n\kappa}-V_0(r)]F_{n\kappa}(r)\\ \frac{d}{dr}F_{n\kappa}(r)&=\frac{\kappa}{r}F_{n\kappa}(r)+[m_r-E_{n\kappa}+V_0(r)]G_{n\kappa}(r)\,.\end{aligned}\tag{13}$$

For electronic atoms, it is customary to make the further approximation $V_0(r)=-Z\alpha/r$ and treat the effects of finite nuclear size in perturbation theory. For muonic atoms, these effects can be estimated from

$$\begin{aligned}\Delta E_{n\kappa}&\simeq\int_0^\infty dr\,[F_{n\kappa}^2(r)+G_{n\kappa}^2(r)]\left[V_0(r)+\frac{Z\alpha}{r}\right]\\ &\simeq R_N^{-2}[F_{n\kappa}^2(R_N)+G_{n\kappa}^2(R_N)]\int_0^{R_N}dr\,r^2\left[V_0(r)+\frac{Z\alpha}{r}\right]\\ &\simeq\frac{Z\alpha}{10}[F_{n\kappa}^2(R_N)+G_{n\kappa}^2(R_N)]\,,\end{aligned}\tag{14}$$

where we have approximated the nucleus by a uniform charge distribution of radius R_N and the muon wave function inside the nucleus by the value of the point-nucleus solution at the nuclear surface. This latter approximation was made to eliminate the unphysical singularity in the relativistic point-nucleus wave functions for $j=\frac{1}{2}$. For the $1s$ state in Fe, $\Delta E\simeq 116$ keV, about 6% of the point-nucleus binding energy. Considering that this energy is known experimentally to within about 0.5 keV, it is clear that more accurate calculations are needed.

D. Numerical methods

1. Eigenvalues

Solving the differential equations (13) and finding the eigenvalues normally involves making an initial guess for the eigenvalue and then "shooting" by stepwise integration outward in r from a small radius and inward from a large radius to a common matching point, where the mismatch in the wave function is used to improve the eigenvalue. Since with any reasonable numerical integration scheme, errors in the starting values at the small and large radii propagate in the solutions without amplification, it is not necessary to have high relative accuracy in these values. Common methods for calculating the starting values are power series for small r and asymptotic series for large r. Another method of comparable accuracy is to consider the potential at the starting radii to be locally constant, so that the required solutions are spherical Bessel functions of appropriate angular momentum.

One method for improving the eigenvalue is the secant method

$$E_{j+1}\simeq\frac{D_jE_{j-1}-D_{j-1}E_j}{D_j-D_{j-1}}\tag{15}$$

where D_j is some suitable measure of the mismatch upon

the jth iteration of the outer and inner wave functions F_o, G_o, and F_i, G_i at the matching radius, e.g.,

$$D_j = F_o/G_o - F_i/G_i \ . \tag{16}$$

Another method is based upon a variational principle (Blatt, 1967; Rinker, 1976). If ψ_0 is a wave function obtained with the initial eigenvalue guess E_0, then an improved eigenvalue estimate is

$$E = (\psi_0, H\psi_0) \ . \tag{17}$$

With ψ_0 obtained by shooting, the expectation value gives E_0 plus a contribution from the discontinuity

$$E = E_0 + F_i G_o - F_o G_i \ , \tag{18}$$

where

$$F_i^2 + G_i^2 = F_o^2 + G_o^2 \tag{19}$$

and

$$\int_0^\infty dr\,[F^2(r) + G^2(r)] = 1 \ . \tag{20}$$

The secant method converges almost quadratically, while the variational method converges quadratically.

2. Solution of the radial Dirac equations

A variety of methods are in current use for the numerical solution of the differential equations. Each has its advocates; however, the present problem is so simple by modern standards that almost any respectable method will work. The primary pitfall is instability, which is a generic term used to describe any phenomenon which leads to uncontrolled error growth. Thus a method may have a small truncation error at any given step, but if successive truncation errors add constructively, the method will be unstable. The instability may lie in the original differential equation itself or in the finite-difference approximation used to obtain the numerical solution. The Dirac equation (13) exhibits the former, as it generally admits a pair of complementary solutions. In regions of negative kinetic energy, one of these decreases and the other increases at approximately the same rate. If one attempts to obtain the decreasing solution numerically, it is inevitable that small components of the increasing solution will get mixed in through truncation errors. These can eventually dominate and render meaningless the finite-difference solution actually obtained. The usual way around this difficulty is always to integrate in the direction in which the desired solution is either increasing or oscillating. This is always possible for (13), as no more than two solutions ever exist for the differential equation.

Other instabilities arise from the finite-difference approximations themselves. One can eliminate these by using low-order methods which admit no more than two solutions (Blatt, 1967). Such extreme measures are not necessary, however, as good high-order methods are known in which all extraneous solutions decay in situations of present interest. Exceptionally stable in this respect are the Adams methods (Shampine and Gordon, 1975), which will integrate even rapidly decreasing functions properly if small enough steps are taken. Less efficient are the widely used Runge-Kutta methods, which are, however, simple to implement and sufficiently accurate and stable. An example of a well known method which is nearly always unstable is Milne's, which fails even to integrate oscillating functions properly (Hamming, 1962). Another widely used method which is stable but asymptotically incorrect and therefore not recommended is Hamming's method (Hamming, 1959; Shampine, 1973). In any case, present-day experimental accuracy dictates that computation must be made in double precision if a computer with less than 12 decimal digit accuracy is used.

A considerable literature now exists on the subject. The reader who is tempted to devise his own method would be well advised first to consult one of the excellent introductory texts, such as Shampine and Gordon (1975) or Hamming (1962).

E. "Model-independent" interpretation

In the earliest analyses, the nucleus was represented by a static phenomenological charge-distribution function. The Dirac equation for the muon was then solved, and parameters such as the nuclear radius were adjusted to fit measured transition energies. In this way it was first determined that nuclear radii were approximately 1.2 $A^{1/3}$ fm rather than 1.4 $A^{1/3}$ fm as had been believed previously (Fitch and Rainwater, 1953). More recently, a number of so-called "model-independent" methods have been devised to interpret spectra in terms of constraints upon ground-state nuclear charge distributions, in order to avoid the unphysical constraints imposed by a specific assumed functional form for the charge distribution. Since this is a subject concerned primarily with the analysis of data rather than the theoretical calculation of energy levels, we shall only briefly sketch it here. For more details, the reader is referred to the reviews of Barrett (1974) and Friar and Negele (1975).

These methods begin with some spherical, trial nuclear charge distribution $\rho_0(r_N)$, and then investigate the effect of an arbitrary variation $\delta\rho(r_N) = \rho(r_N) - \rho_0(r_N)$. In lowest order one obtains

$$E_{n\kappa} \simeq E_0 + Z \int dr_N\, r_N^2 \delta\rho(r_N) \int d\Omega_N\, V_{n\kappa}(\mathbf{r}_N) \ , \tag{21}$$

where $V_{n\kappa}(\mathbf{r}_N)$ is the potential generated by the average muon charge distribution for the state or transition in question, and E_0 is the energy calculated using $\rho_0(r_N)$. It should be emphasized that Eq. (21) is first order and thus of use only if one starts with a trial distribution which is already a good approximation to nature. In this way one obtains a linear integral constraint on $\rho(r_N)$ [or $\delta\rho(r_N)$] for each transition, in terms of calculated and measured energies E_0 and $E_{n\kappa}$. A similar set of constraints can be obtained for each cross section $\sigma(q)$ measured by scattering electrons from the same nucleus. In general, one finds that the muon-derived constraints are

very precise but are limited to slowly varying kernel functions $V_{n\kappa}(r_N)=\int d\Omega_N\, V_{n\kappa}(\mathbf{r}_N)$, while the electron-derived constraints are less precise but more rapidly varying. The two types of measurement are thus complementary. Given enough such constraints of sufficient accuracy, it would be possible to invert them to obtain a unique, "measured" charge distribution within reasonable error limits.

Such a procedure is clearly hopeless when the muonic data alone are used. It has instead become customary to express experimental results in terms of a moment-transformed charge function $R_\alpha(k)$ (Ford and Wills, 1969; Barrett, 1970; see also Ford and Rinker, 1973) defined by

$$\frac{3}{R_\alpha^3(k)}\int_0^{R_\alpha(k)} dr_N\, r_N^{2+k} e^{-\alpha r_N} = 4\pi\int_0^\infty dr_N\, r_N^{2+k} e^{-\alpha r_N}\rho(r_N)\ . \tag{22}$$

With this definition, $R_\alpha(k)$ is the radius of a uniform distribution with the same expectation value of $\langle r_N^k e^{-\alpha r_N}\rangle$ as that of the model $\rho(r_N)$ under consideration. This approach was initiated by Ford and Wills (1969) and extended by Barrett (1970). Its significance arises from the fact that the muon potential function for any state or transition can be parametrized accurately by the form

$$V_{n\kappa}(r_N)\simeq C+Br_N^k e^{-\alpha r_N}\ , \tag{23}$$

so that Eq. (22) becomes an expression of the constraint (21). With optimal fits, C, B, k, and α all vary from transition to transition and element to element. In practice, one optimizes α for a given nucleus and compares the transformed moment function $R_\alpha(k)$ to the values measured for specific values of k. The same approach is also useful for analyzing isotope and isomer shifts (Ford and Rinker, 1974). A generalized form for deformed nuclei has been given by Wagner *et al.* (1977). Similar approaches have been taken to utilize the constraints obtained from electron scattering. If the constraint corresponding to (21) is written

$$\delta\sigma(q)=Z\int d^3r_N\,\delta\rho(r_N)f_q(r_N)\ , \tag{24}$$

then an expansion

$$\rho(r_N)=\sum_{q=0}^{\infty} a_q f_q(r_N) \tag{25}$$

would yield $Z\delta a_q=\delta\sigma(q)$ if the kernels $f_q(r_N)$ were orthonormal. In practice this is not the case, so that correlations remain among the coefficients a_q no matter how well the kernels $f_q(r_N)$ are approximated. In addition, practical limitations on momentum transfer in experiments restricts the number of coefficients that can be determined. Several prescriptions and iterative procedures have been devised to solve Eqs. (24) and (25) (Lenz, 1969; Lenz and Rosenfelder, 1971; Friar and Negele, 1973a; Borysowicz and Hetherington, 1973; Sick, 1973, 1974). For many nuclei the data are now sufficient to complete the inversion with only modest uncertainties and assumptions about unmeasured coefficients. Under the assumption of electron-muon universality (Rinker and Wilets, 1973b; Barber *et al.*, 1979a, 1979b) at the required level of accuracy, the muonic data can also be included with the primary effect of normalizing the scattering data more precisely.

The first notable demonstration of the virtues of this approach occurred in 1973 with the controversy over whether the charge distribution of ^{208}Pb had a depression in its center. Model analyses (Heisenberg *et al.*, 1969) of available electron scattering data and muonic atom transition energies indicated a depression, in serious contradiction to a number of theoretical calculations which displayed the opposite. The issue was finally resolved by an analysis along the above lines (Friar and Negele, 1973a), which showed that although a depression was consistent with the data, charge distributions with increased density near the origin were, too. These authors also showed that if the overall normalization of the measured electron scattering cross sections were in error by 2–3%, reasonable agreement with theoretical calculations could be obtained (see also Barrett, 1974; Friar and Negele, 1975).

F. Corrections for static nuclear moments

In addition to the extended electric monopole charge distribution, the nucleus may possess nonzero magnetic and electric multipole moments in its ground or excited states. The former may be treated with the previously neglected vector potential $\mathbf{A}$, while the latter are represented by higher-order multipoles in the expansion of $V_0(\mathbf{r})$ or its generalization for excited nuclear states. In cases where these moments are small, they merely split the muon energy levels. To describe this splitting, we need to construct a muon-nucleus basis coupled in angular momentum. Denoting the nuclear states by $|IM\rangle$, we have

$$H_N|IM\rangle=E_{N,I}|IM\rangle\ ,\quad \mathbf{I}\cdot\mathbf{I}|IM\rangle=I(I+1)|IM\rangle\ ,$$
$$I_z|IM\rangle=M|IM\rangle\ . \tag{26}$$

We couple these to the Pauli spinors $|\kappa\mu\rangle$ to give total angular momentum $\mathbf{\Lambda}=\mathbf{j}+\mathbf{I}$ and projection Ω

$$|\kappa I\Lambda\Omega\rangle=\langle\kappa\mu IM|\kappa I\Lambda\Omega\rangle|\kappa\mu\rangle|IM\rangle\ , \tag{27}$$

so that

$$\mathbf{\Lambda}\cdot\mathbf{\Lambda}|\kappa I\Lambda\Omega\rangle=\Lambda(\Lambda+1)|\kappa I\Lambda\Omega\rangle$$
$$\Lambda_z|\kappa I\Lambda\Omega\rangle=\Omega|\kappa I\Lambda\Omega\rangle\ . \tag{28}$$

Note that the Clebsch–Gordan series (27) is independent of the sign of κ, since it is $j=|\kappa|-\frac{1}{2}$ which is coupled to I. Using the shorthand $|\pm\zeta\rangle=|\pm\kappa I\Lambda\Omega\rangle$, the coupled muon-nuclear state is

$$\Psi_{n\zeta}(\mathbf{r})=\begin{bmatrix}\frac{1}{r}G_{n\kappa}(r)\ \langle\mathbf{r}|\zeta\rangle\\ \frac{i}{r}F_{n\kappa}(r)\ \langle\mathbf{r}|-\zeta\rangle\end{bmatrix}\ . \tag{29}$$

1. Electric multipole interactions

Writing the muon-nucleus interaction as

$$V(\mathbf{r})=-Z\alpha\int d^3r_N\,\frac{\rho(\mathbf{r}_N)}{|\mathbf{r}-\mathbf{r}_N|}\,, \tag{30}$$

the first-order perturbed energy shift due to higher multipoles in $\rho(\mathbf{r}_N)$ is

$$\begin{aligned}\Delta E_{n\zeta}&=(\Psi_{n\zeta}(\mathbf{r}),[V(\mathbf{r})-V_0(r)]\Psi_{n\zeta}(\mathbf{r}))\\&=Z\alpha\sum_{L=0}^{\infty}(-1)^{L+I+\Lambda-1/2}\tfrac{1}{2}[1+(-1)^L]\left[\frac{4\pi}{2L+1}\right]^{1/2}(2j+1)\begin{Bmatrix}j&I&\Lambda\\I&j&L\end{Bmatrix}\begin{bmatrix}j&L&j\\-\frac{1}{2}&0&\frac{1}{2}\end{bmatrix}\\&\quad\times\int_0^\infty dr\,[F^2_{n\kappa}(r)+G^2_{n\kappa}(r)]\langle I||\int d^3r_N\,\rho(\mathbf{r}_N)Y_L(\hat{r}_N)r_<^L/r_>^{L+1}||I\rangle-\int_0^\infty dr\,[F^2_{n\kappa}(r)+G^2_{n\kappa}(r)]V_0(r)\,.\end{aligned} \tag{31}$$

For the ground state, the monopole term is removed by cancellation with $V_0(r)$. For excited nuclear states and $L=0$, (31) reduces to the so-called "isomer shift." All of the odd multipoles are zero.

The energy shift is proportional to a reduced matrix element of the nuclear charge-density operator $\rho(\mathbf{r}_N)$, customarily reduced via

$$\begin{aligned}&\langle I||Z\int d^3r_N\,\rho(\mathbf{r}_N)Y_L(\hat{r}_N)r_<^L/r_>^{L+1}||I\rangle\begin{bmatrix}I&L&I\\-I&0&I\end{bmatrix}\\&\quad=\langle II\,|\,Z\int d^3r_N\,\rho(\mathbf{r}_N)Y_{L0}(\hat{r}_N)r_<^L/r_>^{L+1}\,|\,II\rangle\\&\quad\underset{r\to\infty}{\to}Q_{IL}/r^{L+1}\,,\end{aligned} \tag{32}$$

where Q_{IL} is the Lth multipole moment of nuclear state I. If the following ansatz is made for the expectation value of $\rho(\mathbf{r}_N)$

$$\langle II\,|\,\rho(\mathbf{r}_N)\,|\,II\rangle=\sum_{L'M'}\beta_{IL'M'}Y^*_{L'M'}(\hat{r}_N)\rho_{IL'}(r_N)\,, \tag{33}$$

then the reduced nuclear matrix element in Eq. (31) becomes

$$\begin{aligned}&\langle I\,||\,Z\int d^3r_N\,\rho(\mathbf{r}_N)Y_L(\hat{r}_N)r_<^L/r_>^{L+1}||I\rangle\\&\quad=Z\beta_{IL0}\begin{bmatrix}I&L&I\\-I&0&I\end{bmatrix}^{-1}\int_0^\infty dr_N\,r_N^2r^L\langle\,/r\rangle^{L+1}\rho_{IL}(r_N)\end{aligned} \tag{34}$$

Equation (31) can be written in terms of the "hyperfine-structure constants" $A_{Ln\zeta}$,

$$\Delta E_{n\zeta}=Z\alpha(-1)^\Lambda\sum_{L=0}^{\infty}\begin{Bmatrix}j&I&\Lambda\\I&j&L\end{Bmatrix}A_{Ln\zeta}\,. \tag{35}$$

These quantities may sometimes be fitted to the measured energy spectrum. For muon states which do not significantly penetrate the nucleus, the result is measurement of the nuclear Lth multipole moment (see, e.g., Dey *et al.*, 1979). For penetrating muon states, information about the radial distribution of multipole charge is obtained. Using a "model-independent" analysis similar to the monopole case (Wagner *et al.*, 1977), this information can be formulated in terms of integral constraints on the multipole charge distribution (see Sec. II.E).

2. Magnetic dipole interactions

In addition to even-L electric multipole moments, the nucleus may possess nonzero magnetic moments for odd L. We restrict consideration to $L=1$ because of the complicated nature of the higher-order terms and the fact that they are quite small when compared to the inherent uncertainties in evaluating the $L=1$ contributions. The M1 hfs may be obtained by evaluating $e\boldsymbol{\alpha}\cdot\mathbf{A}$ in (1) in perturbation theory. A nonrelativistic representation of this operator may be obtained by iterating (1), giving a Schrödinger-like equation for each spinor component with a perturbation to order $\mathbf{A}$

$$\frac{e}{m_r}\mathbf{A}\cdot\mathbf{p}+\frac{e}{2m_r}\boldsymbol{\sigma}\cdot\nabla\times\mathbf{A}\,. \tag{36}$$

The first term is the muon orbital interaction and the second the muon spin-nuclear moment interaction. Although one may proceed with a general nonrelativistic reduction to evaluate these terms, the algebra is simpler if one evaluates $\boldsymbol{\alpha}\cdot\mathbf{A}$ relativistically. The first-order energy shift is given by

$$\begin{aligned}\Delta E_{n\zeta}&=\langle n\zeta\,|\,e\boldsymbol{\alpha}\cdot\mathbf{A}\,|\,n\zeta\rangle\\&=2ie\int_0^\infty dr\,F_{n\kappa}(r)G_{n\kappa}(r)\langle\zeta\,|\,\boldsymbol{\sigma}\cdot\mathbf{A}\,|\,-\zeta\rangle\,,\end{aligned} \tag{37}$$

where we have used $\langle-\zeta|\boldsymbol{\sigma}\cdot\mathbf{A}\,|\,\zeta\rangle=-\langle\zeta\,|\,\boldsymbol{\sigma}\cdot\mathbf{A}|-\zeta\rangle$. Assuming that the nuclear magnetization in state $|I\rangle$ is given by the distribution[1] $g(e/2M_p)\mathbf{I}\mu(r_N)$

[1]Following convention, we write the magnetization in terms of the nuclear Bohr magneton $e/2M_p$, with the proton mass $M_p\simeq938.2796$ MeV, whose units require $e^2=\alpha$ and not $e^2=4\pi\alpha$ as used elsewhere in the present work.

$[\int d^3r_N \mu(r_N)=1]$, the dipole approximation gives

$$e\mathbf{A}(\mathbf{r})=\frac{g\alpha}{2M_p}\int d^3r_N \mu(r_N)\frac{\mathbf{I}\times(\mathbf{r}-\mathbf{r}_N)}{|\mathbf{r}-\mathbf{r}_N|^3}, \tag{38}$$

so that

$$e\boldsymbol{\sigma}\cdot\mathbf{A}=-\frac{g\alpha}{2M_p}\frac{4\pi}{r^3}\mathbf{I}\cdot\boldsymbol{\sigma}\times\mathbf{r}\int_0^r dr_N r_N^2\mu(r_N). \tag{39}$$

Working out the angular momentum algebra eventually yields the formula

$$\Delta E_{n\kappa}=\frac{4\pi\kappa g}{\kappa^2-\frac{1}{4}}\frac{\alpha}{2M_p}[\Lambda(\Lambda+1)-I(I+1)-j(j+1)]\times\int_0^\infty dr\, r^{-2}F_{n\kappa}(r)G_{n\kappa}(r)\int_0^r dr_N r_N^2\mu(r_N). \tag{40}$$

The form-factor integral is similar to that for an electric moment, except of course, that there is no term representing work done against the field in moving a probe inside the distribution. Equation (40) is valid for all muon states. Although it is not immediately obvious, it includes both the r^{-3} orbital terms and the Fermi contact interaction. For the $1s$ state, for example, it works out in the point-nucleus limit to be

$$\Delta E_{1s}=\frac{(2m_r Z\alpha)^3}{\gamma(2\gamma-1)}\frac{g}{3}\frac{\alpha}{2M_p 2m_r}[\Lambda(\Lambda+1)-I(I+1)-\tfrac{3}{4}], \tag{41}$$

which reduces to the correct nonrelativistic value in the limit $\gamma=(1-Z^2\alpha^2)^{1/2}\to 1$. It might perhaps be noted that the point-nucleus expression diverges for $\gamma<\frac{1}{2}$ ($Z>118$).

The above analysis does not take into account mass corrections to the hyperfine structure, which arise from Thomas precession and are of order $(g_N-2)m(AM_p)^{-1}$. Although negligible for heavy elements, these can be important for states with $l\neq 0$ in light muonic atoms (Borie, 1976b).

G. Intrinsic nuclear dynamics

Next we discuss effects arising from the internal degrees of freedom of the nucleus. These effects are generally referred to by two names: nuclear polarization and dynamic hyperfine structure. The first term is used to describe effects which are calculated in first- or second-order perturbation theory (see Fig. 3), leading to shifts in energy (and transition rates) of the muon states. The second describes those which split the coupled muon-nuclear levels into various components and must be calculated to all orders, e.g., by means of matrix diagonalization. Nuclear polarization effects were considered in the earliest analyses of muonic atom data (Cooper and Henley, 1953; Fitch and Rainwater, 1953). Estimates of these effects were necessarily crude due to lack of detailed information about nuclear excitation spectra, as well as the inadequacy of analytic computational approaches. More sophisticated calculations were carried out by Cole (1969) using better nuclear models. These calculations, however had the drawback that they depended upon closure over the intermediate muon states. The first truly accurate calculations, which eliminated the dependence upon closure, were made in the important papers of Chen (1970a) and of Skardhamar (1970) for muonic lead. Significant refinements have been made in calculations since that time; however, the fundamental approach and ideas have not been altered substantially. Dynamic hyperfine structure was first considered by Wilets (1954) and by Jacobsohn (1954). These classic papers set forth all of the basic physical ideas exploited in subsequent work, even though the actual calculations carried out were necessarily limited to simple rotational nuclear models. Nuclear-polarization effects were first combined with dynamic hyperfinc-structure calculations by Chen (1970b). It is this generalized approach which we shall follow in the present treatment, as adopted and extended by Rinker (1976) and Rinker and Speth (1978a). Similar approaches have been used by McLoughlin *et al.* (1976) and Vogel and Akylas (1977).

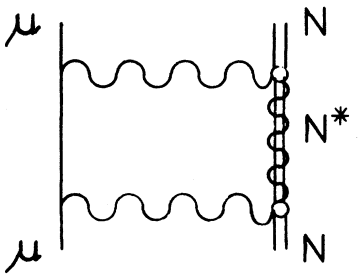

FIG. 3. Nuclear-polarization correction.

1. Formal description

The problem may be described formally by writing the Schrödinger equation for the muon-nucleus system as

$$(H_0+V_P-E_a)|a\rangle=0, \tag{42}$$

where $|a\rangle$ represents the complete muon-nucleus state. H_0+V_P is the zero-order Hamiltonian in Eq. (4). We may assume in addition that the muonic part of H_0 also includes all of the small corrections not involving nuclear excitations or static moments, e.g., quantum electrodynamic (QED) corrections; we need note only that all of these corrections known at present may be represented adequately by effective potentials in the muon coordinates, so that the appropriate matrix elements may be computed as needed. The eigenvalue to be found is E_a. The complete state is expanded in eigenfunctions of H_0:

$$|a\rangle=\sum_{i=1}^{\infty}a_i|i\rangle, \tag{43}$$

with

$$(H_0-\varepsilon_i)\,|\,i\,\rangle=0\ . \tag{44}$$

Our main task is to determine the coefficients a_i. We shall follow a program in which all of these coefficients are determined implicitly at least to first order in V_P, and some are determined explicitly to all orders.

To carry this out, we first define projection operators into a model space s and its complement as

$$P_s=\sum_{p=1}^{s}|\,p\,\rangle\langle\,p\,|\ ,\quad Q_s=\sum_{q=s+1}^{\infty}|\,q\,\rangle\langle\,q\,|\ . \tag{45}$$

The model space is assumed to include all those states which are expected to have large coefficients a_i, so that treatment to all orders in V_P is necessary. Inserting $1=P_s+Q_s$ into Eq. (42) and using standard projection operator properties, one obtains

$$(H_0-E_a+P_sV_P)P_s\,|\,a\,\rangle+P_sV_PQ_s\,|\,a\,\rangle=0\ , \tag{46}$$

and

$$Q_s\,|\,a\,\rangle=-(H_0-E_a)^{-1}Q_sV_P\,|\,a\,\rangle\ , \tag{47}$$

which may be combined to yield the exact result

$$P_s\{\,(H_0-E_a+V_P)P_s\,|\,a\,\rangle-V_P(H_0-E_a)^{-1}Q_sV_P\,|\,a\,\rangle\,\}=0\ . \tag{48}$$

This provides the framework for a sequence of approximations which are of successively higher order in the quantity $Q_s\,|\,a\,\rangle$, which must be small if the procedure is to be useful. It should be noted that the inverse operator $(H_0-E_a)^{-1}$ always exists in Eq. (48), since

$$(H_0-E_a)^{-1}Q_s=\sum_{q=s+1}^{\infty}(\varepsilon_q-E_a)^{-1}\,|\,q\,\rangle\langle\,q\,|\ , \tag{49}$$

and in the situation under discussion, E_a is never one of the ε_q. The requirement that $Q_s\,|\,a\,\rangle$ be small is satisfied if for all p,q

$$|\,\langle\,p\,|\,V_P\,|\,q\,\rangle\,|\ll|\,\varepsilon_p-\varepsilon_q\,|\ . \tag{50}$$

The lowest-order approximation to Eq. (48) which is of interest consists of neglecting the term involving Q_s. If the model space s is chosen to include only one state, the result is the simple static approximation in which no nuclear excitation occurs. If $s>1$, the problem may be solved by a straightforward finite-dimensional matrix diagonalization.

The next level of approximation is obtained by adding $P_s\,|\,a\,\rangle$ to Eq. (47) to get

$$|\,a\,\rangle=P_s\,|\,a\,\rangle-(H_0-E_a)^{-1}Q_sV_P\,|\,a\,\rangle \tag{51}$$

and then neglecting the second term, so that Eq. (48) becomes approximately

$$P_s\{\,(H_0-E_a+V_P)-V_P(H_0-E_a)^{-1}Q_sV_P\,\}P_s\,|\,a\,\rangle=0 \tag{52}$$

This is of the form

$$P_s(H_0-E_a+V_P+\Delta V_P)P_s\,|\,a\,\rangle=0\ , \tag{53}$$

with

$$\Delta V_P=\sum_{q=s+1}^{\infty}\frac{V_P\,|\,q\,\rangle\langle\,q\,|\,V_P}{E_a-\varepsilon_q}\ . \tag{54}$$

To the order of accuracy so far retained, one may treat ΔV_P formally as a first-order perturbation upon the lowest-order "model space" solutions, so that the resulting energy shift is

$$\Delta E_a=\sum_{p,p'=1}^{s}a_s^*a_{s'}\sum_{q=s+1}^{\infty}\frac{\langle\,p\,|\,V_p\,|\,q\,\rangle\langle\,q\,|\,V_p\,|\,p'\,\rangle}{E_a-\varepsilon_q}\ . \tag{55}$$

If $s=1$, this is just the standard second-order nuclear polarization energy shift, whereas if $s>1$, it is a nuclear polarization correction to the hyperfine structure. If the states in s were exactly degenerate, we would simply be dealing with degenerate perturbation theory. Clearly, we could continue the above development to higher orders, but as a practical matter this is pointless, since one can always choose a model space which insures that the neglected higher-order corrections are smaller than the other uncertainties in the calculation.

The infinite sum appearing in Eq. (55) can be evaluated in closed form. We first note that

$$|\,\Delta p\,\rangle=\sum_{i=1}^{\infty}\frac{\langle\,i\,|\,V_p\,|\,p\,\rangle\,|\,i\,\rangle}{E_a-\varepsilon_i} \tag{56}$$

is essentially the standard first-order perturbation of the state $|\,p\,\rangle$ due to V_P. This function satisfies (Dalgarno and Lewis, 1955; Schiff, 1968)

$$(H_0-E_a)\,|\,\Delta p\,\rangle+(V_P-\langle\,p\,|\,V_P\,|\,p\,\rangle)\,|\,p\,\rangle=0\ . \tag{57}$$

Rather than attempting to construct Eqs. (55) or (56) term by term, we may solve Eq. (57) directly and use the result in (55) to calculate the energy correction, with the first s terms in the sum over i in (56) removed explicitly. The only differences between (56) and (57) and normal perturbation theory is that $E_a\neq\varepsilon_p$. Here E_a represents any of the s eigenvalues obtained from a diagonalization of the model space. The result is that Eq. (57) is to be solved s^2 times, once for each combination of basis function and eigenvalue.

A further approximation may be made which saves considerable computational labor. Rather than solve Eq. (57) s times for every basis function $|\,p\,\rangle$, we may instead choose some average energy $\langle E\rangle$ and solve it only once, so that (57) need be solved only s times altogether. This approach introduces ambiguities into the procedure, but the size of the additional errors may be checked by comparing results for different choices of $\langle E\rangle$. These errors are of relative order $(\langle E\rangle-E_a)/(\varepsilon_p-\varepsilon_q)$. Two choices for $\langle E\rangle$ which have been used in previous work are (1) to make a single average over the entire subspace (Chen, 1970b; Vogel and Akylas, 1977), or (2) to set $\langle E\rangle=\varepsilon_p$ for the calculation of each $|\,\Delta p\,\rangle$ (McLoughlin *et al.*, 1976; Rinker and Speth, 1978a). The former gives a more consistent treatment of the off-diagonal corrections and retains the hermiticity of the perturbation matrix (54). The latter gives a more accurate treatment of the

diagonal corrections for states which are dominated by a single coefficient a_i but loses hermiticity for the off-diagonal corrections. Which choice (if either) is appropriate depends more upon the details of an individual calculation than on any overall principle. With any such choice, it is not necessary to have the eigenvalues E_a in order to compute the corrections, so that one may just as well construct ΔV_P first and then diagonalize the "renormalized" interaction $V_P + \Delta V_P$, so that the resulting eigenvalues and eigenvectors include the corrections of Eqs. (55) and (56). To the order of accuracy consistently retained, this is equivalent to using (55) explicitly, but is computationally more convenient. This procedure has been used in all calculations to date.

2. Explicit formulas

Although Eq. (57) can be regarded as a differential equation in any desired coordinates, in practice it is necessary to project out and sum explicitly over all but the muon radial coordinate. Such a treatment avoids the complexities of solving partial differential equations numerically. In addition, it allows one to treat the nucleus semiempirically rather than through some approximate model Hamiltonian.

The initial muon-nuclear spinor $|p\rangle$ is given by Eq. (29). The general first-order correction is

$$|\Delta p\rangle = \sum_{\zeta'} \begin{bmatrix} \frac{1}{r} g_{\zeta'}(r) \,|\, \zeta' \rangle \\ \frac{i}{r} f_{\zeta'}(r) \,|\, -\zeta' \rangle \end{bmatrix}, \tag{58}$$

with $g_{\zeta'}(r)$ and $f_{\zeta'}(r)$ to be determined. These functions satisfy the inhomogeneous differential equations

$$\begin{aligned} \frac{d}{dr} g_{\zeta'}(r) &= -\frac{\kappa'}{r} g_{\zeta'}(r) + [m_r - V_0(r) + E_{n\zeta} - E_{N,\zeta'} + E_{N,\zeta}] f_{\zeta'}(r) - V^{(L)}_{\zeta\zeta'}(r) F_{n\kappa}(r) , \\ \frac{d}{dr} f_{\zeta'}(r) &= \frac{\kappa'}{r} f_{\zeta'}(r) + [m_r + V_0(r) - E_{n\zeta} + E_{N,\zeta'} - E_{N,\zeta}] g_{\zeta'}(r) + V^{(L)}_{\zeta\zeta'}(r) G_{n\kappa}(r) , \end{aligned} \tag{59}$$

where

$$\begin{aligned} V^{(L)}_{\zeta\zeta'}(r) = \langle \zeta \,|\, V^{(L)}(r) \,|\, \zeta' \rangle &= Z\alpha(-1)^{I+\Lambda+j'+j+1/2} \tfrac{1}{2} [1 + (-1)^{l+L+l'}] \\ &\times \left[\frac{4\pi(2j+1)(2j'+1)}{2L+1} \right]^{1/2} \begin{Bmatrix} j & I & \Lambda \\ I' & j' & L \end{Bmatrix} \begin{pmatrix} j & L & j' \\ -\frac{1}{2} & 0 & \frac{1}{2} \end{pmatrix} \delta_{\Lambda\Lambda'} \delta_{\Omega\Omega'} \\ &\times \langle I \,||\, \int d^3 r_N \, \rho(\mathbf{r}_N) Y_L(\hat{r}_N) r_<^L / r_>^{L+1} \,||\, I' \rangle \end{aligned} \tag{60}$$

is a reduced nuclear multipole matrix element, sometimes also referred to as a transition potential. To complete the calculation we need the interaction matrix elements

$$\langle n \,|\, V^{(L)}_{\zeta\zeta'}(r) \,|\, n' \rangle = \int_0^\infty dr \, V^{(L)}_{\zeta\zeta'}(r) [F_{n\kappa}(r) F_{n'\kappa'}(r) + G_{n\kappa} G_{n'\kappa'}(r)] . \tag{61}$$

Second-order perturbed energy shifts are given by

$$\Delta E_{n\zeta} = \sum_{\zeta'} \Delta E_{n\zeta\zeta'} = \sum_{\zeta'} \int_0^\infty dr \, V^{(L)}_{\zeta\zeta'}(r) [F_{n\kappa}(r) f_{\zeta' r} + G_{n\kappa}(r) g_{\zeta'}(r)] . \tag{62}$$

The only numerical subtlety involved arises in solving the imhomogeneous equations (59). These have three solutions in general: two for the homogeneous parts and a third for the complete equations. Unless $E_{n\zeta} - E_{N,\zeta'} + E_{N,\zeta}$ is an eigenvalue of the homogeneous equations, only the third will be finite at both $r=0$ and ∞. One can solve these equations by shooting and extracting the unwanted contributions by imposing boundary conditions. However, unwanted rapidly growing solutions exist for both directions of integration in the general case, so that such extraction can fail unless extremely high numerical precision is used. An alternate method is to rewrite Eqs. (59) explicitly as low-order difference equations (Rinker, 1976) and reassemble them as a large but finite set of simultaneous algebraic equations for the function values $f_i = f(r = ih)$, etc., with the necessary boundary conditions built into the equations. The result is a band matrix which may be inverted by standard techniques. Both methods have drawbacks. If $E_{n\zeta} - E_{N,\zeta'} + E_{N,\zeta}$ is far from any eigenvalue, the instability in the shooting method may make it impossible to extract the desired perturbation. If $E_{n\zeta} - E_{N,\zeta'} + E_{N,\zeta}$ is close to an eigenvalue or the perturbation is very small, truncation error in the low-order band matrix technique may render the result meaningless, particularly if terms must be removed explicitly to obtain the restricted sum in Eqs. (54) or (55). The first problem is solved by computing in multiple precision, while the second is solved

by decreasing the radial increment h. Both require increases in computation time and storage, although the band matrix technique has usually proved easier in practice to adapt to difficult problems. Improvement may sometimes be obtained by scaling the perturbation by an overall multiplicative factor greater than 1 before solving (59) and then rescaling the final answer appropriately downward, noting that the perturbative energy shifts are quadratic in the scale of the perturbation.

At this point the physical problem has been reduced to specifying the nuclear-transition potentials and excitation energies appearing in Eqs. (59)–(61). In addition, one needs to take care of the substantial bookkeeping details involved in solving equations such as (53) and (54), as well as finding numerical solutions to (59). Several computer codes exist to solve this problem for various special cases (Chen, 1970a, 1970b; McLoughlin *et al.*, 1976; Vogel and Akylas, 1977; Rinker, 1979). At least one of these (Rinker, 1979) has been published in general form so that arbitrary nuclear models may be incorporated.

The connection of the transition potential to static nuclear multipole moments was given for the diagonal case in Eq. (32). For nuclear transitions, we have

$$\left|\left\langle I\left|\left|Z\int d^3r_N\,\rho(\mathbf{r}_N)Y_L(\hat{r}_N)r_<^L/r_>^{L+1}\right|\right|I'\right\rangle\right| \underset{r\to\infty}{\to} [(2I+1)B(EL;I\to I')]^{1/2}/r^{L+1}\,. \tag{63}$$

For many transitions of interest, this quantity is known experimentally and can be used to normalize the transition potential (Chen, 1970a), assuming that its sign and radial form factor have been obtained from a theoretical model or inelastic electron scattering. For other transitions and for systematics of the nuclear spectrum in general, however, one must resort to completely theoretical calculations.

3. Radiative transition rates

Radiative transition rates for electric multipole transitions between two states $|a\rangle$ and $|b\rangle$ are given in the long-wavelenth approximation by

$$T(a\to b)=\frac{8\pi Z\alpha}{(2\Lambda_a+1)}\sum_{L=0}^{\infty}(E_a-E_b)^{2L+1}\frac{(L+1)}{L[(2L+1)!!]^2}\left|\left\langle a\left|\left|Z\int d^3r_N\,r_N^L Y_L(\hat{r}_N)\rho(\mathbf{r}_N)+r^L Y_L(\mathbf{r})\right|\right|b\right\rangle\right|^2. \tag{64}$$

If $|a\rangle$ and $|b\rangle$ are defined by

$$|a\rangle=\sum_{i=1}^{s}a_i\,|j_iI_i\Lambda_a\Omega_a\rangle\,,\quad |b\rangle=\sum_{k=1}^{s}b_k\,|j_kI_k\Lambda_b\Omega_b\rangle\,, \tag{65}$$

then the reduced matrix elements may be expressed in terms of basis-state matrix elements,

$$\begin{aligned}\left\langle j_iI_i\Lambda_a\left|\left|Z\int d^3r_N\,r_N^L Y_L(\hat{r}_N)\rho(\mathbf{r}_N)+r^L Y_L(\hat{r})\right|\right|_k I_k\Lambda_b\right\rangle&\\ =(-1)^L[(2\Lambda_a+1)(2\Lambda_b+1)]^{1/2}&\left[(-1)^{j_k+I_k+\Lambda_a}\begin{Bmatrix}I_i & \Lambda_a & j_i\\ \Lambda_b & I_k & L\end{Bmatrix}\left\langle I_i\left|\left|Z\int d^3r_N\,r_N^L Y_L(\hat{r}_N)\rho(\mathbf{r}_N)\right|\right|I_k\right\rangle\delta_{j_ij_k}\right.\\ &\left.+(-1)^{j_i+I_i+\Lambda_b}\begin{Bmatrix}j_i & \Lambda_a & I_i\\ \Lambda_b & j_k & L\end{Bmatrix}\langle j_i||Y_L(\hat{r})||j_k\rangle\delta_{I_iI_k}\int_0^\infty dr\,r^L[G_i(r)G_k(r)+F_i(r)F_k(r)]\right].\end{aligned} \tag{66}$$

Both the nuclear and muon matrix elements appearing in (66) may be computed from quantities already involved in the hfs calculation.

4. Examples

a. General case of nuclear polarization

Detailed information about the nuclear excitation spectrum is known experimentally in only a few cases with sufficient completeness to carry out a reliable calculation. Even in these cases theoretical effort is required to fill in the gaps in experimental knowledge. It is therefore desirable to have a simple treatment based upon general considerations. Because the polarization energy shift is represented by a complete sum over the nuclear spectrum, one can hope to make use of the sum rules which express related sums in terms of ground-state expectation values. We illustrate this point with the following example (Rinker and Speth, 1978b). Consider the monopole part of the residual interaction, and consider only those terms in the sum (55) in which the muon remains in its initial state. Then the required matrix elements are

$$\langle n\,|\,V_{\xi\xi'}^{(0)}(r)\,|\,n'\rangle=-Z\alpha\int d^3r_N\langle I0\,|\,\rho(\mathbf{r}_N)\,|\,I'0\rangle\times\int_0^\infty dr\,r_>^{-1}[F_{n\kappa}^2(r)+G_{n\kappa}^2(r)]\,. \tag{67}$$

The second integral is just the muon-generated monopole potential, parametrized by Ford and Wills (1969) in the form $C+Br_N^k$ (see Sec. II.E). The constant term does not contribute because of the orthogonality of the nuclear wave functions, so the energy shift becomes

$$\Delta E_{n\xi}=(Z\alpha)^2B^2\sum_{I'\neq I}[E_{N,I}-E_{N,I'}]^{-1}\times|\langle I0|\int d^3r_N\,r_N^k\rho(\mathbf{r}_N)\,|\,I'0\rangle\,|^2\,. \tag{68}$$

This is a sum over only the nuclear excitations, and in principle can be evaluated in closed form in terms of ground-state expectation values of the operator r'^k. This is, unfortunately, difficult to do reliably. In his analysis, Chen (1970a) replaced a corresponding energy denominator by an average value and removed it from the sum. The result in that case is

$$\Delta E_{n\zeta} \simeq (Z\alpha)^2 B^2 \langle E_{N,I} - E_{N,I'} \rangle^{-1} \times \langle I0 | \int d^3r_N \, d^3r'_N r_N^k r_N'^k \rho(\mathbf{r}_N, \mathbf{r}'_N) | I0 \rangle \ . \quad (69)$$

To evaluate the integral, one needs to know two-body correlations in the ground-state nuclear wave function. At the present time, no microscopic nuclear theory can produce such quantities reliably.

A sum which is simpler to evaluate (in the absence of momentum and isospin-dependent nuclear forces) is energy weighted,

$$S = \sum_{I' \neq I} [E_{N,I'} - E_{N,I}] \, | \langle I0 | \int d^3r_N \, r_N^k \rho(\mathbf{r}_N) | I'0 \rangle |^2 = \frac{k^2}{2M_p} \langle I0 | \int d^3r_N \, r_N^{2k-2} \rho(\mathbf{r}_N) | I0 \rangle \ . \quad (70)$$

With the same average replacement of the excitation energies, the polarization shift is

$$\Delta E_{n\zeta} = (Z\alpha)^2 B^2 \langle E_{N,I'} - E_{N,I} \rangle^{-2} S \ . \quad (71)$$

Since S depends only upon the ground-state expectation value of a one-body operator, it can be evaluated much more reliably. The price paid is a further departure from the energy weighting of interest. This departure would be unimportant if the nuclear excitations for a given multipole were strongly peaked about one particular energy. However, this is often not the case.

The above discussion illustrates the connection between nuclear-polarization energy shifts and sum rules. Things are more complicated in general because the excited muon states must be taken into account, introducing a complicated interdependence of solutions to Eqs. (59)–(62) with explicit nuclear models for transition energies, strengths, and form factors. Because of these difficulties, Ericson and Hüfner (1972) restricted consideration to high-lying muon (more generally, exotic particle) states and showed that the nuclear polarization energy shift of a level nl due to excitations of multipolarity $L \neq 0$ is

$$\Delta E_{nlL} = -\frac{\alpha}{2} \alpha_{\rm pol}(L) \langle r^{-2L-2} \rangle_{nl} \ , \quad (72)$$

where $\alpha_{\rm pol}(L)$ is the nuclear polarizability

$$\alpha_{\rm pol}(L) = \frac{8\pi\alpha}{(2L+1)^2} \sum_f (E_{N,f} - E_{N,0})^{-1} B(EL;0 \to f) = \frac{L}{L+1} \left[\frac{(2L-1)!!}{\pi} \right]^2 \int_0^\infty dE_N \, E_N^{-2L} \sigma(L, E_N) \ . \quad (73)$$

The second line is an alternate form written in terms of the photoabsorption cross section

$$\sigma(L, E_N) = (2\pi)^3 \alpha \frac{(L+1) E_N^{2L-1}}{L[(2L+1)!!]^2} B(EL, E_N) \frac{df}{dE_N} \ . \quad (74)$$

Equation (72) was obtained from classical arguments for $L = 1$ and from nonrelativistic quantum arguments for $L \geq 1$ using closure over the intermediate muon states, neglecting muonic excitation energies. It assumes the asymptotic form (63) for the transition potential (60) and this is valid only for states with $l \geq L > 0$, so that the expectation value in (72) does not diverge as $R_N \to 0$. The principal physical restriction is that muon excitation energies be small compared to nuclear excitation energies. This condition is usually fulfilled for states with $l > L$, but it can also hold in other cases [for example, $l = L = 1$ in light muonic atoms ($Z \lesssim 20$), where $L = 1$ is the dominant contribution]. In such cases the muon orbit lies almost entirely outside the nucleus. For most states of interest for tests of QED (see Sects. III.D.1 and III.D.2) this condition is fulfilled, and (70)–(72) can be used to give a reliable estimate of the nuclear-polarization correction. Similar formulas may be derived for $L = 0$ and $L > l$, but these are quite inaccurate due to the short range of the transition potential compared to the variation in the muon wave functions. This situation introduces large errors in the closure and nonrelativistic approximations.

If the nuclear excitations for a given multipolarity L and isospin projection τ are concentrated about some average resonant energy $\langle E_N(L\tau) \rangle$, one may make use of the energy-weighted sum rules

$$S_1(L,\tau) = \sum_f (E_{N,f} - E_{N,0}) B(EL\tau;0 \to f) = \frac{L(2L+1)^2 Z}{8\pi M_p} \langle r_N^{2L-2} \rangle \left[\frac{Z}{A}(1-\tau) + \frac{N}{A}\tau \right] \quad (75)$$

to obtain the explicit formula

$$\Delta E_{nl,L} \simeq -\frac{6\alpha(Z\alpha)^4}{n^3} \frac{m}{M_p} \frac{1}{R_N} \left[\frac{Z}{A} \left[\frac{m}{\langle E_N(L0) \rangle} \right]^2 + \frac{N}{A} \left[\frac{m}{\langle E_N(L1) \rangle} \right]^2 \right] \times \frac{(n+l)!}{n(n-l-1)![(2l+1)!]^2} \frac{L(2l-2L)!}{2L+1} \left[\frac{2Z\alpha m R_N}{n} \right]^{2L-1} \ . \quad (76)$$

We have used nonrelativistic point-nucleus muon wave functions and kept only the leading term in an expansion in powers of the nuclear radius $R_N = (5\langle r_N^2 \rangle/3)^{1/2}$, where we have concentrated the transition charge density. This is a

minor improvement over Eq. (72), which concentrates the transition charge density at the origin; however, the restriction $l > L > 0$ is still assumed in carrying out the integrals. This expansion is accurate for values of the parameter $(2Z\alpha m R_N/n) \lesssim 1$. In general, $L=1$ excitations dominate for cases in which Eq. (76) is valid, in which case it takes the especially simple form

$$\Delta E_{nl,1} \simeq -\frac{4m\alpha(Z\alpha)^5}{n^4}\frac{m}{M_p}\frac{N}{A}\left[\frac{m}{\langle E_N(11)\rangle}\right]^2 \frac{(n+l)!(2l-2)!}{n(n-l-1)![(2l+1)!]^2} . \tag{77}$$

These formulas can be quite accurate. For example, (77) gives -4.9 eV for the $4f$ states in lead, whereas a numerical calculation gives -5.0 and -4.6 eV for the $4f_{5/2}$ and $4f_{7/2}$ states, respectively. They can also be applied to other exotic atoms for states in which the strong interaction can be neglected.

A further attempt at a general formulation was made by Rinker and Speth (1978b). Rather than avoid completely the details of nuclear excitations, they constructed a semiempirical nuclear model intended to approximate the energies and form factors of giant multipole resonances throughout the periodic table, as well as to satisfy identically the energy-weighted sum rules (75) and the corresponding sum for $L=0$

$$S_1(0\tau) = \sum_f (E_{N,f} - E_{N,0}) \,|\, \langle 0 | \int d^3 r_N \, r_N^2 \rho_N(\mathbf{r}_N) \,|\, f\rangle \,|^2$$
$$= \frac{2Z}{M_p}\langle r_N^2\rangle \left[\frac{Z}{A}(1-\tau)+\frac{N}{A}\tau\right] . \tag{78}$$

These sums wee concentrated in a single resonant state for each $(L\tau)$, with excitation energies

$$\langle E_N(L\tau)\rangle = \begin{cases} [100(1-\tau)+200\tau](1-A^{-1/3})A^{-1/3}, & L=0 \\ 95(1-A^{-1/3})A^{-1/3}, & L=1 \\ [75(1-\tau)+160\tau](1-A^{-1/3})A^{-1/3}, & L\geq 2 \end{cases} \tag{79}$$

Energy shifts were obtained by solving Eqs. (59)–(62) numerically, using simple analytic forms for the nuclear form factors. Thus important errors in the closure and nonrelativistic approximations were eliminated. These shifts are plotted in Fig. 4. Values for states not shown may be obtained by extrapolating the results of Fig. 4, noting that the energy shift varies with n for constant l mainly through the overall normalization of the muon wave functions, i.e., n^{-2l-3}.

The values in Fig. 4 agree essentially by construction with more detailed calculations for ^{208}Pb and are thus probably reliable for other heavy nuclei as well, so long as deformation (hfs) effects are either negligible or otherwise accounted for. For light nuclei, however, additional caution must be exercised. Here, the energy-weighted sums (75) are exceeded experimentally by as much as a factor of two (Ahrens *et al.*, 1975, 1976). Although the model depends upon these sums, this fact does not imply that the results in Fig. 4 are in error by the same factor. More to the point is the ratio of the model polarizability for the dominant multipole $L=1,\tau=1$

$$\alpha_{\rm pol}^{(\rm model)}(1) = \tfrac{1}{9} 8\pi\alpha S_1(11)/\langle E_N(11)\rangle^2 \tag{80}$$

to the measured value of the polarizability (73). This ratio is 1.0 ± 0.2 for all nuclei measured by Ahrens *et al.* (1975,1976) except for ^{40}Ca, where it is 0.7. The reason that the energy-weighted sums differ by larger factors is that the excess transition strength comes at high excitation energies, where they are exaggerated in Eq. (75) relative to the polarizability sum (73).

b. Helium

The first nuclear-polarization calculation for muonic helium was carried out by Joachain (1961) for the $2s_{1/2}$ state using the nonrelativistic closure approximation for the sum over excited muon states, as later exploited by Ericson and Hüfner (1972). This calculation used experi-

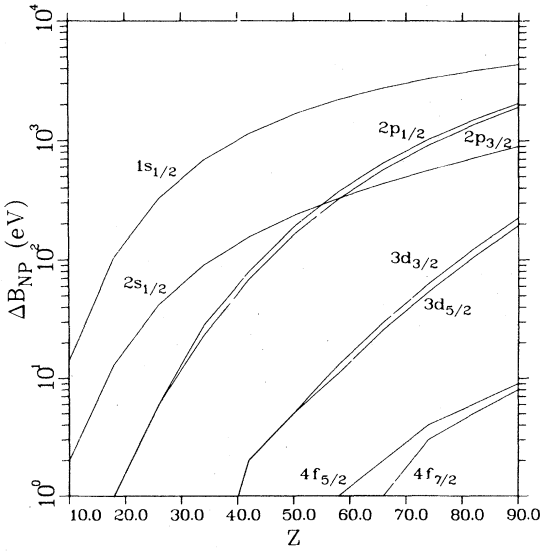

FIG. 4. Nuclear-polarization binding energy shifts (Rinker and Speth, 1978b).

mental information to provide bounds on the nuclear matrix elements. For the ns state and $L\neq 0$, we may write in analogy to Eq. (72)

$$\Delta E_{ns,L} = -\frac{\alpha}{2}\left[\frac{2Z\alpha m R_N}{n}\right]^3 \frac{(2L+1)}{(2L+3)(2L-1)} \times R_N^{-2-2L}\alpha_{\rm pol}(L) \ . \quad (81)$$

We have approximated the muon wave function by its nonrelativistic point-nucleus value at the origin and concentrated the transition charge density in Eq. (60) at the nuclear surface with radius R_N.

The dominant multipole for very light nuclei is $L=1$. Inserting the measured value for ^{4}He $\alpha_{\rm pol}\simeq 0.073$ fm^3 into Eq. (81) gives 10 meV for the $2s_{1/2}$ state. As discussed following Eq. (74), however, this procedure is not really justified for $l=0$. The energy shift diverges as R_N^{1-2L} as $R_N\to 0$ and so is quite sensitive to this parameter. In addition, the L-dependent terms in Eqs. (73) and (74) show an enhancement of higher multipoles, so that the dipole approximation is not necessarily sufficient even if it dominates the photoabsorption cross section. Finally, the closure approximation itself greatly limits the accuracy of such a calculation. Nonrelativistically, this approximation amounts to representing the true solutions of Eq. (59) by

$$g_{\xi'}(r) = -V^{(L)}_{\xi\xi'}(r)G_{n\kappa}(r)/(E_{N,\xi'}-E_{N,\xi}) \ ,$$
$$f_{\xi'}(r) = 0 \ . \quad (82)$$

The consequences of this are shown in Fig. 5 for a typical perturbation with $L=1$. It is clear that the result is very poor in just the region where the integrand in (62) is large.

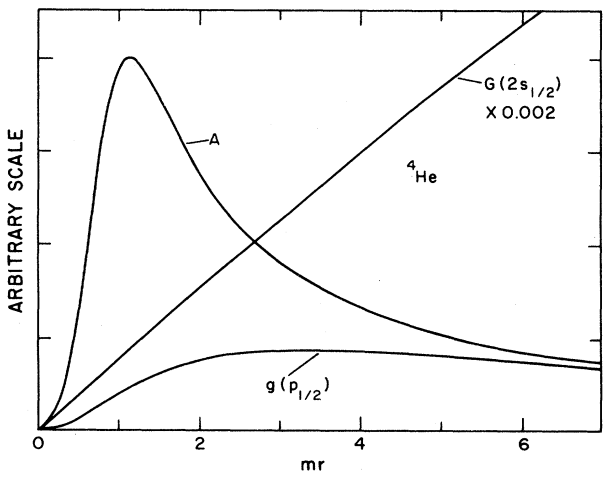

FIG. 5. Wave-function perturbations due to nuclear polarization for ^{4}He (Rinker, 1976). G is the unperturbed $2s_{1/2}$ wave function (scaled smaller as shown), g is a typical first-order $p_{1/2}$ perturbation, and A is the perturbation calculated in the closure approximation (82).

An improved analysis for $l=0$ along the same lines, but which avoids explicit use of the closure approximation and is convergent as $R_N\to 0$, has been given by Ericson (1981).

More detailed calculations have since been carried out. Bernabeau and Jarlskog (1974) used a covariant formulation with the full electromagnetic interaction constrained, where possible, by measured structure factors. The muon states were also treated properly, except that the spatial variation of the initial muon wave function was neglected. The result was $\Delta E=-3.1$ meV for the $2s_{1/2}$ state in ^{4}He. Henley *et al.* (1976) computed and corrected the closure approximation rather than the main result directly. Such an approach would be particularly useful if corrections to the closure approximation were small; however, that turns out not to be the case here, as is seen from Fig. 5. As a result, the corrections were difficult to calculate accurately. In addition, the polarizability sum σ_{-2} for the model used was too large by a substantial margin, affecting the results adversely (Bernabeau and Jarlskog, 1976; Rinker, 1976). Rinker (1976) followed the methods outlined in Sec. II.G.2, using transition potentials normalized by the measured photoabsorption cross sections $\sigma(L,E)$ and simple semiempirical radial form factors. Results for the $2s$ state were -4.9 meV for ^{3}He and -3.1 meV for ^{4}He, of which 60% and 80%, respectively, arose from dipole excitations. These results were in agreement with Bernabeau and Jarlskog. In both cases, uncertainties were estimated to be 10–20%. The entire subject was then re-examined by Friar (1977) with general agreement as to the validity of the previously made approximations.

c. Lead

The other classic simple system which has been the subject of much study is muonic ^{208}Pb, particularly the low-lying states. Because of its size and high atomic number, nuclear-polarization effects here take on an entirely different character than in helium. The penetration of the muon wave function into the nuclear interior substantially increases the importance of monopole excitations and invalidates the approximations which have proved useful for very light nuclei or for very high-lying states.

Early estimates were made by Cooper and Henley (1953), Lakin and Kohn (1954), Nuding (1957), Greiner (1961), and Greiner and Marschall (1962). All of these calculations depended upon closure or upon explicit construction of the sums (55) or (56) rather than solution of Eq. (57), thereby introducing substantial errors in the treatment of the muon perturbations. The first calculations which avoided this problem were carried out by Chen (1970a) and by Skardhamar (1970), both of whom solved nonrelativistic versions of Eq. (59) and thereby treated the sum over muon excitations with reasonable accuracy. Chen actually made two separate calculations. In one, he used the random-phase approximation to compute the excited nuclear state energies and transition po-

tentials. In the other, he used closure over the excited nuclear states and evaluated the resulting non-energy-weighted sums using shell-model wave functions in a harmonic oscillator basis. Skardhamar constructed collective, phenomenological excited states with macroscopic transition form factors.

Attention focused upon the correction for the $1s$ state, as this was the largest, and it was hoped that by fitting nuclear charge distribution parameters to measured higher-lying transitions, one could in some sense measure the $1s$ polarization energy shift (Anderson *et al.*, 1969). It was almost immediately found that the data suggested the calculated shifts were too small by as much as several keV. This seemed remarkable in view of the confidence and agreement with which the theoretical results were reported. Chen quoted $\Delta E_{1s} = -6.0 \pm 0.6$ keV, while Skardhamar gave -6.8 ± 2.0 keV. Nevertheless, the disagreement persisted in further measurements and analyses (Jenkins *et al.*, 1971; see also Martin *et al.*, 1973; Ford and Rinker, 1973; Kessler *et al.*, 1975). An additional attempt was made to calculate the monopole contribution using nuclear Hartree-Fock wave functions, both with and without the muon present (Galonska *et al.*, 1973; Faessler *et al.*, 1975). Although conceptually straightforward, these calculations were technically difficult and fundamentally incomplete, including only rearrangement rather than true polarization effects (Rinker and Speth, 1978a). Rearrangement effects are characteristic of Hartree–Fock, which includes only one-particle–one-hole excitations. Not included are those terms of order α in the polarization sum in which both muon and nucleus are excited. Nevertheless, these calculations provided a useful independent verification that the results of Chen and Skardhamar were not wrong by large amounts. In the meantime, peculiarities in the $p_{3/2}-p_{1/2}$ splittings were noticed in all lead isotopes (Ford and Rinker, 1973, 1974). Similar difficulties with the $3d_{5/2}-3d_{3/2}$ splittings (Anderson *et al.*, 1969) were explained by Shakin and Weiss (1973) as resulting from mixing with the strong 3^- state at 2.6 MeV. This state was later observed and its isomer shift measured in the muonic spectrum of ^{208}Pb by Shera *et al.* (1977), with good agreement with the predicted theoretical intensity (Rinker and Speth, 1978a). Further work by the same group (Hoehn *et al.*, 1980) produced similar results for the 2^+ state in ^{204}Pb. It was conjectured (Ford and Rinker, 1974) and later emphasized (Rinker and Speth, 1978a) that similar mixing with 1^- states could alter the $2p$ splitting to the point of invalidating the earlier empirical conclusions about the size of the $1s$ correction (see also Abela *et al.*, 1980). (The $2p_{3/2}$-$2p_{1/2}$ and $2p-1s$ energy differences measure nearly the same radial moment of the nuclear charge distribution and thus provide a strong internal consistency check.) It was shown that the data could be fit at least as well by postulating a shift in the $2p$ splitting as by a shift in the $1s$ binding energy. The claims by Rinker and Speth were coupled with a new calculation of the corrections, using the formalism presented here and highly detailed RPA calculations adjusted to reproduce a substantial body of experimental excitation data. This new calculation, which was essentially similar to Chen's but used relativistic muon kinematics and a greatly refined nuclear model, gave an even smaller value for the $1s$ shift (-3.9 keV). It should perhaps be noted that the earlier calculations were less reliable insofar as corrections to the $2p$ splitting were concerned because important relativistic effects on the muon wave functions were neglected. A subsequent simultaneous fit to both muonic-atom and electron scattering data (Yamazaki *et al.*, 1979) supported the idea that it was the calculated $2p$ splitting which was at fault rather than the $1s$ energy. However, no appropriate 1^- states have been found, and the discrepancy remains unresolved.

d. Deformed nuclei

From the earliest days, it was recognized that substantial mixing could occur among the muon levels and those of strongly deformed rotational nuclei. The first calculations of these effects were made by Wilets (1954) and by Jacobsohn (1954), in which the nuclear ground-state rotational band was coupled to the muon $2p$ levels and diagonalized [see the discussion immediately after Eq. (50)]. This procedure was used for a number of years to analyze the dynamic hyperfine spectra of such muonic atoms. However, fitted quadrupole moments tended to come out too large by a few percent as compared to those obtained through other experiments, and other irregularities in the spectra were observed. With this as motivation, Chen (1970b) applied the analysis described in Eqs. (53)–(57). He found that his numerical results could roughly be summarized by a renormalization of the intrinsic quadrupole moment of such a magnitude as to bring the various experiments into agreement. This work was later generalized by Vogel and Akylas (1977), and numerous renormalization coefficients were computed. Rotational model energy spectra and transition charge densities, however, remained firmly embedded in the analyses.

Additional contributions due to nuclear states outside the rotational band have been considered by other authors. Martorell and Scheck (1976) used sum rules to estimate the effects of dipole polarization. Measurements and more sophisticated calculations have been carried out by Yamazaki *et al.* (1978) for isotopes of samarium using the general computer code RURP (Rinker, 1979), which allows states of arbitrary multipolarity, energy, transition strength, and multipole moment to be used (see Secs. G.1–3), thus removing the rotational model restrictions. (See also Powers *et al.*, 1979; Missimer and Simons, 1979; Powers, *et al.*, 1977).

e. Transitional nuclei

Between the region of strongly deformed rotating nuclei ($A \simeq 150-170$) and the heavy spherical nuclei

($A \simeq 208$) lies a transition region in which nuclei have peculiar shapes and are capable of changing from prolate to oblate with little provocation. An analysis in which the simple rotational model is built in is therefore inappropriate, as is an approach based upon a spherical nucleus approximation. For such nuclei it is necessary to provide the nuclear spectrum as known, preferably, from experiment. Calculations and experiments have been carried out both with and without the corrections of Eq. (54). The primary limitation has been that independent experimental information concerning the spectra is incomplete, while theoretical predictions are inaccurate or nonexistent. The result is that, in general, too many model assumptions are needed to analyze the muonic atom data by itself, although in certain specific cases the requirements of internal consistency have pointed out some real discrepancies. A considerable amount of work is being done at the present time (see, for example, Hoehn *et al.*, 1977; Hoehn *et al.*, 1981), but further work is needed, particularly in independent (e.g., inelastic electron scattering) measurements of nuclear spectra and excitation strengths.

H. Translational nuclear motion

1. Nonrelativistic corrections

The nonrelativistic two-body problem can always be written in terms of relative and center-of-mass coordinates such that, in the absence of external fields, one of the objects is regarded as fixed in space (infinitely massive), while the other acquires a reduced mass

$$m_r = mM_N/(m+M_N) . \tag{83}$$

For two point particles, the binding energies are simply proportional to the mass of the moving particle, so that the effect of a less than infinitely massive nucleus is simply to scale the muon binding energies by a factor $M_N/(m+M_N)$. If either particle has finite size, however, a rescaling of the lengths involved must be included in addition. (It should perhaps be noted that both of these effects are included automatically when the Schrödinger equation is solved numerically using the muon-reduced mass.) To see how this length rescaling arises, consider the radial Schrödinger equation for a particle of reduced mass m_r, written in terms of the dimensionless variable $x = m_r r$,

$$-\frac{1}{2}\frac{d^2}{dx^2}\phi(x)+\left[v(x)+\frac{l(l+1)}{2x^2}-\varepsilon\right]\phi(x)=0 . \tag{84}$$

In the above, $\phi(x)$ is the scaled wave function, and $v(x)$ and ε are the scaled potential and energy $V(x/m_r)/m_r$ and E/m_r, respectively. The eigenvalues of (84) are pure numbers, in terms of which dimensioned eigenvalues for any given problem are obviously $E = m_r\varepsilon$. However, suppose $V(r)$ contains a length scale c, which must necessarily enter in a dimensionless combination with r, i.e., r/c. Then the dimensionless eigenvalues will depend in general upon the scaled parameter $m_r c$, so that $\varepsilon = \varepsilon(m_r c)$ and $E = m_r \varepsilon(m_r c)$. As an example, consider the shift in energy of a given transition between two isotopes of the same element, keeping the nuclear radius fixed. The change in reduced mass is

$$\Delta m_r \simeq \frac{m^2}{(m+M_N)^2}\Delta M_N , \tag{85}$$

so that the change in transition energy is

$$\Delta E = \Delta m_r \frac{dE}{dm_r} = \Delta m_r \left[\varepsilon + m_r c \frac{d\varepsilon}{d(m_r c)}\right] . \tag{86}$$

Since

$$\frac{dE}{dc} = m_r^2 \frac{d\varepsilon}{d(m_r c)} , \tag{87}$$

we obtain

$$\Delta E = \frac{\Delta m_r}{m_r}\left[E + c\frac{dE}{dc}\right] . \tag{88}$$

Note that E is negative and dE/dc is positive in realistic cases, so that the finite-size effect tends to reduce the isotope mass shift from its point-nucleus value.

2. Relativistic corrections

Relativistically, the center-of-mass motion cannot be factored out rigorously due to the difference in time scale associated with two particles moving at different, nonzero velocities (see, e.g., Breit, 1937). For example, one might imagine a Dirac Hamiltonian for two interacting fermions as

$$H = \boldsymbol{\alpha}_1\cdot\mathbf{p}_1 + \beta_1 m_1 + \boldsymbol{\alpha}_2\cdot\mathbf{p}_2 + \beta_2 m_2 + V(\mathbf{r}_1,\mathbf{r}_2) . \tag{89}$$

In the Dirac theory, however, $H\psi = i\partial\psi/\partial t$, and it is not clear what to use for t. The correct wave equation for the problem is the much more complicated Bethe-Salpeter equation, which is notoriously difficult to solve in practice. Since, for our problem, the nuclear mass is much greater than the muon mass, it is possible to factor out the nuclear degrees of freedom systematically from the wave function and define an approximate Dirac equation for the muon, evaluating the mass corrections in powers of m/M_N. This we shall do in the scattering approximation rather than through the Bethe-Salpeter equation, following the approach of Grotch and Yennie (1969) and the analyses of Friar and Negele (1973b) and Barrett *et al.* (1973). Using a different approach, Gross (1969) has obtained essentially the same result to order m/M_N. See also Fricke (1973).

We first write down the Feynman amplitude for lowest-order fermion-boson scattering (see Fig. 6 for kinematical definitions)

$$S_{fi} = -Ze^2\bar{u}(p_3)\gamma^\mu u(p_1)\frac{F(q^2)}{q_0^2-\mathbf{q}^2+i\varepsilon}\frac{(p_4+p_2)_\mu}{(4E_2E_4)^{1/2}} , \tag{90}$$

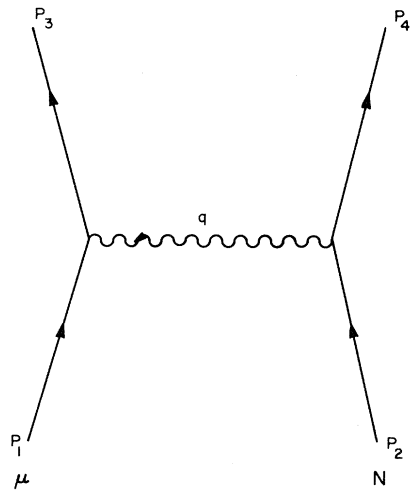

FIG. 6. Kinematics for the recoil correction.

where $q=p_2-p_4=p_3-p_1$ is the momentum transferred to the muon and $F(q^2)$ is the nuclear form factor. The electromagnetic current density of the nucleus is normalized such that

$$\langle p_4 \mid j_\mu \mid p_2 \rangle = \frac{-Ze}{(4E_2E_4)^{1/2}} F(q^2)(p_4+p_2)_\mu \ . \tag{91}$$

In more detail, Eq. (90) is

$$S_{fi} = \frac{-Ze^2}{(4E_2E_4)^{1/2}} \frac{F(q^2)}{q^2} \bar{u}(p_3) \times [\gamma_0(E_2+E_4)-\boldsymbol{\gamma}\cdot(\mathbf{p}_2+\mathbf{p}_4)]u(p_1) \ . \tag{92}$$

If we regard the nucleus as a slowly moving object, we have, to a good approximation,

$$E_2 \simeq M_N + p_2^2/2M_N$$
$$E_4 \simeq M_N + p_4^2/2M_N \ . \tag{93}$$

Reverting to the notation $\boldsymbol{\gamma}=\gamma_0\boldsymbol{\alpha}$, using $u^+(p)=\bar{u}(p)\gamma_0$, and evaluating Eq. (92) to order $1/M_N$ in the CM system ($\mathbf{p}_2=-\mathbf{p}_1$, $\mathbf{p}_4=-\mathbf{p}_3$), we have

$$S_{fi} = -u^+(p_3)\frac{Ze^2}{q^2}F(q^2)\left[1+\frac{\boldsymbol{\alpha}\cdot(\mathbf{p}_3+\mathbf{p}_1)}{2M_N}\right]u(p_1) \ . \tag{94}$$

This is of the form $u^+(p_3)V_{\text{eff}}u(p_1)$. As $M_N\to\infty$, $V_{\text{eff}}\to -Ze^2F(q^2)/q^2$, which is a static potential if written in the Coulomb gauge $q^\mu=(0,\mathbf{q})$. We are motivated to use the Coulomb gauge because

$$\frac{1}{q^2}=\frac{1}{q_0^2-\mathbf{q}^2}\simeq\frac{-1}{\mathbf{q}^2}\left[1+\frac{q_0^2}{\mathbf{q}^2}+\cdots\right], \tag{95}$$

and $q_0\to 0$ as $M_N\to\infty$. Adopting this gauge, we note the kinematical relations

$$\mathbf{p}_3=\mathbf{p}_1+\mathbf{q}, \quad E_3=E_1$$
$$E_3^2=\mathbf{p}_3^2+m^2=E_1^2=\mathbf{p}_1^2+m^2 \ , \tag{96}$$

which give

$$\mathbf{p}_3^2-\mathbf{p}_1^2=\mathbf{q}\cdot(\mathbf{p}_3+\mathbf{p}_1)=0 \ . \tag{97}$$

Thus any term proportional to $\mathbf{q}\cdot(\mathbf{p}_1+\mathbf{p}_3)$ may be added to V_{eff} without changing the first-order scattering amplitude. In particular, we can add inside the brackets of Eq. (94) the term

$$-\frac{\boldsymbol{\alpha}\cdot\mathbf{q}}{\mathbf{q}^2}\frac{\mathbf{q}\cdot(\mathbf{p}_1+\mathbf{p}_3)}{2M_N} \ . \tag{98}$$

This term will be helpful later on, as it makes V_{eff} explicitly dependent only upon the transverse muon current. Thus we have for $V_{\text{eff}}(q)$

$$V_{\text{eff}}(q) = -\frac{Ze^2F(\mathbf{q}^2)}{\mathbf{q}^2}\left[1+\left[\alpha-\frac{\boldsymbol{\alpha}\cdot\mathbf{q}}{\mathbf{q}^2}\right]\cdot\frac{(\mathbf{p}_1+\mathbf{p}_3)}{2M_N}\right] . \tag{99}$$

It should be emphasized that the additional term proportional to $\mathbf{q}\cdot(\mathbf{p}_1+\mathbf{p}_3)$ does not vanish off shell, when $E_1\neq E_3$ or $E^2\neq\mathbf{p}^2+m^2$. Thus iteration of $V_{\text{eff}}(q)$ does not give the correct second-order scattering. Furthermore, it leads to differences when evaluated in bound-state perturbation theory. This illustrates a basic ambiguity of the scattering approximation. One may make certain definitions in a given order (in this case to eliminate unwanted terms), but these definitions must be kept track of and evaluated in higher order if necessary. Accounting for these makes the mass corrections some of the most confusing corrections to evaluate. Nevertheless, it can be shown (Grotch and Yennie, 1969) that Eq. (99) gives the total mass correction to order $\mathbf{p}/M_N$. For further discussion of this point, see the review of Erickson (1977).

We now need to evaluate Eq. (99) for a bound state in configuration space. The first manipulation is to move all momenta $\mathbf{p}_1$ to the right and all $\mathbf{p}_3$ to the left, so that when evaluated as $u^+(p_3)V_{\text{eff}}(q)u(p_1)$, they can be replaced by the operator $\mathbf{p}$. Some algebra gives

$$V_{\text{eff}}(q) = -Ze^2\left\{\frac{F(\mathbf{q}^2)}{\mathbf{q}^2}+\left\{\frac{F(\mathbf{q}^2)}{\mathbf{q}^2},\frac{\boldsymbol{\alpha}\cdot\mathbf{p}}{2M_N}\right\} - \frac{1}{2M_N}\left[\boldsymbol{\alpha}\cdot\mathbf{p},\left[\mathbf{p}^2,\frac{F(\mathbf{q}^2)}{\mathbf{q}^4}\right]\right]\right\} . \tag{100}$$

The first term is the static Coulomb potential, and the second comes from the original term $\boldsymbol{\alpha}\cdot(\mathbf{p}_1+\mathbf{p}_3)$. The third arises from the transverse current projection.

We Fourier transform $\mathbf{q}$ to configuration space and retain $\mathbf{p}$, which can be evaluated between muon spinors. This gives

$$V_{\rm eff}= V(r)+\frac{1}{2M_N}\{V(r),\boldsymbol{\alpha}\cdot\mathbf{p}\}-\frac{1}{2M_N}[\boldsymbol{\alpha}\cdot\mathbf{p},[\mathbf{p}^2,W(r)]]$$
$$=V(r)+\frac{1}{M_N}[E_0V(r)-\beta mV(r)$$
$$-V^2(r)+W'(r)V'(r)]\,, \tag{101}$$

where we have anticipated expectation values and written

$$H_0\psi=E_0\psi,\quad H_0=\boldsymbol{\alpha}\cdot\mathbf{p}+\beta m+V(r)\,, \tag{102}$$

so that

$$\boldsymbol{\alpha}\cdot\mathbf{p}\psi=[E_0-\beta m-V(r)]\psi\,, \tag{103}$$

and where

$$V(r)=-Z\alpha\int d^3r_N\,\frac{\rho(r_N)}{|\mathbf{r}-\mathbf{r}_N|} \tag{104}$$

and

$$W(r)=\frac{Z\alpha}{2}\int d^3r_N\,\rho(r_N)\,|\mathbf{r}-\mathbf{r}_N|\,. \tag{105}$$

Putting $V_{\rm eff}$ into a two-body Hamiltonian

$$H=\boldsymbol{\alpha}\cdot\mathbf{p}+\beta m+\mathbf{p}^2/2M_N+V_{\rm eff}\,, \tag{106}$$

in which we have treated the nucleus nonrelativistically and used $\mathbf{p}_N=-\mathbf{p}$ because we are in the center-of-mass frame, we get

$$H=H_0+\frac{1}{2M_N}(E_0^2-m^2)-\frac{m}{M_N}\beta V(r)+\frac{1}{2M_N}h(r)\,, \tag{107}$$

where

$$h(r)=2W'(r)V'(r)-V^2(r)\,, \tag{108}$$

and we have used $\langle p^2\rangle=\langle[E_0-V(r)]^2-m^2\rangle$. The terms in M_N^{-1} will be treated as first-order perturbations.

We first note that the last term is diagonal with respect to the muon spinors. It may be written in the form (Friar and Negele, 1973b)

$$\frac{1}{2M_N}h(r)=-\frac{1}{2M_N}\left[P_1^2(r)+\frac{4}{3r}P_1(r)Q_2(r)+\frac{1}{3r^4}Q_2(r)Q_4(r)\right], \tag{109}$$

where

$$Q_n(r)=4\pi Z\alpha\int_0^r dr_N\,r_N^n\rho(r_N)\,,$$
$$P_n(r)=4\pi Z\alpha\int_r^\infty dr_N\,r_N^n\rho(r_N)\,. \tag{110}$$

We see from Eqs. (109) and (110) that $h(r)$ has a long-range part, behaving as $Z^2\alpha^2\langle r_N^2\rangle/3r^4$ outside the nucleus. This is evidently a retardation effect, as it depends upon the nuclear size. The following identities

$$P_1(r)=-rV'(r)-V(r),\quad Q_2(r)=r^2V'(r)\,,$$
$$Q_4(r)=r^4V'(r)-2r^3V(r)+6\int_0^r dr_N\,r_N^2V(r_N) \tag{111}$$

may be used to rewrite $h(r)$ in the more compact form

$$h(r)=-V^2(r)-\frac{2}{r^2}V'(r)\int_0^r dr_N\,r_N^2V(r_N)\,. \tag{112}$$

Next, we show that using the reduced mass $m_r=mM_N/(m+M_N)\simeq m(1-m/M_N)$ cancels most of the remaining perturbation. Define

$$H_r\psi=[\boldsymbol{\alpha}\cdot\mathbf{p}+\beta m_r+V(r)]\psi=E_r\psi\,, \tag{113}$$

so that $E_r-E_0=\beta(m_r-m)\simeq-\langle\beta\rangle m^2/M_N$. Evaluating the total energy given by Eq. (107) then yields

$$E=E_r+\frac{m^2}{M_N}\langle\beta\rangle+\frac{1}{2M_N}(E_0^2-m^2)$$
$$-\frac{m}{M_N}\langle\beta V(r)\rangle+\frac{1}{2M_N}\langle h(r)\rangle\,. \tag{114}$$

The third and fourth terms may be manipulated to give

$$-\frac{m^2}{M_N}\langle\beta\rangle+\frac{m^2}{M_N}-\frac{B_0^2}{2M_N}+\frac{B_0}{M_N}\langle P_1(r)\rangle\,, \tag{115}$$

where $B_0=m-E_0$, and we have used the identities $\langle\beta\rangle E_0=m+\langle\beta V(r)\rangle$ and $m\langle\beta\rangle=m-B_0+\langle P_1(r)\rangle$. The first term in (115) cancels that arising from use of the reduced mass in H_r. The second is state independent and may thus be discarded, since we are interested only in computing transition energies. The final result for the energy shift *beyond* that due to using the reduced mass is thus

$$\Delta E=E-E_r=-\frac{B_0^2}{2M_N}+\frac{1}{2M_N}\langle h(r)+2B_0P_1(r)\rangle\,. \tag{116}$$

The bracketed terms vanish for a point nucleus. For a finite nucleus, they behave as $-(Z\alpha)^2\langle r_N^2\rangle/6M_Nr^4$ outside the nuclear charge distribution and thus dominate the correction to this order for tests of QED in very light muonic atoms.

The origin of the term $-B_0^2/2M_N$ is essentially kinematic. It may be derived alternatively using the relativistic generalization of the reduced mass (Todorov, 1973; Pilkuhn, 1979).

The relativistic recoil correction derived above still does not contain all computationally significant terms. Salpeter (1952) originally derived additional corrections by using the Bethe-Salpeter equation; the presence of the additional terms is associated with the use of hole theory rather than single-particle theory. The contributions are of three types: corrections to the exchange of two Coulomb photons, recoil with transfer of one transverse photon, and processes with two transverse photons. The full calculation has been carried out only for point nuclei and, for s states, only for $n=2$. For details see Fulton and Martin (1954) or Grotch and Yennie (1969). The result is

$$\Delta E=\frac{4(Z\alpha)^5m}{3\pi n^3}\frac{m}{M_N}\left[2\ln\frac{(Z\alpha)^2m}{2\Delta E_n}+\{\tfrac{1}{4}\ln(z\alpha)^{-2}-\tfrac{1}{12}-a_n\}\delta_{l0}-\frac{7}{4}\frac{(1-\delta_{l0})}{l(l+1)(2l+1)}\right], \tag{117}$$

with

$$a_n \simeq -\frac{7}{2}\left[\ln\frac{2}{n}+1+\sum_{i=1}^{n-1}\frac{1}{i}+\frac{1}{2n}\right] . \quad (118)$$

It is easily seen that ΔE is of order Zm/M_N times the self-energy correction (171). A calculation for the case of muonic atoms, including the effects of finite nuclear size, does not exist. The same difficulties that arise in the calculation of the self-energy correction (Sec. III.B) will play a role in the calculation of these recoil corrections.

I. Electron screening

Particularly in the case of heavy elements, not all of the atomic electrons are ejected by Auger transitions during the muonic cascade. In addition, unoccupied electron states can be refilled during the cascade. The remaining electrons interact with the muon and thus have an effect on the binding energy. In principle, this effect can be formulated in a manner entirely analogous to the muon-nucleus interaction. In practice, the static monopole effect is treated in the same way, but polarization effects are treated as rearrangement effects in the Hartree-Fock approximation. Justification for such a separation and treatment is similar to that for the nuclear polarization: polarization effects are small because the frequency of muon motion is substantially different from that of electron (nucleon) motion. In this case, however, it is the electrons which move much faster, rather than the muon. The limitation to rearrangement effects is probably less significant here than for the nuclear polarization due to the decreased importance of excitation of the relatively heavy muon.

The predominant effect is calculated using the additional static potential $V_e(r)$ generated by the average electron density $\rho_e(r_e)$. Traditionally, one regards the influence of the electrons as being smallest for the inner orbits (this is true in any case for transition energies), and one therefore subtracts the constant $V_e(0)$ from the effective screening potential. We then have

$$V_e(r)=\frac{4\pi\alpha}{r}\int_0^r dr_e\,\rho_e(r_e)(r_e^2-rr_e) , \quad (119)$$

where $\rho_e(r_e)$ is the spherically averaged electron density. It is normalized such that

$$4\pi\int_0^\infty dr_e r_e^2\rho_e(r_e)=\text{number of electrons} . \quad (120)$$

The electron density is usually calculated using a Hartree-Fock (Mann and Rinker, 1975; von Egidy and Desclaux, 1978) or Hartree-Fock-Slater approach (Vogel, 1973a). The electron screening correction is either calculated as a first-order perturbation or taken to be the difference in binding energies computed with and without the inclusion of $V_e(r)$. Since the muon is usually found much closer to the nucleus than to the electrons (see Fig. 1), one may assume, as a first approximation, that it screens one unit of the nuclear charge. The electronic orbits are then simply the states of a normal atom with atomic number $Z-1$. This approximation is thus known as the "Z-1 approximation."

A more sophisticated calculation which includes rearrangement effects (Vogel, 1973b; Fricke, 1969a; Fricke and Telegdi, 1975) treats the muon-electron system self-consistently [compare to Faessler *et al.* (1975)]. One uses a relativistic Hartree-Fock-Slater program and takes into account the interaction between the muon and the electrons when computing the electron density. In this case the electron density depends upon the muonic quantum numbers n, l, and j. These rearrangement effects were estimated by Vogel (1973b) and Fricke and Telegdi (1975). For states with $n \geq 8$ in heavy elements these effects are non-negligible. In the states of interest for tests of QED the screening correction is reduced slightly with respect to the Z-1 approximation.

A very simplified treatment (Tauscher *et al.*, 1978), which computes $\rho_e(r_e)$ using unperturbed relativistic wave functions for the electrons in Z-1 approximation for K electrons, Z-3 approximation for L electrons, and so on, gives a screening correction that, for the $5g$-$4f$ transitions in lead, and other transitions useful in QED tests, is nearly identical with the results of self-consistent calculations, provided similar assumptions about the electron populations are made. A polarization correction is estimated as in the work of Ericson and Hüfner (1972). This provides a crude estimate of rearrangement corrections (which of course are automatically included in a self-consistent calculation). One can expect that the simplified approach would break down for transitions involving higher principal quantum numbers.

An important source of uncertainty in the calculation of screening corrections is our lack of knowledge as to the number of electrons present during the muonic cascade. For heavy elements, such as lead, one finds from energy conservation (Fricke and Telegdi, 1975; Vogel *et al.*, 1977; Vogel, 1973a; see also Vogel, Winther, and Akylas, 1977) that at least 15 electrons must remain when the muon has reached a state with $n=8$. The K electrons can be ejected by an Auger transition (with $\Delta n=1$) only when $n<7$. For such values of n, radiative transitions dominate. The K electrons are responsible for over 80% of the effective electron density [i.e., contribution to $\rho_e(r_e)$ for which $\mathbf{r}$ is less than the appropriate muonic Bohr radius] for all $n<14$. At least for heavy elements it is thus extremely probable that all ten K and L electrons are present during radiative transitions between states with $n \leq 8$. These electrons are responsible for more than 95% of the screening correction. A similar conclusion was reached by Bovet *et al.* (1980) in connection with a study of pionic x rays. Recent experimental results on the electronic K x-ray energies in heavy muonic atoms (Schneuwly and Vogel, 1980) also indicate that the inner electronic shells are almost instantaneously refilled during the muonic cascade.

These estimates have been experimentally tested by measuring muonic x rays corresponding to transitions between states of higher principal quantum number n; their energies are most sensitive to electron screening (Vogel

et al., 1977; Vuilleumier *et al.*, 1976). Some typical results for Rh, Hg, and Pb are summarized in Table I. The good agreement between theory and experiment for these cases confirms that we understand the electron screening correction to a level of a few percent of the correction, at least for the transitions under discussion.

In the case of lighter elements ($Z \leq 20$) the situation is not so clear. The rates for refilling of electron vacancies are uncertain, and as a result very little is known about the electron population. Preliminary results (Ruckstuhl *et al.*, 1979) indicate that the electron screening shift of the $4f$-$3d$ transitions in muonic ^{28}Si is about half of that expected if all Z-1 electrons were present, so that one K electron is probably absent.

III. QUANTUM ELECTRODYNAMIC (QED) CORRECTIONS

Additional contributions to the energy levels of muonic atoms come about as a result of the interaction between the lepton field and the quantized electromagnetic field. These include radiative corrections, due to the emission and/or absorption of real or virtual photons, and vacuum polarization. As a result of the radiative corrections, the muon acquires form factors and no longer behaves precisely as a point Dirac particle (the anomalous magnetic moment is one experimental consequence). Vacuum polarization results in a modification of the photon propagator due to virtual pair production and reannihilation; this leads to a modification of Coulomb's law at distances small compared to the electron's Compton wavelength and thus to numerically important shifts of muonic energy levels. See Sec. III.D for a detailed discussion of experimental tests; here we discuss calculational methods.

A. Vacuum polarization

1. Order $\alpha Z\alpha$

a. e^+e^- pairs

The most important QED effect is the virtual production and annihilation of a single e^+e^- pair [Fig. 7(b)]. It has as a consequence an effective interaction of order $\alpha Z\alpha$, which is usually called the Uehling or Serber-Uehling potential (Uehling, 1935; Serber, 1935). This interaction describes the most important modification of Coulomb's law. Numerically it is so important that one cannot treat this effect using perturbation theory, but must add the Uehling potential to the nuclear electrostatic potential before solving the Dirac equation in order to obtain sufficient accuracy. Like most other QED corrections, the Uehling potential is most conveniently derived using the scattering approximation. The reason for this is that Feynman diagrams deliver a prescription for computing scattering amplitudes in momentum space, while the computation of atomic energy levels is usually done in configuration space using a static potential. The scattering approximation provides a useful connection between the two pictures. One writes down the scattering amplitude corresponding to the diagrams under consideration, and tries to find a potential which reproduces this scattering amplitude in Born approximation. (When it exists, the Fourier transform of the scattering amplitude satisfies this requirement). This potential is then used to compute the energy-level shift.

We recall from the discussion of the recoil correction that the amplitude for Coulomb scattering of a lepton by a heavy nucleus is given by

TABLE I. Experimental transition energies E_{exp}, calculated transition energies E_{th}, screening correction E_{scr}, all in eV.

Element	Transition	E_{exp}	E_{th}	$E_{th}-E_{exp}$	E_{scr}
$^{103}_{45}$Rh[a]	$8h$-$5g$	138 966(34)	138 968(3)	2(34)	−189(2)
	$7h$-$5g$	111 786(35)	111 795(3)	9(35)	− 98(2)
	$6g$-$4f$	198 697(27)	198 708(3)	11(27)	− 66(1)
	$5g$-$4f$	129 010(33)	129 015(3)	5(33)	− 20(1)
$^{nat}_{80}$Hg[a]	$8i$-$6h$	219 609(32)	219 633(5)	24(33)	−406
	$6h_{11/2}$-$5g_{9/2}$	221 857(28)	221 876(4)	19(29)	−108(2)
	$6h_{9/2}$-$5g_{7/2}$	223 418(28)	223 433(4)	15(29)	−107(2)
	$7h_{11/2}$-$5g_{9/2}$	354 614(34)	354 661(5)	47(35)	−318
$^{208}_{82}$Pb[b]	$6h_{11/2}$-$5g_{9/2}$	233 199(12)	233 196(5)	− 3(13)	−115
	$7h_{11/2}$-$5g_{9/2}$	372 724(16)	372 714(5)	−10(17)	−348
	$7h_{9/2}$-$5g_{7/2}$	374 842(36)	374 828(5)	−14(36)	−348
	$9i_{13/2}$-$6h_{11/2}$	292 324(27)	292 304(5)	−20(27)	−774
	$7i_{13/2}$-$6h_{11/2}$	140 138(13)	140 148(5)	10(14)	−153

[a]Vuilleumier *et al.*, 1976. [b]Vogel *et al.*, 1977.

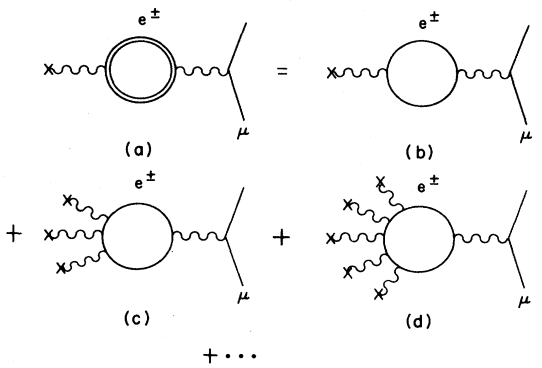

FIG. 7. Decomposition of the vacuum-polarization correction.

$$S_{fi}=\bar{u}(p')\gamma^0 u(p)V_{\rm eff}(q)(2\pi)^4\delta^4(p'-p-q)$$
$$=u^+(p')u(p)[-eA_0(q)](2\pi)^3\delta^3(\mathbf{p}'-\mathbf{p}-\mathbf{q})\ . \tag{121}$$

The quantity $eA_0(q)$ defined in Eq. (121) can be related to the scattering potential by means of the relation

$$eA_0(q)=-4\pi Z\alpha\frac{F(q)}{q^2}2\pi\delta(E'-E)$$
$$=\int d^3r\, V(r)e^{-i\mathbf{q}\cdot\mathbf{r}}2\pi\delta(E'-E)\ . \tag{122}$$

We shall now apply the above result to the derivation of the Uehling potential. As is well known, the effect of vacuum polarization is best described as a modification of the photon propagator (Bjorken and Drell, 1964), as is illustrated in Fig. 8, so that

$$q^{-2}\to q^{-2}+q^{-2}\Pi(q^2)q^{-2}+\cdots\ . \tag{123}$$

This effect can be described roughly as an order-α strengthening of the photon propagator, a description which is sufficient to estimate its quantitative importance in many practical cases. To leading order in the fine-structure constant α, we have (after renormalization) (Jauch and Rohrlich, 1955; Akhiezer and Berestetskii, 1965)

$$\frac{\Pi(q^2)}{q^2}=\frac{2\alpha}{3\pi}\frac{q^2}{4m_e^2}\int_1^\infty dz\left[\frac{1}{z^2}+\frac{1}{2z^4}\right]\frac{(z^2-1)^{1/2}}{z^2+q^2/4m_e^2}$$
$$=\frac{\alpha}{3\pi}[\tfrac{1}{3}-(3-\delta^2)(1-\phi\delta)]=U_2(q) \tag{124}$$

with $\delta=\coth\phi$, $\sinh^2\phi=q^2/4m_e^2$.

From this we immediately obtain the corresponding potential $V_{\rm VP1}(q)$ in momentum space. One simply replaces q^{-2} by $q^{-4}\Pi(q^2)$ in Eq. (121), where $q=(0,\mathbf{q})$.

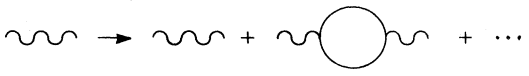

FIG. 8. Vacuum-polarization insertion in the photon propagator.

We then have

$$V_{\rm VP1}(q)=\frac{\Pi(q^2)}{q^2}eA_0(q)=-4\pi Z\alpha\frac{F(q)}{q^2}U_2(q)\ . \tag{125}$$

For numerical applications, it is (perhaps unfortunately) more convenient to work in configuration space. The relatively simple expression (125) for the Uehling potential becomes a rather complicated convolution integral, which is tedious to compute. The rather considerable literature which has appeared on the subject of the evaluation of vacuum polarization has been devoted almost exclusively to improved numerical methods which permit the efficient evaluation of this potential (Fullerton and Rinker, 1976; Klarsfeld, 1977b; Huang, 1976; Dubler, 1978).

From Eqs. (122) and (125) we obtain for the Uehling potential

$$V_{\rm VP1}(r)=-\frac{Z\alpha}{2\pi^2}\int d^3r_N\,\rho(r_N)\int d^3q\,e^{i\mathbf{q}\cdot(\mathbf{r}-\mathbf{r}_N)}\frac{U_2(q)}{q^2}\ . \tag{126}$$

Using Eq. (124) for $U_2(q)$ and

$$\int d^3q\,\frac{e^{i\mathbf{q}\cdot\mathbf{r}}}{q^2+4m_e^2z^2}=\frac{2\pi^2}{r}e^{-2m_erz}\ , \tag{127}$$

we obtain

$$V_{\rm VP1}=-\frac{2\alpha Z\alpha}{3\pi}\int d^3r_N\,\frac{\rho(r_N)}{|\mathbf{r}-\mathbf{r}_N|}\chi_1(2m_e|\mathbf{r}-\mathbf{r}_N|)$$
$$=-\frac{2\alpha Z\alpha}{3m_er}\int_0^\infty dr_N\,r_N\rho(r_N)[\chi_2(2m_e|r-r_N|)$$
$$-\chi_2(2m_e|r+r_N|)]\ , \tag{128}$$

where the functions χ_n are defined by

$$\chi_n(x)=\int_1^\infty dz\,\frac{(z^2-1)^{1/2}}{z^{n+1}}\left[1+\frac{1}{2z^2}\right]e^{-xz}\ . \tag{129}$$

(Several other notations for these functions appear in the literature.)

The direct numerical evaluation of χ_2 from the integral representation requires too much computer time for general use. A series expansion which is valid for $r\lesssim m_e^{-1}\simeq 386$ fm has been given by McKinley (1969b). This was used by Vuilleumier *et al.* (1978) and by Engfer *et al.* (1974) for the computation of the vacuum polarization (VP) corrections which appear in that work. Another type of expansion in polynomials and exponential integrals was given by McKee (1968) and later extended to higher order (Rinker and Wilets, 1975). Both series are of comparable accuracy. Rational approximations, which have been optimized in the Chebychev sense for minimum computation time consistent with a given upper bound for the (weighted) error, have been given by Fullerton and Rinker (1976). Other approximations were

given by Huang (1976) and Dubler (1978). In addition, Klarsfeld (1977b) has exploited the fact that the functions $\chi_n(z)$ can be expressed as linear combinations of the modified Bessel functions (Abramowitz and Stegun, 1965) $K_0(z)$, $K_1(z)$, and

$$Ki_1(z)=\int_z^\infty dx\, K_0(x)\,dx, \quad Ki_1(0)=\pi/2 . \tag{130}$$

These functions are frequently available in standard computer program libraries.

A useful approximation which is valid for distances large compared to the nuclear radius is given by Fullerton and Rinker (1976; see also Blomqvist, 1972),

$$V_{\mathrm{VP1}}(r)\simeq-\frac{2\alpha Z\alpha}{3\pi r}[\chi_1(2m_e r)+\tfrac{2}{3}m_e^2\langle r_N^2\rangle\chi_{-1}(2m_e r) + \tfrac{2}{15}m_e^4\langle r_N^4\rangle\chi_{-3}(2m_e r)+\cdots], \tag{131}$$

where the radial moments of the nuclear charge distribution are given by

$$\langle r_N^k\rangle=\int d^3r_N\, r_N^k\rho(r_N) . \tag{132}$$

b. $\mu^+\mu^-$ pairs

The VP correction due to a virtual $\mu^+\mu^-$ pair can be treated exactly as described above, with the replacement of the electron mass by the muon mass. Because the muon mass is much larger, the effect is numerically much smaller, and for practical calculations, the $q=0$ limit is usually taken in Eq. (124) before transforming to configuration space. In this limit, the expression is much simpler; Eqs. (124) and (126) become

$$U_2(q)\simeq\frac{\alpha}{15\pi}\frac{q^2}{m^2}, \quad V_{\mathrm{VP1}}(r)\simeq-\frac{4\alpha Z\alpha}{15m^2}\rho(r) . \tag{133}$$

The difference between this and the expectation value of the exact Uehling potential is only 4 eV for the 1s state in lead and is thus usually ignored.

c. Effect on higher nuclear multipoles

For nuclei which have a magnetic moment or an electric quadrupole moment, there is a corresponding magnetic or quadrupole component of the vacuum-polarization potential. For the case of the quadrupole component, this can be obtained easily from Eq. (126) or from (128) if $\rho(\mathbf{r}_N)$ is taken to be not spherically symmetric. The magnetic component is obtained analogously to (125) in momentum space by multiplying $e\mathbf{A}(q)$, the Fourier transform of the vector potential $\mathbf{A}$ in (1) and (2), by $\Pi(q^2)/q^2$. The properties of the quadrupole component have been discussed by Pearson (1963), McKee (1968), and McKinley (1969b). The effect of the quadrupole VP is to increase the spread among the hyperfine states by a few tenths of a percent. The effect is just comparable to experimental uncertainties.

d. Effect on the recoil correction

We observe that vacuum polarization also has an effect on the relativistic recoil correction discussed in Sec. II.H. To the extent that the Uehling potential may be regarded as static (e.g., the virtual electron-positron pairs respond almost instantaneously to the motion of the nucleus), this effect may be calculated from Eq. (116), adding the Uehling potential to the electrostatic potential due to the nuclear charge distribution. Vacuum polarization modifies B_0, $h(r)$, and $P(r)$ appearing in Eq. (116), providing the usual order-α strengthening of the photon propagator. This results in an increase in the recoil correction of the order of one percent.

e. Hadronic vacuum polarization

The contribution of virtual hadronic states (Fig. 9) is obtained from the total cross section for $e^+e^-\to$ hadrons by observing that

$$\frac{\Pi_H(q^2)}{q^2}=U_H(q^2)=\frac{|\mathbf{q}|^2}{4\pi^2\alpha}\int_{4m_\pi^2}^\infty dt\frac{\sigma_{e^+e^-\to\mathrm{had}}(t)}{t+|\mathbf{q}|^2} . \tag{134}$$

Substitution in Eq. (125) gives

$$V_{\mathrm{HVP}}(q)=-4\pi Z\alpha\frac{F(q^2)}{q^2}U_H(q^2) . \tag{135}$$

As was also observed by Gerdt *et al.* (1978), it is a good approximation to take

$$U_H(q^2)\simeq\frac{\alpha}{3\pi}\frac{|\mathbf{q}|^2}{m_H^2} \tag{136}$$

with

$$m_H^{-2}=\frac{3}{4\pi\alpha^2}\int_{4m_\pi^2}^\infty dt\,\sigma_{e^+e^-\to\mathrm{had}}(t)/t . \tag{137}$$

A recent calculation of m_H^{-2} by Borie (1981) is in fair agreement with that of Gerdt *et al.* (1978) but uses a better parametrization of the cross section for $e^+e^-\to$hadrons, particularly as regards the continuum contribution. Borie (1981) also verified that the approximation (136) is valid by calculating the corrections to the binding energies of a number of muonic atoms without making use of it and obtaining agreement with results

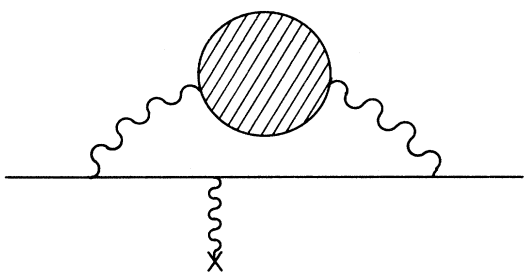

FIG. 9. Hadronic vacuum-polarization correction of order $\alpha(Z\alpha)$.

calculated with this approximation. She found $m_H^{-2}=0.23\ m_\pi^{-2}$. [Gerdt *et al.* (1978) have $m_H^{-2}=0.25\ m_\pi^{-2}$]. We observe that Eq. (136) is very similar in form to (133). One might therefore expect that the contribution of hadronic vacuum polarization can be very simply obtained from that for muonic vacuum polarization by

$$\Delta E_{\rm HVP}\simeq\frac{5m^2}{m_H^2}\Delta E_{\mu\rm VP}\simeq 0.66\Delta E_{\mu\rm VP}\ . \tag{138}$$

Borie's numerical results agree with this simple estimate to within 0.1 eV. These results are not consistent with those of Sundaresan and Watson (1975b); however, we are unable to give a reason for the discrepancy.

2. Order $\alpha^2 Z\alpha$

a. e^+e^- pairs

The Källen-Sabry correction (VP2) (Källen and Sabry, 1955) corresponds to diagrams in which a virtual photon appears in the VP loop ("cracked-egg" diagrams) and to the "double-bubble" diagram containing two e^+e^- pairs in the photon propagator (Fig. 10). These diagrams correspond to an interaction of order $\alpha^2 Z\alpha$. Their contribution can be evaluated in momentum space exactly as in the derivation of the Uehling potential described above, with the result

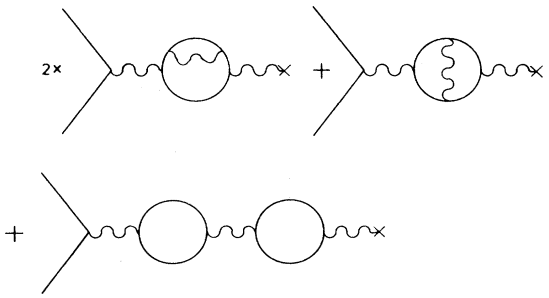

FIG. 10. Vacuum-polarization corrections of order $\alpha^2(Z\alpha)$.

$$V_{\rm VP2}(q)=-4\pi Z\alpha\frac{F(q)}{q^2}U_4(q) \tag{139}$$

where (Källen and Sabry, 1955; Barbieri and Remiddi, 1973; Borie, 1975a)

$$\begin{aligned}U_4(q)=U_2^2(q)-(\alpha/\pi)^2\Big(&\tfrac{3}{4}-\tfrac{13}{24}\delta^2-(\delta(5-3\delta^2)/8)\ln\Theta+\tfrac{1}{4}\ln^2\Theta[(33+22\delta^2-7\delta^4)/24-\delta(3-\delta^2)]\\&-\delta(1-\delta^2/3)\{L_2(\Theta^2)-L_2(\Theta)+\ln\Theta\ln[(1-\Theta^2)(1+\Theta)]\}-[1-(1-\delta^2)^2/4]\\&\times\{L_3(1)+L_3(\Theta^2)-2L_3(\Theta)-4\ln\Theta[L_2(\Theta^2)-L_2(\Theta)]/3\\&-\ln^2\Theta\ln[(1-\Theta^2)(1+\Theta)]/3\}\Big)\ .\end{aligned} \tag{140}$$

Here $\Theta=\exp(-2\phi)$, and

$$L_2(\Theta)=-\int_0^\Theta\ln(1-x)\frac{dx}{x}\ ,$$
$$L_3(\Theta)=\int_0^\Theta L_2(x)\frac{dx}{x} \tag{141}$$

are Spence functions (Gröbner and Hofreiter, 1966).

A useful expression for $V_{\rm VP2}(r)$ was first given by Blomqvist (1972), in terms of an integral representation and as a power series in $m_e r$. Other calculations were made by Sundaresan and Watson, 1972. Numerical values for large radii have been given by Vogel (1974). Chebychev fits to these values and to the series of Blomqvist have been given by Fullerton and Rinker (1976) and by Fullerton (1981). These fits are more efficient to evaluate numerically but are no more accurate than the original representations. More recently, Chlouber and Samuel (1978) and Huang (1976) have given expansions useful in the computation of $V_{\rm VP2}(r)$. Asymptotically, we have

$$V_{\rm VP2}(r)\underset{r\to\infty}{\to}-\frac{Z\alpha}{r}\left[\frac{\alpha}{\pi}\right]^2\frac{e^{-2m_e r}}{m_e r}\times\left[\int_1^\infty dx\,f(x)+O(m_e r)^{-1/2}\right]\ , \tag{142}$$

with

$$f(x)=\frac{3x^2-1}{x(x^2-1)}\cosh^{-1}x-\frac{\ln 8x(x^2-1)}{(x^2-1)^{1/2}}\ . \tag{143}$$

The integral is equal to $\pi^2/4-8\ln^2 2$, so that

$$V_{\rm VP2}(r)\underset{r\to\infty}{\to}\frac{Z\alpha^3}{r}\frac{e^{-2m_e r}}{m_e r}\left[\frac{8}{\pi^2}\ln^2 2-\frac{1}{4}\right]\ . \tag{144}$$

b. Mixed μ-e vacuum polarization

The mixed $\mu-e$ vacuum polarization (Fig. 11) is calculated in momentum space analogously to the Uehling and Källen–Sabry corrections. From Eqs. (125) and (133) we find

$$\begin{aligned}\Delta V_{\mu e}(q)&=2\frac{\Pi_\mu(q^2)}{q^2}\frac{\Pi_e(q^2)}{q^2}eA_0(q)\\&\simeq-\frac{\alpha}{\pi}\left[4\pi Z\alpha\frac{F(q^2)}{q^2}\right]\frac{q^2}{15m^2}U_2(q)\ ,\end{aligned} \tag{145}$$

where $U_2(q)$ is defined in Eq. (125), and the approximation $q^2<<m^2$ is made. The contribution of such terms is very small.

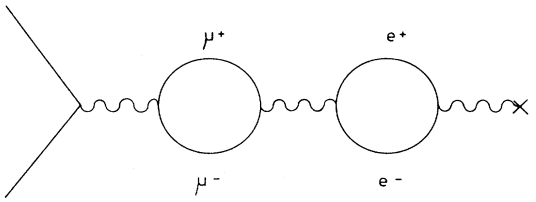

FIG. 11. Mixed μ-e vacuum-polarization correction of order $\alpha^2(Z\alpha)$.

3. Orders $\alpha(Z\alpha)^n$, $n = 3, 5, 7 \ldots$

For heavy elements, modifications to the free-electron propagator appearing in the calculation of the Uehling effect (Sec. III.A.1) become important. These modifications may be regarded as Coulomb corrections to the electron propagators in a generalized sense (e.g., corrections due to multiple interactions with a not-necessarily-pointlike electrostatic potential). As a result, one must deal with vacuum polarization effects which are nonlinear in the nuclear charge Z. The dominant diagrams of this type ("Medusa" diagrams) are shown in Fig. 7. Corresponding diagrams with an even number of nuclear vertices vanish due to charge-conjugation invariance (Furry's theorem). The diagram with a single nuclear vertex (Fig. 7b) represents the previously discussed Uehling effect. The higher-order diagrams are in principle reduced only by successive factors $(Z\alpha)^2$, which is not necessarily a small parameter[2]; hence it is necessary to perform a more complete calculation.

A straightforward application of the techniques of Feynman graphs quickly encounters formidable computational difficulties in higher orders. In an effort to circumvent these difficulties, all successful calculations to date have used the static bound-interaction picture, in which electron-positron propagators are computed in the external static nuclear field (Fig. 7a) and thus effectively sum all powers of $Z\alpha$. In this picture, one computes the electron-positron charge density induced in the vacuum by the nuclear field, subtracts the Uehling contribution (this is necessary in order to obtain a mathematically well-defined induced charge density and take into account charge renormalization), and treats the potential arising from the resulting charge density as a perturbation; energy-level shifts are then calculated using lowest-order perturbation theory in the usual manner. The price paid for this formal simplification is that one must deal with exact Coulomb propagators, which are notoriously difficult to work with, either numerically or analytically.

One begins with a formal expression for the electron-positron charge induced in the vacuum

$$\rho(\mathbf{r}) = -\frac{e}{2}\left[\sum_{\text{oc}} |\psi_E(\mathbf{r})|^2 - \sum_{\text{un}} |\psi_E(\mathbf{r})|^2\right], \tag{146}$$

where the $\psi_E(\mathbf{r})$ are the electron wave functions of energy E calculated in the applied external electric potential $V(\mathbf{r})$ generated by the nucleus. (Note that in this section, unlabeled coordinates refer to polarization electrons.) The terminology "oc" and "un" mean occupied and unoccupied electron states, respectively. Equation (146) is charge-conjugation invariant and satisfies the physical requirement that addition or removal of an electron changes the total charge of the system by one unit. It may be written in other (equivalent) ways which amount only to relabeling of the particle states involved. One usually takes the Dirac sea ($E < -m_e$) to be occupied and the remaining states to be unoccupied. For normal atoms, this results in a vacuum with zero net charge. One may alternatively define the vacuum to have other charge states. For example, treating certain bound atomic states as occupied includes electron screening effects within the same framework. As another example, for very strong fields ($Z\alpha > 1$ in the point-nucleus approximation), bound electron states leave the regime of discrete energies ($-m_e < E < m_e$) and enter the negative-energy continuum, yielding a vacuum with nonzero net charge even if only those states with $E < -m_e$ are occupied. Such situations have elicited substantial interest in their own right (Pieper and Greiner, 1969; Rein, 1969; Popov, 1971; Fulcher and Klein, 1973; Rafelski *et al.*, 1974a, 1974b) but will not be discussed here further, as they have no present practical relevance to muonic atoms.

Equation (146) is neither convergent nor manifestly gauge invariant as it stands. Furthermore, it contains the linear (Uehling) contribution, which has already been evaluated and must be removed if the higher-order effects are to be identified. The most straightforward procedure for regularizing Eq. (146) is due to Pauli and Villars (1947). This method consists of subtracting from (146) an identical expression calculated for a fictitious lepton of arbitrary mass M, and at the end taking the limit $M \to \infty$. Such a procedure is manifestly gauge invariant and clearly contributes nothing but a renormalization of the induced charge, as the range of vacuum-polarization effects due to a lepton of mass M is limited to $r \lesssim M^{-1}$. This subtraction reduces the nominal quadratic divergence of Eq. (146) to the well-known logarithmic divergence of the term linear in Z, which is absorbed in charge renormalization. The higher-order terms thus regularized are finite and well defined, so long as care is taken to evaluate each corresponding term consistently. An illustration of this method is discussed below.

In principle one may solve Eq. (146) for any arbitrary $V(\mathbf{r})$. An assumption of spherical symmetry, however, results in a substantial simplification of the calculation. Such an assumption is not so severe as it might seem. The Uehling term, already known for a point source,

[2]Explicit calculation, however, shows that the $(Z\alpha)^3$ diagram is relatively much smaller than this. For example, the $(Z\alpha)^3$ contribution to the $5g$-$4f$ transitions in lead ($Z\alpha \simeq 0.6$) is only about 2% of the order-$Z\alpha$ contribution. The higher-order contributions decrease in successive ratios closer to $(Z\alpha)^2$.

may be folded over any arbitrary nonspherical nuclear charge distribution. Thus if spherical symmetry is assumed in Eq. (146) and the Uehling term removed, deviations from spherical symmetry cause errors only in the higher-order terms, which are relatively small. Assuming that $V(\mathbf{r})-V(r)$ is spherically symmetric, Eq. (146) may be rewritten in the notation of Rinker and Wilets (1975) as

$$4\pi r^2\rho(r)=-\frac{e}{2}\sum_\kappa 2\,|\kappa|\int_{m_e}^{\infty}dE[F^2_{-E\kappa}(r)+G^2_{-E\kappa}(r)-F^2_{E\kappa}(r)-G^2_{E\kappa}(r)]+\frac{e}{2}\sum_{\substack{\text{bound}\\ \text{states}}}2\,|\kappa|\,[F^2_{n\kappa}(r)+G^2_{n\kappa}(r)]\ , \tag{147}$$

where the continuum wave functions are normalized to

$$G_{E\kappa}(r)\underset{r\to\infty}{\to}\left[\frac{|E+m_e|}{\pi p}\right]^{1/2}\sin(pr+\delta)\ ,$$
$$F_{E\kappa}(r)\underset{r\to\infty}{\to}\left[\frac{|E-m_e|}{\pi p}\right]^{1/2}\cos(pr+\delta)\ , \tag{148}$$

and δ is an appropriate phase shift of the potential $V(r)$. The bound-state wave functions are normalized to

$$\int_0^\infty dr\,[F^2_{n\kappa}(r)+G^2_{n\kappa}(r)]=1\ . \tag{149}$$

If $V(r)$ is a simple enough function, Eq. (147) can be evaluated analytically, the various orders in $V(r)$ (equivalently, $Z\alpha$) isolated, and the divergences and ambiguities removed. Such a program was first carried out by Wichmann and Kroll (1956) using the point-nucleus approximation $V(r)=-Z\alpha/r$. For computational purposes they rewrote Eq. (147) in terms of the Dirac Green's function

$$K^{\mu\nu}_{z\kappa}(r_1,r_2)=\sum_E\frac{w^\mu_{E\kappa}(r_1)w^\nu_{E\kappa}(r_2)}{z-E} \tag{150}$$

where $w^1_{E\kappa}(r)=F_{E\kappa}(r)$ and $w^2_{E\kappa}(r)=G_{E\kappa}(r)$. Cauchy's integral then yields

$$4\pi r^2\rho(r)=-\frac{e}{2}\sum_\kappa 2\,|\kappa|\,\frac{1}{2\pi i}\left[\int_{c_1}dz\,\mathrm{Tr}\{K_{z\kappa}(r,r)\}+\int_{c_2}dz\,\mathrm{Tr}\{K_{z\kappa}(r,r)\}\right]. \tag{151}$$

The contour c_1 encloses in the counterclockwise direction all eigenvalues with $E<-m_e$, while c_2 encloses in the clockwise direction all those with $E>-m_e$. In order to evaluate Eq. (151), a limiting procedure must be defined to extend the contours to infinity, as well as appropriate regularization procedures to eliminate the divergences and ambiguities.

With an explicit representation for the Laplace transform of $\mathrm{Tr}\{K_{z\kappa}(r,r)\}$ and a lengthy analysis based primarily upon uniqueness and gauge invariance, Wichmann and Kroll showed that the only physical contribution to Eq. (151) arises from the integral along the imaginary energy axis, i.e.,

$$4\pi r^2\rho(r)=-\frac{e}{2}\sum_\kappa 2\,|\kappa|\,\frac{1}{i\pi}\int_{-i\infty}^{i\infty}dz\,\mathrm{Tr}\{K_{z\kappa}(r,r)\}\ . \tag{152}$$

This useful result was obtained without using the Pauli-Villars prescription. It was later shown by Gyulassy (1974, 1975) to be valid for any spherically symmetric $V(r)$. The complete result of Wichmann and Kroll is quite complicated and will not be reproduced here. It was first put into computationally convenient form by Blomqvist (1972) in terms of expansions in $Z\alpha$ and r. The order-$(Z\alpha)^3$ potential was evaluated numerically for large r by Vogel (1974). These results may be expressed efficiently as (Rinker, 1979)

$$V_3(r)\simeq 10^{-4}\frac{(Z\alpha)^3}{r}f(m_e r)$$
$$V_5(r)\simeq 0.340(Z\alpha)^2V_3(r) \tag{153}$$
$$V_7(r)\simeq 0.176(Z\alpha)^4V_3(r)\ ,$$

where

$$f(x)=\begin{cases}\dfrac{1.528-0.489x}{1+2.672x+1.410x^2+1.374x^3}, & x\le 1\\[2ex] \dfrac{-0.413+0.367x+0.207x^2}{x^6}, & x>1.\end{cases} \tag{154}$$

Although formally valid for any $Z\alpha<1$, these results suffer from the internal flaw that just in the region of interest (large Z) the effects of finite nuclear size play an important role (see Fig. 12). The nonlinearity of the higher-order terms in Z precludes the possiblity of simple superposition (folding) of the result over the nuclear charge distribution, in contrast to the applicability of such a treatment for the term linear in Z. Thus an accurate treatment requires building the effects of finite nuclear size into the calculation from the start. The need for such a treatment became acute in the early 1970s when precision measurements of high-lying transition energies in heavy elements showed systematic discrepancies from theory. Although it seemed unlikely that such effects could account for the discrepancies then believed to exist, proof could come only from explicit calculations. Even the sign of the effect could not be deduced conclusively from simple arguments. The various calculations performed in connection with tests of QED will be discussed in Sec. III.D.1. Here we present an approach which is valid for all muonic states.

This calculation (Rinker and Wilets, 1973a, 1975) evaluated Eq. (147) directly by actually constructing numerical electron wave functions in the potentials generated by realistic nuclear charge distributions. The term linear in $V(r)$ was removed numerically. This approach also made use of the Pauli-Villars regularization. The gauge invariance of this prescription and the necessity for internal consistency can be seen from the following

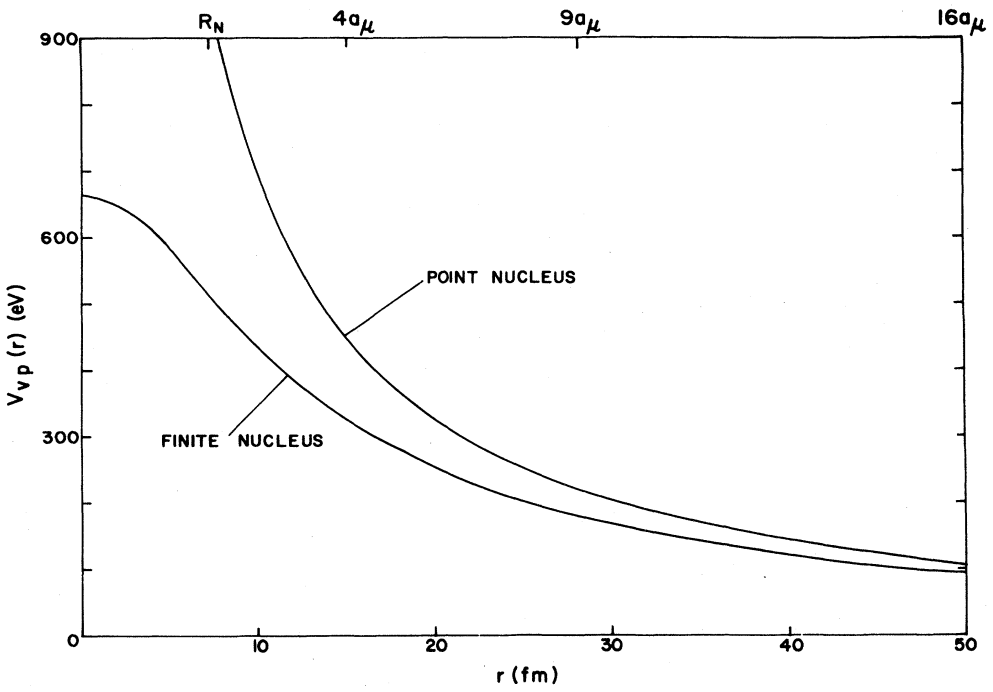

FIG. 12. Vacuum-polarization potentials of order $\alpha(Z\alpha)^{n\geq 3}$ for $Z=82$, calculated both for a realistic nuclear charge distribution and in the point-nucleus approximation (Rinker and Wilets, 1975).

simple argument (Rinker and Wilets, 1975). It can be shown that as $M\to\infty$, the Fermi gas model provides the solution to Eq. (147) for all terms nonlinear in Z. Intuitively, we expect the Fermi gas subtraction to produce the proper gauge invariance, as for a static applied electric field, gauge invariance means that Eq. (147) should be unaltered by the addition of any constant term to $V(r)$; and for a constant potential, the Fermi gas is the exact result. Alternatively, one may say that the calculation must be arranged so that a constant (but nonzero) potential produces no polarization of the vacuum. In a plane-wave basis, the result is

$$\rho_M(r)=\frac{1}{6\pi^2}(\{[E+V(r)]^2-M^2\}^{3/2}-\{[E-V(r)]^2-M^2\}^{3/2})$$
$$\underset{\substack{E\to\infty\\M\to\infty}}{\to}\frac{1}{3\pi^2}[3(E^2-M^2)^{1/2}EV(r)+V^3(r)+O(V^3(r)M^4/E^4)]\,, \tag{155}$$

where $V(r)$ is the electrostatic potential generated by the nucleus and E is the maximum plane-wave energy to which the sum (147) is carried. The ordering of limits to be taken is $E\to\infty$ and then $M\to\infty$. The quadratic divergence in the term linear in $V(r)$ is that expected from a non-gauge-invariant calculation. Along with the proper correction of order $V(r)$ to the Fermi gas model, it cancels the corresponding term in Eq. (147) for the physical mass, reducing the divergence to the well-known logarithmic charge renormalization. The contact term $V^3(r)/3\pi^2$ is the only counter term which survives in higher order to be subtracted from Eq. (147).

Another ordering of the limits in Eq. (147) may be used, however. If we instead carry out the limits $E\to\infty$ and $M\to\infty$ in (147) before summing over κ, we find for any given κ

$$\rho_{M\kappa}(r)=\frac{|\kappa|}{4\pi^2r^2}\left\{\left[[E+V(r)]^2-M^2-\left[\frac{\kappa}{r}\right]^2\right]^{1/2}-\left[[E-V(r)]^2-M^2-\left[\frac{\kappa}{r}\right]^2\right]^{1/2}\right\}$$
$$\underset{\substack{E\to\infty\\M\to\infty}}{\to}\frac{|\kappa|}{2\pi^2r^2}\left\{\left[1+O\left[\frac{\kappa^2}{E^2r^2}\right]\right]V(r)+O\left[\frac{V^3(r)}{E^2}\right]\right\}. \tag{156}$$

There is no surviving $V^3(r)$ term. If, however, we integrate Eq. (156) over all allowable $|\kappa^{\pm}| \leq r\{[E \mp V(r)]^2 - M^2\}^{1/2}$, where $\pm$ refers to positive/negative energy states, we regain Eq. (155). Thus internal consistency in the counting of states and the ordering of limits $|\kappa| \to \infty$, $E \to \infty$ is crucial, even though the sums are separately convergent.

Figure 13 shows the net charge density induced in the vacuum for $|\kappa| = 1$ and 2, as calculated by Rinker and Wilets for lead. For the high-lying muon states, the results of all authors are in satisfactory agreement. For the low-lying states, the only systematic calculations which have been carried out are by Rinker and Wilets (1975). Their results are plotted in Fig. 14. These may be compared to the binding energy shifts of order $\alpha(Z\alpha)$ plotted in Fig. 15 (note that the effects have opposite sign). Although internal consistency checks suggest that the numbers in Fig. 14 are accurate in spite of the formidable numerical difficulties, the calculations have not been independently repeated.

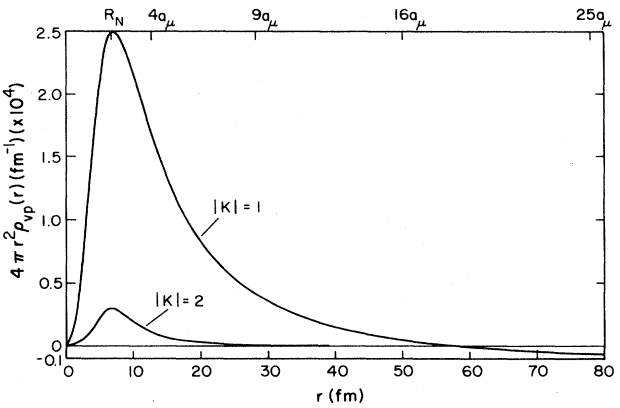

FIG. 13. Vacuum-polarization electron densities of order $\alpha(Z\alpha)^{n\geq 3}$ for both $|\kappa| = 1$ and 2.

4. Order $\alpha^2(Z\alpha)^2$

The virtual Delbrück effect corresponds to the graphs shown in Fig. 16. It can be interpreted in two ways: (a) a virtual photon emitted by the muon is scattered by the nuclear electrostatic potential (analogous to Delbrück scattering) and is then reabsorbed by the muon; (b) the muon polarizes the vacuum linearly (to order e), the electron-positron pair interacts with the nucleus, and the muon interacts again with the polarization field (again to order e). The former interpretation is more useful when the methods of Feynman graphs are used to calculate the shift in binding energy, since the results given in the rather extensive literature on light-by-light scattering (Karplus and Neumann, 1950; Costantini *et al.*, 1971;

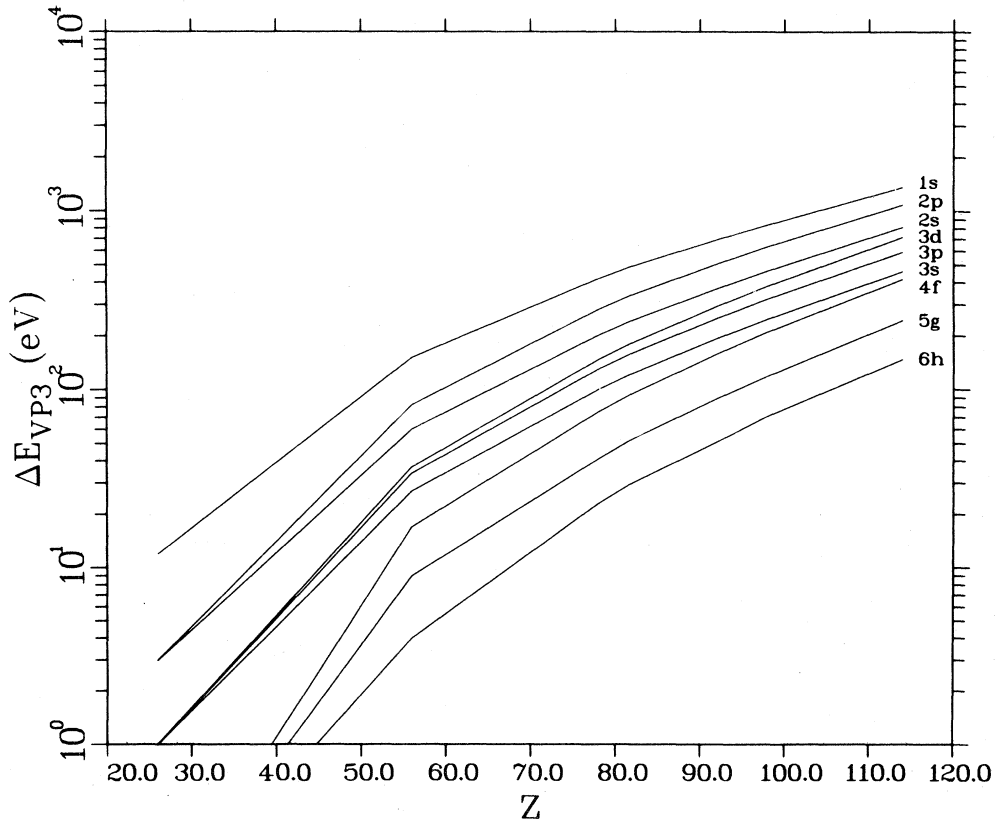

FIG. 14. Order-$\alpha(Z\alpha)^{n\geq 3}$ vacuum-polarization energy shifts (Rinker and Wilets, 1975).

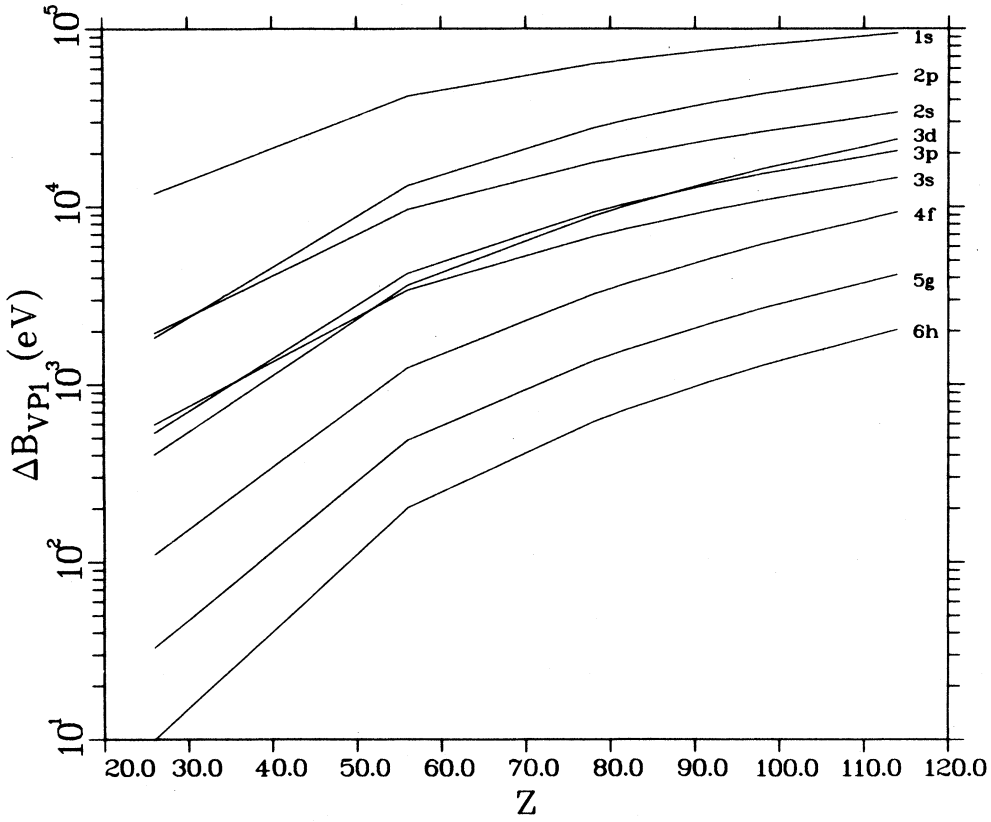

FIG. 15. Order-$\alpha(Z\alpha)$ vacuum-polarization binding energy shifts.

Papatzacos and Mork, 1975) can be utilized. The second interpretation was used by Wilets and Rinker (1975), since this enabled them to use the same procedure originally developed for nonlinear corrections to the Uehling potential. It is reassuring that both approaches gave very similar results for the energy shifts of interest in tests of QED.

A complete calculation of the virtual Delbrück effect would involve using full Coulomb propagators for the muon and for the electron loop in the so-called bound interaction picture (Jauch and Rohrlich, 1955). The full calculation would probably be too large for existing computer facilities. For the purpose of determining whether its contribution might be significant in tests of QED, an estimate based on reasonable approximations should be sufficient. We describe here the calculation of Borie

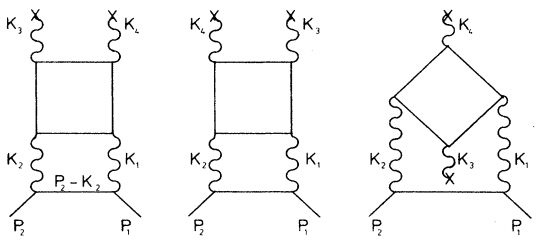

FIG. 16. Feynman diagrams contributing to the virtual Delbrück effect.

(1976a). (See also Fujimoto, 1975; Calmet and Owen, 1978).

As has already been discussed (Sec. III.A.1.a), the scattering approximation is frequently useful for the calculation of radiative corrections to atomic energy levels, at least provided no infrared divergences are present. The calculations of the virtual Delbrück effect by Borie (1976a) and Fujimoto (1975) are based on this approximation. According to this prescription, one calculates the scattering amplitude which corresponds to the graphs in question and constructs a potential which reproduces this scattering amplitude in Born approximation. Although this approximation runs into difficulties in the calculation of the self-energy due to the presence of infrared divergences, it should be valid whenever a vacuum polarization insertion is present, since the electron mass provides a natural cutoff at low energies. The approximation also involves the use of the free muon propagator; this will be justified in more detail below. Physically it corresponds to using the closure approximation for the muon propagator. Furthermore, since the average muon velocity is small ($v \simeq Z\alpha/n \simeq 0.15c$ for the $4f$ state in lead), it is sufficient to use a low-energy approximation for the muon propagator, at least for those levels which are relevant for tests of QED. It turns out that the correction is dominated by the Coulomb (longitudinal) components of the electromagnetic field. A calculation based on these approximations can thus be expected to

give the correct sign and order of magnitude for the correction, and will be sufficient if the correction is not too large.

The energy shift corresponding to the graphs of Fig. 16 is then simply the expectation value of the potential obtained from the scattering amplitude. If we denote this potential by $\Delta V(q)$ (in momentum space; i.e., the Fourier transform of the physical potential), then the energy shift of the muonic level is given by

$$\Delta E_{n\kappa}=\frac{1}{2\pi^2}\int_0^\infty dq\, q^2\Delta V(q) \times\int_0^\infty dr\, j_0(qr)[F_{n\kappa}^2(r)+G_{n\kappa}^2(r)] \simeq\frac{1}{2\pi^2}\int_0^\infty dq\, q\Delta V(q)\frac{\beta}{2\gamma(1+q^2/\beta^2)\gamma} \times\sin[2\gamma\tan^{-1}(q/\beta)]\,, \tag{157}$$

where $F_{n\kappa}$ and $G_{n\kappa}$ are the small and large components of the wave function. The second part is obtained by using relativistic point Coulomb wave functions with $n=j+1/2$ (circular orbits), with $\gamma=(n^2-\alpha^2Z^2)^{1/2}$ and $\beta=2Z\alpha m/n$.

We now proceed to justify the use of the scattering approximation for the virtual Delbrück effect. In the presence of an external electromagnetic field, the propagator $S_F^B(x,y)$ of a lepton is defined by (Furry, 1951)

$$[i\gamma^\mu\partial_{\mu x}-e\not{A}(x)-m]S_F^B(x,y) =S_F^B(x,y)[-i\gamma^\mu\partial_{\mu y}-e\not{A}(y)-m] =\delta(x-y)\,. \tag{158}$$

Its Fourier transform is given by

$$S_c(p,q)=\int d^4x\int d^4y\, e^{i(px-qy)}S_F^B(x,y) \tag{159}$$

and the free propagator by

$$S_F(p)=(\not{p}-m)^{-1}\,. \tag{160}$$

Its Fourier transform is a solution to Eq. (158) when the external field vanishes.

One can show (Jauch and Rohrlich, 1955) that

$$S_c(p,q)=(2\pi)^4S_F(p)\delta(p-q) +S_F(p)e\not{A}(p-q)S_F(q)+S_F(p) \times\int\frac{d^4p'}{(2\pi)^4}\int\frac{d^4q'}{(2\pi)^4}e\not{A}(p-p')S_c(p',q') \times e\not{A}(q'-q)S_F(q)\,. \tag{161}$$

Equation (161) can be represented graphically, as in Fig. 17, in which a single line represents a free propagator and a double line represents a Coulomb propagator. A photon line ending on X indicates an interaction with the external field.

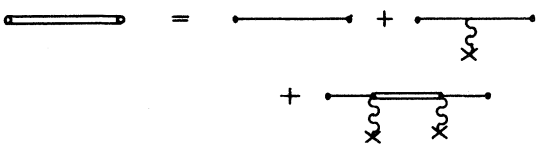

FIG. 17. Graphical representation of Eq. (161).

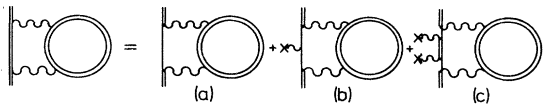

FIG. 18. Vacuum-polarization corrections of order $\alpha^2(Z\alpha)^{2n}$.

The VP corrections of order $\alpha^2(Z\alpha)^{2n}$, $n=1,2,\ldots$ are exhibited graphically in Fig. 18. On the right-hand side we have inserted Eq. (161) for the muon propagator. In contrast to the calculation of the self-energy, in which infrared-divergent contributions to the various terms cancel each other, the contributions of diagrams 18(a), 18(b), and 18(c) are separately infrared convergent since the electron mass acts as a natural infrared cutoff. The contribution of diagram 18(b) has already been calculated (with free-electron propagator) in connection with the fourth-order muon Lamb shift (Borie, 1975b) and is small; for the $5g$-$4f$ transition in lead it results in a change of 0.02 eV. Coulomb corrections to the electron propagator are unlikely to change this result significantly. Since diagrams 18(b) and 18(c) are separately infrared convergent, the contribution from 18(c) is at least a factor $Z\alpha$ smaller than that from 18(b) (see Erickson and Yennie, 1965), and we have just seen that the contribution from 18b is too small to have a measurable effect on the energy level. The only contribution which might be important would then be that from 18(a), in which the Coulomb propagator for the muon is replaced by the free propagator. From the above discussion, this should be a very good approximation.

As a next step, we decompose the electron propagators according to Eq. (161). Only terms containing an even number of vertices on the electron loop contribute according to Furry's theorem (charge-conjugation invariance). The diagrams in Fig. 19 remain. Figure 19(a) corresponds to a radiative correction to the mass renormalization and does not contribute to the binding energy. The contributions of Figs. 19(b), 19(c), and 19(d) are the virtual Delbrück graphs which must be calculated.

Our notation as to momenta is defined in Fig. 16. The scattering amplitude corresponding to the first graph is given by

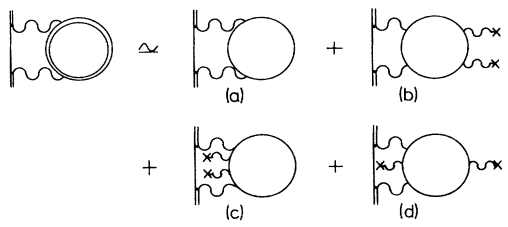

FIG. 19. Order-α^2, $\alpha^2(Z\alpha)^2$, . . . vacuum-polarization corrections to the binding energy of a muonic atom.

$$S=\int\frac{d^4k_1}{(2\pi)^4}\int\frac{d^4k_2}{(2\pi)^4}\int\frac{d^4k_3}{(2\pi)^4}\int\frac{d^4k_4}{(2\pi)^4}\bar{u}(p_2)\left[(-ie\gamma_\nu)\frac{1}{\not p-\not k_2-m+i\varepsilon}(-ie\gamma_\mu)\right]u(p_1)$$

$$\times(2\pi)^8\delta(p_1+k_1-p_2+k_2)\delta(k_1+k_2+k_3+k_4)\left[\frac{-i}{k_1^2+i\varepsilon}\right]\left[\frac{-i}{k_2^2+i\varepsilon}\right](-1)(-ie)^4A_\lambda(k_3)A_\sigma(k_4)$$

$$\times\int\frac{d^4p}{(2\pi)^4}\,\mathrm{Tr}\left\{\gamma^\mu\frac{1}{\not p-m_e+i\varepsilon}\gamma^\nu\frac{1}{\not p-\not k_2-m_e+i\varepsilon}\gamma^\lambda\frac{1}{\not p-\not k_2-\not k_3-m_e+i\varepsilon}\gamma^\sigma\frac{1}{\not p+\not k_1-m_e+i\varepsilon}\right\}, \tag{162}$$

where $eA_\lambda(q)=-Ze^2F(q^2)/q^2\cdot 2\pi\delta(q_0)\delta_{\lambda 0}$ (see Sec. III.A.1.a). In Eq. (162) we replace

$$\frac{1}{i\pi^2}\int d^4p\,\mathrm{Tr}\left\{\gamma^\mu\frac{1}{\not p-m_e+i\varepsilon}\gamma^\nu\frac{1}{\not p-\not k_2-m_e+i\varepsilon}\gamma^\lambda\frac{1}{\not p-\not k_2-\not k_3-m_e+i\varepsilon}\gamma^\sigma\frac{1}{\not p+\not k_1-m_e+i\varepsilon}\right\} \tag{163}$$

by $G_{\mu\nu\lambda\delta}(k_1,k_2,k_3,k_4)$ in order to take into account all three diagrams. Some properties of the fourth-order vacuum polarization tensor and references are given in the Appendix. We let $q=p_2-p_1$ and obtain

$$S=-\frac{Z^2(4\pi\alpha)^4}{(2\pi)^{10}}\int d^4k_2\frac{1}{(k_2^2+i\varepsilon)[(q-k_2)^2+i\varepsilon]}\int d^4k_3\,\delta(k_3^0)\delta(q_0+k_3^0)\frac{F(k_3^2)F[(q+k_3)^2]}{|\mathbf{k}_3|^2|\mathbf{q}+\mathbf{k}_3|^2}$$

$$\times\bar{u}(p_2)\gamma^\nu\frac{\not p_2-\not k_2+m}{(p_2-k_2)^2-m^2+i\varepsilon}\gamma^\mu(up_1)i\pi^2G_{\mu\nu00}(q-k_2,k_2,k_3,-q-k_3)\,. \tag{164}$$

If we neglect terms of relative order $m(Z\alpha/n)^2$ in both numerator and denominator of the muon propagator, we obtain

$$S=i\frac{Z^2\alpha^4}{4\pi^4}\int\frac{d^4k_2}{(k_2^2+i\varepsilon)[(q-k_2)^2+i\varepsilon]}\frac{\delta(q_0)}{2m\omega'-i\varepsilon}\int\frac{d^3k_3F(k_3^2)F[(q+k_3)^2]}{|\mathbf{k}_3|^2|\mathbf{q}+\mathbf{k}_3|^2}$$

$$\times\bar{u}(p_2)\left\{2m\gamma^0G_{0000}+\tfrac{1}{2}q^i\gamma_0(G_{0i00}-G_{i000})+\frac{1}{2}\left[(p_1+p_2)^j(1+\gamma^0)+\frac{i\sigma^{kj}}{2}q_k\right](G_{0j00}+G_{j000})\right\}u(p_1)\,. \tag{165}$$

The arguments of the components of $G_{\mu\nu00}$ are, of course, the same as in Eq. (164). The first term of Eq. (165), involving G_{0000}, corresponds to the static-muon approximation. This approximation was made at the beginning by Fujimoto (1975) and by Wilets and Rinker (1975). Its validity was verified explicitly by Borie (1976a); the contribution of the other terms corresponding to muon recoil is a factor 50 less than the leading contribution in the case of levels of interest for tests of QED, although these terms could become more important for the *ls* state in heavy elements. In addition, we set the nuclear form factors equal to unity; as a result, the potential which we shall obtain will not be a useful approximation at short distances (of the order of magnitude of the nuclear radius). This is unimportant for states of interest in tests of QED. For more tightly bound states, our result will still give the correct order of magnitude for this contribution.

The only vector quantity remaining after integration over k_2 and k_3 is $\mathbf{q}$. By symmetry, the last term in Eq. (165) then vanishes. We finally obtain

$$S=i\delta(q_0)\bar{u}(p_2)\gamma^0u(p_1)\frac{\alpha^4Z^2}{4\pi^4}\int\frac{d^4k_2}{k^2(q-k_2)^2}\frac{1}{2m\omega'-i\varepsilon}\int\frac{d^3k_3}{|\mathbf{k}_3|^2|\mathbf{q}+\mathbf{k}_3|^2}[2mG_{0000}+\tfrac{1}{2}q^i(G_{0i00}-G_{i000})]\,. \tag{166}$$

A comparison with the amplitude for potential scattering in Born approximation (99), (122) indicates that the desired Delbrück potential is given in momentum space by

$$\Delta V(q)=-\frac{iZ^2\alpha^4}{8\pi^5}\int\frac{d^4k_2}{k_2^2(q-k_2)^2}\int\frac{d^3k_3}{|\mathbf{k}_3|^2|\mathbf{q}+\mathbf{k}_3|^2}\left[\frac{G_{0000}}{\omega'-i\varepsilon}+\frac{q^i(G_{0i00}-G_{i000})}{4m\omega'-i\varepsilon}\right]. \tag{167}$$

Using the identity

$$\frac{1}{\omega'-i\varepsilon}=P\frac{1}{\omega'}+i\pi\delta(\omega') \tag{168}$$

(P denotes the principle value integral) and the fact that G_{0000} is an even function of $\omega'=k_{20}=-k_{10}(q_0=k_{30}=0)$, one finds

$$\Delta V(q)=\frac{Z^2\alpha^4}{8\pi^4}\int\frac{d^3k_3}{|\mathbf{k}_3|^2|\mathbf{q}+\mathbf{k}_3|^2}\left[\int\frac{d^3k_2}{|\mathbf{k}_2|^2|\mathbf{q}-\mathbf{k}_2|^2}G_{0000}-\frac{i}{4\pi m}\int\frac{d^4k_2}{(\omega'^2-|\mathbf{k}_2|^2)(\omega'^2-|\mathbf{q}-\mathbf{k}_2|^2)}\frac{q^i(G_{0i00}-G_{i000})}{\omega'}\right] \tag{169}$$

Retardation effects are thus seen to be unimportant in the first term of Eq. (169), in agreement with the conclusions of other authors who have calculated this effect.

In order to calculate $\Delta V(q)$, it is now necessary to integrate over the momenta k_2 and k_3. The components of the fourth-order VP tensor are given, as in Papatzacos and Mork (1975) and Borie (1976a), as integrals over the Feynman parameters x, y, and z. The two k integrations require the introduction of four further Feynman parameters. The resulting sevenfold integral had to be performed numerically. Some details are given by Borie (1979). Since the calculation is not particularly simplified by neglecting the electron mass, and since the value of $q\simeq Z\alpha m/n$ which is relevant for the transitions of interest here is not really much larger than m_e, the electron mass was not neglected.

Since the nuclear form factors were set equal to unity in Eq. (167), the quantity $\Delta V(q)/(Z\alpha)^2$ is independent of atomic number. This quantity was computed numerically for several values of q between 10^{-5} fm^{-1} and 1 fm^{-1}, which is the appropriate range of momentum transfer for a bound muon. Several different integration methods were used, with the results shown in Table II. Many numerical QED calculations use some version of the adaptive Monte Carlo routine RIWIAD (Lautrup, 1971) for computing multiple integrals; however, this program required more computer time than was available to obtain sufficiently accurate results. Some results obtained in tests, using three iterations and 128 points per iteration, are given in the table. Another method which was used consisted of doing five integrations using an iterated Gaussian method [RGAUSS; see Lautrup (1971)], varying the number of iterations along each of the five axes until the results remained stable. The results of the fivefold integration are estimated to be reliable to about 10% (better for small q). The last two integrations were performed using either Simpson's rule (10 points per axis) or Gauss' method (12 points per axis). The numerical results obtained using these three different methods are similar, as can be seen in Table II; the numerical uncertainties can be estimated from the spread in the results. Since the resulting energy shifts turned out to be small, it did not seem to be worth the effort to improve on the numerical accuracy. One also notes that the contribution due to muon motion [from the second term of Eq. (167)] is negligible for $q<m\simeq 0.535$ fm^{-1}. For transitions of interest in tests of QED, the momentum transfer of interest is 0.1–0.2 fm^{-1} or less; the approximations used in the calculation (neglect of nuclear form factors, nonrelativistic motion of the muon) break down for larger values of q in any case.

For $q>>m_e\simeq 2.6\times10^{-3}$ fm^{-1}, the potential is given approximately by

$$\Delta V(q)=\frac{\pi\alpha^2}{q^2}(Z\alpha)^2C\ , \tag{170}$$

where $C\simeq 0.10\pm0.03$ was obtained from a weighted average of values of $\Delta V(q)$ for $q=1$ fm^{-1} in Table II. Fujimoto (1975) obtained a somewhat smaller value for C. Deviations from the behavior (170) are noticeable for $q\simeq 0.1$ fm$^{-1}\simeq 25\alpha m_\mu$, i.e., precisely the range of interest for the calculation of muonic energy levels. For $q<<m_e$, $\Delta V(q)$ approaches a constant. This means that $\Delta V(r)<\exp(-m_e r)$ for $r\to\infty$.

The behavior of $\Delta V(r)$ is shown (for $Z=80$) in Fig. 20. The potential is attractive, leading to an increase in binding energy. At small distances, $\Delta V(r)$ is approximately proportional to r^{-1}; this behavior would of course be modified if the nuclear form factors had been correctly taken into account. A rough estimate of the effect can be obtained by multiplying $\Delta V(q)$ by the nuclear form factor (strictly speaking, this procedure is some-

TABLE II. Effective potential for the virtual Delbrück effect as a function of q; the results of various integration methods are given in order to check the numerical accuracy. The displayed quantity $-q^2\Delta V(q)/(Z\alpha)^2$ is dimensionless.

Integration method q (fm^{-1})	7 G	5 G + 2 Simpson	RIWIAD (3 iterations, 128 intervals)
10^{-5}	-1.4×10^{-10}	-0.6×10^{-10}	. . .
10^{-4}	-1.4×10^{-8}	-0.6×10^{-8}	. . .
10^{-3}	-6.8×10^{-7}	-0.5×10^{-7}	$(-8.0\pm4.0)\times10^{-7}$
10^{-2}	0.9×10^{-5}	1.4×10^{-5}	$(0.6\pm0.4)\times10^{-5}$
10^{-1}	7.0×10^{-5}	4.0×10^{-5}	$(4.9\pm1.3)\times10^{-5}$
1	8.0×10^{-5}	4.5×10^{-5}	$(5.6\pm2.3)\times10^{-5}$

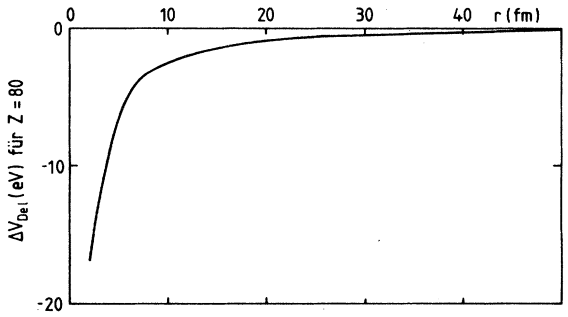

FIG. 20. ΔV_{Del} (eV) as a function of the muon-nuclear separation r, for mercury.

what inconsistent). The contribution to the binding energy of the $1s$ state of medium to heavy elements is thereby reduced somewhat; there is almost no effect on states with high orbital angular momentum.

Table III shows the contribution of the virtual Delbrück effect to several muonic transitions which are of interest for tests of QED (see also Table VII below). The estimated uncertainty of 20% is due to the numerical uncertainty in the evaluation of $\Delta V(q)$, and probably overestimates the error in the transition energies, which turned out to be far less sensitive to variations in $\Delta V(q)$ than the binding energies themselves.

Although the potential which has been derived cannot be expected to give a reliable energy shift for the ground state of heavy muonic elements, it is still of interest to apply the previous results to the $1s$, $2s$, and $2p$ states of heavy elements, to get an idea of the size of the effect in this case. Some results for Nd ($Z=60$) and Hg ($Z=80$) are given in Table IV, along with other corrections of order $\alpha^2 Z\alpha$. Rinker and Steffen (1977) estimate an even smaller value for the contribution. We observe that the virtual Delbrück effect and the fourth-order muon Lamb shift tend to cancel each other. In any case, both corrections are much smaller than the theoretical uncertainties

TABLE III. Contribution of the virtual Delbrück effect to various muonic transitions.

Element	Transition	Contribution (eV)
$_{2}$He	$2s$-$2p$	0.00002
$_{12}$Mg	$4f$-$3d$	0.002
	$3d$-$2p$	0.013
$_{14}$Si	$4f$-$3d$	0.003
	$3d$-$2p$	0.027
$_{45}$Rh	$5g$-$4f$	0.1
	$4f$-$3d$	0.4
$_{56}$Ba	$5g$-$4f$	0.3
	$4f$-$3d$	1.0
$_{80}$Hg	$7i$-$6h$	0.2
	$7i$-$5g$	0.5
	$6h$-$5g$	0.4
	$5g$-$4f$	1.1
$_{82}$Pb	$6h$-$5g$	0.4
	$5g$-$4f$	1.2

arising from nuclear polarizability, two-photon recoil, binding corrections to the self-energy, hadronic vacuum polarization, and nuclear charge density.

B. Self-energy

1. Orders $\alpha(Z\alpha)^n$, $n \geqslant 1$

The muon Lamb shift takes into account the self-energy of the muon (more precisely, the difference between the self-energy of a bound and a free muon), and the muon anomalous magnetic moment. In principle, this contribution to the binding energy should be calculated in the bound-interaction picture, taking into account the effect of the nuclear Coulomb field on the

TABLE IV. Contributions of various higher-order corrections to the binding energies of selected states in some muonic atoms. ΔE_{Del} is the virtual Delbrück effect [order $\alpha^2(Z\alpha)^2$]; $\Delta E_{\mathrm{LS}}^{(4)}$ is the fourth-order Lamb shift [order $\alpha^2(Z\alpha)$]; $\Delta E_{\mathrm{VP}}^{(4)}$ is the fourth-order muonic vacuum polarization [order $\alpha^2(Z\alpha)$]; $\Delta E_{\mu e}$ is the mixed μ-e vacuum polarization [order $\alpha^2(Z\alpha)$].

Element	Level	ΔE_{Del}	$\Delta E_{\mathrm{LS}}^{(4)}$	$\Delta E_{\mathrm{VP}}^{(4)}$	$\Delta E_{\mu e}$
$^{146}_{60}$Nd	$1s_{1/2}$	18.9±4.7	−16.3	1.4	0.9
	$2s_{1/2}$	4.4±0.8	−2.6	0.2	0.2
	$2p_{1/2}$	6.9±1.4	−0.7	0.1	0.1
	$2p_{3/2}$	6.3±1.2	−1.1	0.1	0.0
$^{200}_{80}$Hg	$1s_{1/2}$	35.8±9.8	−23.7	2.1	1.4
	$2s_{1/2}$	10.2±1.9	−4.1	0.4	0.2
	$2p_{1/2}$	17.3±3.8	−3.0	0.4	0.2
	$2p_{3/2}$	16.0±3.4	−3.5	0.3	0.1
	$2d_{3/2}$	5.2±0.5	0.1	0.0	0.0
	$2d_{5/2}$	5.1±0.5	−0.2	0.0	0.0

muon propagator. Figure 21 shows the reduction of the self-energy graph in the bound-interaction picture to a set of vertex graphs [here double lines represent lepton wave functions or propagators in the presence of an external field, single lines the corresponding quantities in the absence of the external field (see Jauch and Rohrlich, 1955)]. In practice, this contribution is approximated by the vertex correction [Fig. 21(b)]. However, this contribution by itself contains infrared divergences arising from low values of the photon momentum, which are compensated by similar terms from diagram 21(c); this illustrates the inapplicability of simple perturbation expansions in bound-state problems. Here, the binding provides an infrared cutoff which is neglected when using free-lepton propagators as in Fig. 21(b). The point is that, when one continues the expansion in powers of $V \propto Z\alpha$, one discovers that the extra factors $Z\alpha$ can be compensated by factors p^{-1}, where $p \simeq mZ\alpha$, in the momentum integrals. If the contribution of Fig. 21(b) is approximated by calculating the Coulomb propagator and muon form factors in the nonrelativistic limit, one obtains the commonly used result, namely,

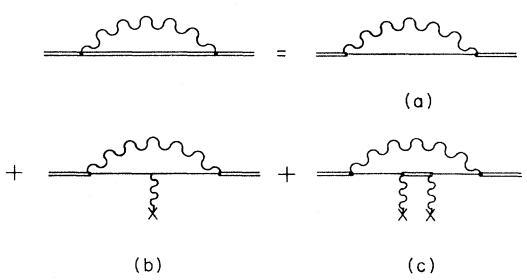

FIG. 21. Contributions to lepton self-energy. See text for explanation.

$$\Delta E_{nl} = -\frac{\alpha}{3\pi m^2}\langle \nabla^2 V(r)\rangle_{nl}\left[\ln\left[\frac{m}{2\Delta E_{nl}}\right]+\frac{11}{24}\right]-\frac{\alpha}{2\pi m^2}\langle -i\boldsymbol{\alpha}\cdot\nabla V(r)\rangle\ , \tag{171}$$

where ΔE_{nl} is Bethe's average excitation energy (Bethe, 1947), defined by

$$\ln\left[\frac{m}{2\Delta E_{nl}}\right]=\frac{2}{\langle \nabla^2 V(r)\rangle_{nl}}\sum_{n'l'}|\langle nl\,|\,\mathbf{p}\,|\,n'l'\rangle|^2(E_{n'l'}-E_{nl})\ln\left[\frac{m}{2\,|E_{n'l'}-E_{nl}|}\right]. \tag{172}$$

One arrives at more familiar forms for the last term of Eq. (171) by observing that

$$\langle -i\boldsymbol{\alpha}\cdot\nabla V(r)\rangle = m_r\int_0^\infty dr\,\frac{dV(r)}{dr}G_{n\kappa}(r)F_{n\kappa}(r)=\left\langle -\frac{1}{4}\nabla^2 V(r)-\frac{1}{2r}\frac{dV(r)}{dr}\boldsymbol{\sigma}\cdot\mathbf{L}\right\rangle . \tag{173}$$

One sees that the Bethe sum involves terms of all orders in the external potential, although terms of higher order than $Z\alpha$ are treated only approximately.

It does not make sense in this case to try to make an order-by-order extraction of contributions. Methods for a full calculation which avoids the pitfalls of perturbation expansions have been given by Cheng *et al.* (1978), Desiderio and Johnson (1971), Cheng and Johnson (1976), Mohr (1974a, 1974b, 1975, and Brown *et al.* (1959). These involve lengthy and difficult numerical calculations which, for the case of muonic atoms, have only been performed for the ground state of heavy elements, and therefore the approximation (171) due to Barrett *et al.* (1968); Barrett, 1968 is used in most cases. The main uncertainty (aside from relativistic contributions to the propagators in diagram 21(c), and the q^2 dependence of diagram 21(b), which are neglected) is the appropriate value of the Bethe sum (172), which is complicated by the effect of nuclear size. For the 1*s* state one has used strict upper and lower bounds due to Bethe and Negele (1968). More recently Klarsfeld (1977a, 1977b) calculated a number of values of Bethe logarithms to use in this connection. The validity of this approximation for the 1*s* state was confirmed by the numerical results of Cheng *et al.* (1978). It has been shown with the aid of Klarsfeld's results that the mean of the Bethe-Negele bounds provides a reasonable semiempirical approximation to the more laboriously calculated values (Rinker and Steffen, 1977). This mean value is given by

$$\ln\left[\frac{m}{2\Delta E}\right]\simeq\tfrac{1}{2}\ln\left[\frac{m_r^2\langle p^2\rangle}{4\langle dV/dr)^2\rangle}\right], \tag{174}$$

with $\langle p^2\rangle=\langle [E-V(r)]^2-m_r^2\rangle$. Equation (174) incorporates the high-energy cutoff of (172) due to the finite nuclear size. This cutoff limits the momenta in intermediate states to $p \lesssim R_N^{-1}$, where R_N is the nuclear radius. Where this momentum is smaller than that corresponding to Bethe's average excitation energy for a point nucleus, Eq. (174) provides a better estimate of the Bethe sum than does the point-nucleus calculation. Otherwise, the opposite is the case. This second situation occurs when the muon overlap with the nucleus is small ($\langle \nabla^2 V\rangle=\langle 4\pi\rho\rangle \to |\psi(0)|^2$), i.e., for all non-*s* states in very light muonic atoms, and for the high-lying states in heavy muonic atoms. For $l\neq 0$, the vertex correction is then given by

$$\Delta E_{nl}\simeq\frac{4\alpha(Z\alpha)^4}{3\pi n^3}m_r\left[\left[\frac{m_r}{m}\right]^2\ln K_{nl}+\frac{3}{8}\frac{m_r}{m}\frac{1}{(2l+1)\kappa}\right], \tag{175}$$

with values of $\ln K_{nl}=\ln[2\Delta E/(Z\alpha)^2 m_r]$ taken from the

TABLE V. Point-nucleus Bethe sums $\ln K_{nl}$ for use with transitions between states having negligible overlap with the nucleus. Values are taken from Klarsfeld and Maquet (1973).

n	$l=0$	$l=1$	$l=2$	$l=3$	$l=4$	$l=5$
1	2.98413					
2	2.81177	−0.03002				
3	2.76766	−0.03819	−0.00523			
4	2.74982	−0.04195	−0.00674	−0.00173		
5	2.74082	−0.04403	−0.00760	−0.00220	−0.00077	
6	2.73566	−0.04531	−0.00815	−0.00250	−0.00096	−0.00041

work of Klarsfeld and Maquet (1973). These are given in Table V. For such states (including most of those of interest for tests of QED using muonic atoms), the vertex correction is dominated by the spin-orbit part of the muon's anomalous magnetic moment.

A rough estimate of neglected higher-order effects (Fig. 21c) was given by Barrett *et al.* (1968). Comparison of this estimate, along with Eqs. (171) and (174), to the numerical calculations of Cheng *et al.* (1978) showed that if

$$\Delta E_{nl}^{(2)}=\frac{\alpha}{3\pi m_r}\left\langle\left[\frac{dV(r)}{dr}\right]^2\right\rangle\frac{\ln(\langle p^2\rangle/m_r^2)}{(\langle p^2\rangle-m_r^2)} \tag{176}$$

is added to Eq. (171), using Eq. (174), a slight improvement with respect to the theoretical results is obtained in all cases where comparison may be made.

2. Orders $\alpha^2(Z\alpha)^n$, $n\geqslant 1$

Higher-order self-energy corrections (of order $\alpha^2 Z\alpha$), corresponding to the diagrams in Fig. 22, have been calculated by Borie (1975b). The contribution of diagrams 20a–e (with a $\mu^+\mu^-$ pair in the VP loop) was calculated as in the work of Appelquist and Brodsky (1970) and Barbieri *et al.* (1972a, 1972b). The contribution of diagram 20a, with an e^+e^- pair in the loop, was taken from the work of Barbieri *et al.* (1973). The result is

$$\Delta E_{\rm LS}^{(4)}=\frac{1}{m_\mu^2}\langle\nabla^2 V\rangle\left[m_\mu^2\frac{\partial F_1^{(4)}}{\partial q^2}\right]_{q^2=0}+\frac{(g-2)^{(4)}}{4m_\mu^2}\left[\langle\nabla^2 V\rangle+\left\langle\frac{2}{r}\frac{dV}{dr}\boldsymbol{\sigma}\cdot\mathbf{L}\right\rangle\right], \tag{177}$$

with

$$\left[m_\mu^2\frac{\partial F_1^{(4)}}{\partial q^2}\right]_{q^2=0}=\left[\frac{\alpha}{\pi}\right]^2\left[\frac{\pi^2}{2}\left[\ln 2-\frac{49}{216}\right]-\frac{4819}{5184}-\frac{3}{4}\zeta(3)+\frac{1}{9}\ln^2\left[\frac{m_\mu}{m_e}\right]-\frac{29}{108}\ln\left[\frac{m_\mu}{m_e}\right]+\frac{\pi^2}{54}+\frac{395}{1296}\right]$$

$$=2.69\left[\frac{\alpha}{\pi}\right]^2, \tag{178}$$

and

$$\tfrac{1}{2}(g-2)^{(4)}=\left[\frac{\alpha}{\pi}\right]^2\left[\frac{197}{144}+\frac{\pi^2}{2}\left[\frac{1}{6}-\ln 2\right]+\frac{3}{4}\zeta(3)+\frac{1}{3}\ln\left[\frac{m_\mu}{m_e}\right]-\frac{25}{36}+O\left[\frac{m_e}{m_\mu}\right]\right]=0.766\left[\frac{\alpha}{\pi}\right]^2. \tag{179}$$

Note that $(g-2)^{(4)}/2$ is the fourth-order contribution to the anomalous magnetic moment of the muon (Bailey *et al.*, 1979; Lautrup *et al.*, 1972).

C. Anomalous interactions

Any contribution to the energy levels of a muonic atom whose source is a difference between the muon-nucleus and the electron-nucleus interaction (other than those due to mass differences) is called an anomalous interaction. For example, such a difference could be present if the muon were not pointlike; one consequence of a finite radius for the muon would be a difference between the cross sections for ep and μp scattering (Hughes and Kinoshita, 1977). A finite muon radius would also result in a disagreement between nuclear radii determined by means of electron scattering and those determined from muonic atoms (Rinker and Wilets, 1973b; Dubler *et al.*, 1974). From this work one can conclude that

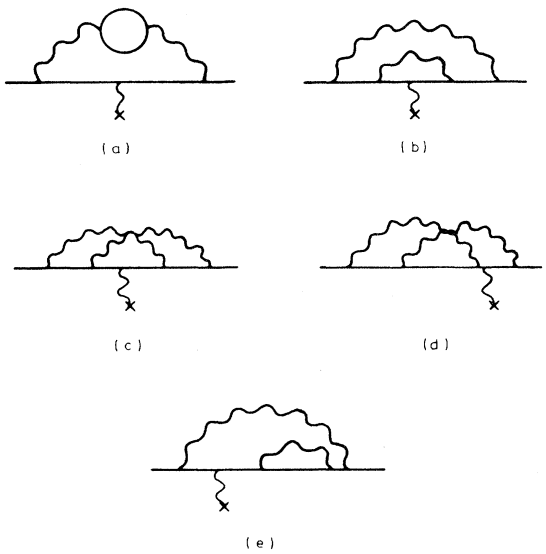

FIG. 22. Fourth-order Lamb shift diagrams. Diagram (a) enters once with an e^+e^- pair and once with a $\mu^+\mu^-$ pair.

$$\langle r_\mu^2\rangle^{1/2}-\langle r_e^2\rangle^{1/2}<0.17 \text{ fm} . \tag{180}$$

A tighter bound is obtained from the latest measurement of $g_\mu-2$ (Bailey *et al.*, 1979), which gives

$$\langle r_\mu^2\rangle^{1/2}<0.03 \text{ fm} . \tag{181}$$

The latest result from $e^+e^-\rightarrow\mu^+\mu^-$ at PETRA is $\langle r_\mu^2\rangle^{1/2}<0.01$ fm (Barber *et al.*, 1979a, 1979b). Another possible source of an anomalous interaction would be the exchange of a scalar particle which couples differently to the muon than to the electron. Such a particle, the Higgs boson, is predicted to exist in unified gauge theories of the weak and electromagnetic interactions (Bernstein, 1974; Weinberg, 1974; Abers and Lee, 1973). The exchange of a scalar particle results in a Yukawa interaction between a lepton and a nucleus (Fig. 23). According to Jackiw and Weinberg (1972), this interaction is given by

$$V_\phi(r)=g_\phi\frac{e^{-m_\phi r}}{r} , \tag{182}$$

with

$$g_\phi=\sqrt{2}Gm_l^2A\xi=1.8\times10^{-7}\frac{m_l^2}{m_\mu^2}A\xi . \tag{183}$$

Here m_l is the lepton mass, m_ϕ the mass of the Higgs boson, A the atomic mass number of the nucleus, G the weak coupling constant, and ξ a dimensionless constant of order unity. We shall discuss explicit bounds of g_ϕ as a function of the ϕ mass in connection with particular experiments later.

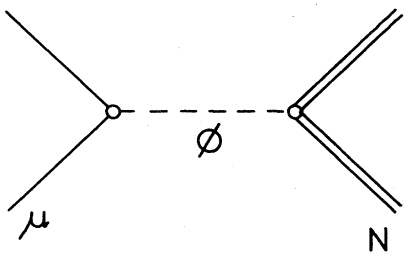

FIG. 23. Muon-nuclear interaction mediated by a Higgs boson.

D. Experimental tests of QED with muonic atoms

The predictions of QED have been verified to a very high degree of accuracy. (See, e.g., Brodsky and Drell, 1970; Bailey and Picasso, 1970; Combley, Farley, and Picasso, 1981; Van Dyck, Schwinberg, and Dehmelt, 1977; Drell, 1979.) As a consequence, QED is regarded as the most successful theory in physics, and is taken as the example for all other theories, such as the presently popular QCD, which describes the interaction of quarks and gluons. After a qualitative discussion of the physical origin of the effects whose computation was discussed in Sec. III.A and III.B, we discuss in detail the more recent experimental tests of QED with muonic atoms.

As first approximation, the motion of a muon or electron can be described by the Dirac equation. The lepton is regarded as a pointlike particle with spin $\frac{1}{2}$, which interacts with a given (classical) electromagnetic field. The quantization of the electromagnetic field results in departures from this simple picture, which are often known as "radiative corrections" (although perhaps improperly so for the case of vacuum polarization). These are due to the interaction of the electron or muon with the electromagnetic field and involve the emission and/or absorption of photons. These photons may be real, as in the well-known case of bremsstrahlung emission by an accelerated charged particle, or virtual,[3] in which case they are reabsorbed, either by the lepton or by another particle. The fact that these radiative effects have experimentally measurable consequences accounts for the great interest which has been devoted to the subject of QED, since it is possible to test the theory to a high degree of precision, providing a challenge both to theorists and to experimentalists.

[3]The concept of a virtual photon is useful for the application of perturbation theory. Such photons have a "mass" due to the fact that they do not obey the simple dispersion law $\omega=ck$. In addition, and in contrast to real radiation, they are not in general polarized perpendicular to their direction of propagation.

It is well known that QED describes many phenomena, such as the anomalous magnetic moment of the electron and muon, atomic energy levels (including the Lamb shift), the hyperfine structure of muonium and positronium, and the scattering of high-energy leptons ($e^+e^-\to e^+e^-,\mu^+\mu^-,\gamma\gamma,\ldots$) with a remarkable precision. One might ask why one should study tests of QED with muonic atoms when these other tests have already verified the essential correctness of QED. As we shall see, the tests with muonic atoms are complementary.

Another point of interest is that even if one believes in QED, the question remains as to whether the muon might have some sort of anomalous interaction with itself or with hadrons. As far as we know, the muon behaves exactly like a heavy electron; the reason for this is an as-yet-unexplained puzzle, which was made even more interesting by the recent discovery of the τ lepton. A model for an anomalous muon-hadron interaction is provided by the gauge theories which unify the weak and electromagnetic interactions. In such theories there is the possibility of exchanging a so-called "Higgs boson" between a muon and a nucleus (Fig. 23), which would result in an extra nonelectromagnetic contribution to the binding energy. Muonic atoms can be used to shed light on these questions, although at the moment there is no evidence for such anomalous interactions.

Muonic atoms are particularly well suited for the study of vacuum polarization. This effect was investigated shortly after the discovery of the positron (Heisenberg, 1934; Furry and Oppenheimer, 1934; Serber, 1935; Uehling, 1935) and is thus one of the earliest-studied QED effects. It is due to the virtual production and reannihilation of electron-positron (or $\mu^+\mu^-$, $\pi^+\pi^-$, $\bar{p}p$,...) pairs. The presence of these virtual pairs slightly modifies the electric field produced by a given charge distribution. The effect is analogous to classical electrostatics in a medium; in that case the observed electric field is the superposition of the fields produced by the "true" and "polarization" charges. In the case of vacuum polarization, this separation is similar in principle; however, the analogy should not be pushed too far, since in this case the induced "polarization charge" is mathematically not well defined even though the resulting electric field is. The result of a detailed calculation (including renormalization) shows that at large distances (compared to the electron Compton wavelength $m_e^{-1}\simeq 386$ fm), the "true" nuclear charge is screened by the virtual electron charge. By definition, the classical observed nuclear charge is the charge which at macroscopic distances results in the observed Coulomb interaction with a test charge. If the test charge came closer to the nucleus, it would "feel" the "bare" nuclear charge, which is larger than the classically defined charge Ze. We thus expect that vacuum polarization results in a modification of Coulomb's law at distances less than m_e^{-1}, such that the electric field strength is increased. Such a modification of the Coulomb interaction between two charged particles should result, among other things, in a shift of the energy levels of hydrogenlike atoms. One should expect increased binding for all cases in which the radius of the lepton orbit is less than, or comparable to, the electron Compton wavelength.

In order to get a feeling for the magnitude of the effect, we consider the hydrogen atom. In the case of normal hydrogen the radius of the electron orbits is given by the Bohr radius

$$a_0=(m_e\alpha)^{-1}\simeq 52\,918 \text{ fm} \tag{184}$$

and the momentum of the electron is approximately given by $\alpha m_e c$. The effects of vacuum polarization are then small compared to those of other radiative corrections, notably the self-energy and additional spin-orbit interaction resulting from the anomalous magnetic moment of the electron. For example, the $2s_{1/2}$ state lies 4.38 μeV (1057.9 Mhz) above the $2p_{1/2}$ state (Fig. 24) (see Lundeen and Pipkin, 1975; Andrews and Newton, 1976). The contribution due to vacuum polarization is only -0.11 μ eV (-27 Mhz).

If we now replace the electron by a negatively charged muon, the Bohr radii are reduced by a factor $m/m_e\simeq 207$ as compared to those for normal atoms

$$a_{0\mu}\simeq 256 \text{ fm} \tag{185}$$

and are generally less than m_e^{-1}. The effects of VP are correspondingly much larger. In muonic hydrogen, the $2s_{1/2}$ level lies 202.0 meV *below* the $2p_{1/2}$ level (Fig. 25). The difference in binding energy due to VP is 206.4 meV, while that due to the self-energy and anomalous magnetic moment is only 0.6 meV. Even higher-order VP corrections are non-negligible in this case. Thus muonic atoms can be used to test vacuum-polarization effects with minimal disturbance from other radiative corrections.

Of course in order to test QED it is necessary to choose transitions between orbits which are not significantly affected by the effects of nuclear structure or by the remaining atomic electrons. However, if one is careful about the choice of transition, it is possible to study a nearly hydrogenlike system even in the limit of strong fields (i.e., $Z\alpha$ not small, as is the case for lead).

1. Heavy elements

With high-Z elements ($Z>40$) one hopes to be able to test QED in the case of strong electromagnetic fields. A

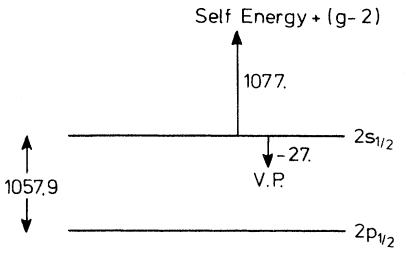

FIG. 24. Lamb shift in hydrogen. Intervals are given in Mhz.

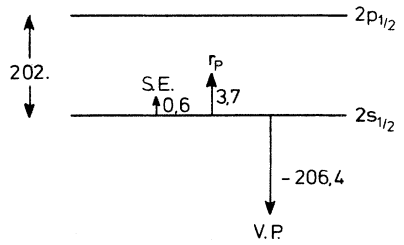

FIG. 25. Lamb shift in muonic hydrogen. Intervals are given in meV.

muon in the $4f$ level of muonic lead experiences an electric field strength of about 4.7×10^{19} V/m at a mean distance of 50 fm from the nucleus. In this case we are dealing with a system in which one of the important expansion parameters, namely $Z\alpha$, is not small. We may expect that effects such as Coulomb corrections to the electron propagator in vacuum polarization are measurable in just such systems, and should attempt to look for these effects by investigating transitions between hydrogenlike states in heavy muonic atoms. These states are chosen to have large orbital angular momentum, in order to minimize uncertainties in the calculated transition energies which arise from uncertainties in nuclear properties. The states in question should also have Bohr radii which are small in comparison to the radii of the electron orbits.

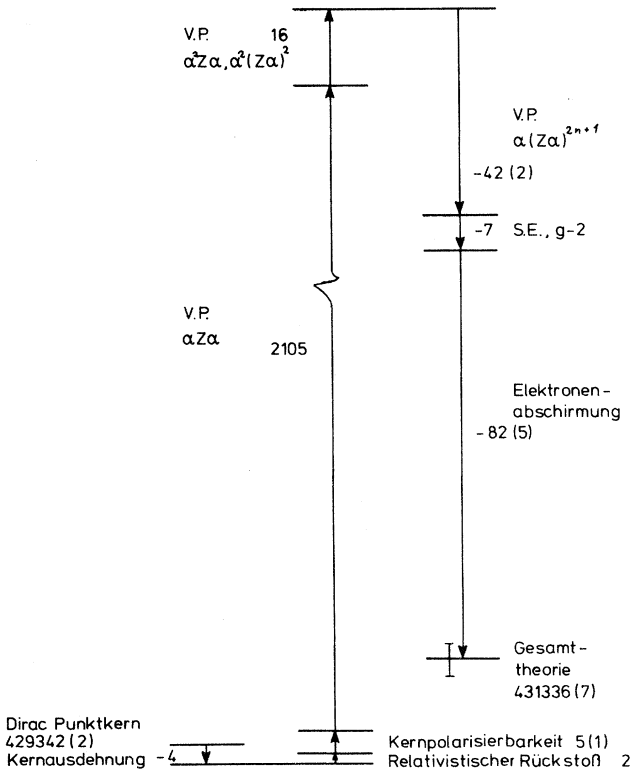

FIG. 26. Theoretical contributions (eV) to the $5g_{9/2}-4f_{7/2}$ transition in muonic lead.

The theoretical contributions to the $5g_{9/2}-4f_{7/2}$ transition in muonic lead are shown schematically in Fig. 26. The contributions to the theoretical transition energies for other cases are summarized in Table VI.

Between 1970 and 1976 there were indications of a discrepancy between theoretical and experimental transition energies for such transitions, hinting at a possible breakdown in the validity of QED in the limit of strong fields. This problem occupied a number of physicists and stimulated considerable work during this time.

In 1970 a group from Karlsruhe and CERN measured the $5g$-$4f$ transitions in lead and bismuth (Backenstoss *et al.*, 1970), finding agreement (within the experimental uncertainties) with the results of a calculation by Fricke (1969b) which included the VP corrections of order $\alpha^2Z\alpha$ and $\alpha(Z\alpha)^3$ for the first time. However, a subsequent experiment by a group from Chicago and Ottawa (Dixit *et al.*, 1971), with better resolution and smaller errors, indicated a systematic discrepancy between theory and experiment. These data included several elements throughout the periodic table. For the $5g$-$4f$ transitions in lead, the difference between theory and experiment amounted to 130 ± 20 eV, which also was in contradiction to the earlier result of Backenstoss *et al.* ($E_{\rm th}-E_{\rm exp}\simeq-30\pm40$ eV).

In 1972 several authors detected an error in the previous calculation of the order $\alpha(Z\alpha)^3$ corrections, as well as the fact that the "double-bubble" diagram of order $\alpha^2Z\alpha$ had been included twice (Blomqvist, 1972; Bell, 1973; Sundaresan and Watson, 1972). This substantially reduced the discrepancy between the results of the Chicago experiment and the theoretical predictions. However, the discrepancy was not completely eliminated (it amounted to 50 ± 20 eV for lead), and this was ground for concern.

In order to clarify the contradiction between the two earlier experiments, another CERN group (Walter *et al.*, 1972) undertook the measurement of similar transitions in Rh, Hg, and Tl. In this experiment the calibration procedure was somewhat improved by using ^{103}Rh and ^{203}Tl as targets. For these elements it is possible to measure delayed gamma rays from the muon capture reactions

$$^{203}\mathrm{Tl}(\mu,n\nu)^{202}\mathrm{Hg}^*;\ ^{202}\mathrm{Hg}^*\rightarrow{}^{202}\mathrm{Hg}+\gamma(439.5\ \mathrm{keV}),$$

$$^{103}\mathrm{Rh}(\mu,n\nu)^{102}\mathrm{Ru}^*;\ ^{102}\mathrm{Ru}^*\rightarrow{}^{102}\mathrm{Ru}+\gamma(474.8\ \mathrm{keV}) \quad (186)$$

in the muonic x-ray spectra. The same lines are also measured as calibration lines, thus making it possible to control possible systematic errors arising from differences in the experimental geometry when the muonic x-ray spectra and calibration spectra were taken, which could cause a shift in the calibration line (within the statistical uncertainty of ±17 eV this effect was found to be zero). The results of this experiment were consistent with those of Dixit *et al.* (1971) and were taken as a confirmation of those results. The situation at the end of 1972 is summarized in Fig. 27; the difference between theory and experiment (in eV) is shown as a function of transition en-

ergy for all of the above-mentioned experiments. The discrepancy for transition energies around 400 keV was considered to be serious.

At this point most further work was coming from the theoretical side. In 1973 a fully self-consistent calculation of the electron-screening effect for all of the relevant transitions appeared (Vogel, 1973b; see also Fricke, 1969b). In any case this correction was too small to explain the discrepancy for the $4f$-$3d$ transitions in barium ($\delta E_{\rm scr} \simeq -17$ eV, $E_{\rm th} - E_{\rm exp} \simeq 81 \pm 21$ eV). Transitions among higher states (such as 7-6, 7-5, 6-5, 8-6 in Hg, Tl, Pb), which are more sensitive to screening corrections, were measured in order to check the validity of the calculated screening correction (see Sec. II.I).

In addition, the Coulomb correction to the electron propagator [the vacuum-polarization corrections of order $\alpha(Z\alpha)^3$, etc.], including the effect of finite nuclear size, were more thoroughly investigated. Older calculations (Fricke, 1969b; Blomqvist, 1972; Bell, 1973; Sundaresan and Watson, 1972) were based on the work of Wichmann and Kroll (1956), in which the Laplace transform of the induced charge density for the case of pointlike sources for the external field was calculated. From this it was possible to determine an effective potential, which was used to calculate energy shifts. At small distances this potential should be modified by the effect of finite nuclear size. One approach (Brown *et al.*, 1975a, 1975b, 1975c; Arafune, 1974) consisted of simplifying the calculation by setting the electron mass equal to zero and calculating directly the long-range part of the finite-size effect. At first glance it would appear that setting $m_e = 0$ should not be a good approximation, as the bound electron states which enter importantly in Eq. (146) exist only for $m_e \neq 0$. Nevertheless, it was shown analytically by both groups that errors in such an approach are of order m_e^2 and not m_e. This conclusion was later supported by numerical calculations (Rinker and Wilets, 1975), in which it was shown that the charge contributed by the bound states is very nearly canceled by the low-lying continuum states for any mass $\lesssim m_e$. These calculations yielded a small shift (4–7 eV in barium and lead) of the wrong sign to account for the discrepancies between theory and experiment.

A further calculation was performed by Gyulassy (1974, 1975) which essentially followed the approach of Wichmann and Kroll except that the Pauli-Villars method of regularization was used and the electron Green's function was corrected for finite nuclear size by the use of simple models for the nuclear charge distribution (uniformly charged sphere, shell of charge). It turns out that the main modification is a change in the s-wave contribution ($j = \frac{1}{2}$, $\kappa = -1$) to the electron propagator. Gyulassy (1975) showed that small differences (of about 1 eV) between his number (6 eV for the $5g$-$4f$ transitions in lead) and those of Arafune (1974) and Brown *et al.* (1974) could be accounted for by the approximation made in taking the electron mass equal to zero, or in expansions in the ratio (R_N/a_{0_μ}). The work of these authors removed this important source of theoretical uncertainty and confirmed the theoretical values for the measured transitions, up to as yet uncalculated higher-order QED corrections and contributions due to an anomalous interaction. The situation as of 1974 was summarized in two reviews of Watson and Sundaresan (1974) and of Engfer *et al.* (1975).

The possible effects of an anomalous interaction were investigated by several authors. If a light scalar boson ($m_\phi < 20$ MeV) with a muon-nucleus coupling of about $g_\phi \sim 10^{-7}$ existed, the discrepancy could be explained (Jackiw and Weinberg, 1972; Barshay, 1974; Adler, 1974; Adler, Dashen, and Treiman, 1974). Such a scalar boson would also have an effect on the anomalous magnetic moment of the muon, at a level which would have been observed ($\Delta a_\mu \simeq 7 \times 10^{-9}$). No such contribution has been detected (Borie, 1979). The influence of a ϕ boson on the energy levels of light muonic atoms would also have been observable (see next section), and measurements in such atoms rule out the existence of a scalar boson with mass < 10 MeV, with a muon-nucleus coupling of the strength suggested by the Weinberg-Salam model. Other anomalous contributions (Adler, 1974) could be ruled out on similar grounds. The only remaining theoretical explanation for the previously discussed discrepancy is the uncalculated higher-order QED corrections. The contribution of the fourth-order Lamb shift was calculated by Borie (1975b). The leading contribution for states of high orbital angular momentum is due to the extra spin-orbit interaction arising from the muon's anomalous magnetic moment. For the $5g$-$4f$ transitions in lead, this contribution is 0.025 eV, which is much too small to explain the reported discrepancy.

At about this time Chen (1975) made the suggestion that the virtual Delbrück diagrams of order $\alpha^2(Z\alpha)^2$ (Fig. 16) might be responsible for the discrepancy, and calculated a correction of -30 eV to the theoretical energy of the $5g$-$4f$ transitions in lead. However, an approximate calculation by Wilets and Rinker (1975) indicated that the correction was only $+1$ eV, increasing the discrepancy slightly. These calculations of the order-$\alpha^2(Z\alpha)^2$ correction involved a number of approximations, and were carried out using a noncovariant formalism (the central field problem is intrinsically noncovariant); it thus seemed to be desirable to calculate the effect of these diagrams using the methods of QED. The most complete calculation, published by Borie (1976a), confirms the approximate calculation of Wilets and Rinker and gives results for all measured transitions. This result was also confirmed for the $5g$-$4f$ transitions in lead by Fujimoto (1975). Thus no theoretical explanation for the discrepancy could be found.

At this point some movement took place on the experimental front. The problem was partially solved, also in 1975, when a group at the National Bureau of Standards discovered that the energy of a nuclear gamma line in gold (at $\simeq 411$ keV), which had been used for calibration in the experiments, had been in error by 12 eV (Deslattes *et al.*, 1975). All of the experimental transition energies, but especially those around 400 keV, had to be corrected

TABLE VI. Comparison between theoretical and experimental energies of several muonic transitions which are sensitive to vacuum polarization. Only recent experiments (since 1974) are included. All energies are in eV. E_{PT} = transition energy from Dirac equation for a point nucleus; δE_{FS} = correction due to finite nuclear size; δE_{VP} = vacuum polarization corrections of order $\alpha Z\alpha$, $\alpha^2 Z\alpha$, $\alpha(Z\alpha)^{n\geq 3}$, $\alpha^2(Z\alpha)^2$; δE_{LS} = muon self-energy, anomalous magnetic moment, muonic vacuum polarization; δE_R = relativistic recoil correction; δE_{NP} = nuclear polarization; δE_{ES} = electron screening (self-consistent with $Z-1$ electrons); E_{th} = total theoretical energy; E_{exp} = measured energy.

Element	Transition	E_{PT}	δE_{FS}	$\alpha Z\alpha$	$\alpha^2 Z\alpha$	$\frac{\delta E_{VP}}{\alpha(Z\alpha)^{n\geq 3}}$	$\alpha^2(Z\alpha)^2$
$_{12}Mg$[a]	$3d_{3/2}$-$2p_{1/2}$	56 213.9±0.2	−2.8±0.0	179.36±0.00	1.26	−0.11±0.00	0.01
	$3d_{5/2}$-$2p_{3/2}$	56 038.9±0.2	−0.9±0.0	177.55±0.00	1.24	−0.11±0.00	0.01
$_{14}Si$[a]	$3d_{3/2}$-$2p_{1/2}$	76 670.7±0.2	−7.4±0.0	276.8±0.00	1.94	−0.23±0.00	0.03
	$3d_{5/2}$-$2p_{3/2}$	76 345.5±0.3	−2.6±0.0	273.2±0.00	1.91	−0.23±0.00	0.03
$_{15}P$[a]	$3d_{3/2}$-$2p_{1/2}$	88 117.2±0.3	−11.9±0.2	335.4±0.00	2.34	−0.31±0.00	0.03
	$3d_{5/2}$-$2p_{3/2}$	87 688.1±0.3	−4.1±0.2	330.38±0.00	2.30	−0.30±0.00	0.03
$_{20}Ca$[b]	$3d_{3/2}$-$2p_{1/2}$	157 518 ±1	−78±2	734±2	5	−1±0.00	0.0
	$3d_{5/2}$-$2p_{3/2}$	156 152 ±1	−28±1	716±2	5	−1±0.00	0.0
$_{45}Rh$[c]	$4f_{5/2}$-$3d_{3/2}$	280 984 ±1	−20±0	1350±3	9	−9±1	0.4
	$4f_{7/2}$-$3d_{5/2}$	277 929 ±1	−7±1	1311±3	9	−9±1	0.4
$_{50}Sn$[b]	$4f_{5/2}$-$3d_{3/2}$	348 234 ±2	−50±1	1795±3	12	−13±1	0.7
	$4f_{7/2}$-$3d_{5/2}$	343 554 ±2	−19±1	1731±3	12	−13±1	0.7
$_{56}Ba$[b]	$4f_{5/2}$-$3d_{3/2}$	439 068 ±2	−143±1	2434±1	17	−21±1	1.0
	$4f_{7/2}$-$3d_{5/2}$	431 652 ±2	−55±1	2328±1	16	−19±1	1.0
	$5g_{7/2}$-$4f_{5/2}$	200 543 ±1	−0±0	762±1	5	−9±0	0.3
	$5g_{9/2}$-$4f_{7/2}$	199 193 ±1	−0±0	748±1	5	−9±0	0.3
$_{56}Ba$[d]	$4f_{5/2}$-$3d_{3/2}$	439 068 ±2	−143±1	2434±1	17	−21±1	1.0
	$4f_{7/2}$-$3d_{5/2}$	431 652 ±2	−55±1	2328±1	16	−19±1	1.0
$_{56}Ba$[e]	$4f_{5/2}$-$3d_{3/2}$	439 068 ±2	−143±1	2434±1	17	−21±1	1.0
	$4f_{7/2}$-$3d_{5/2}$	431 652 ±2	−55±1	2328±1	16	−19±1	1.0
$_{58}Ce$[e]	$4f_{5/2}$-$3d_{3/2}$	471 845 ±2	−193±1	2665±1	19	−24±1	1
	$4f_{7/2}$-$3d_{5/2}$	463 290 ±2	−74±1	2550±1	18	−22±1	1
$_{80}Hg$[c]	$5g_{7/2}$-$4f_{5/2}$	414 181 ±2	−9±0	2046±3	14	−40±2	1
	$5g_{9/2}$-$4f_{7/2}$	408 463 ±2	−3±0	1972±3	14	−39±2	1
$_{81}Tl$[c]	$5g_{7/2}$-$4f_{5/2}$	424 850 ±2	−9±1	2116±1	15	−42±2	1
	$5g_{9/2}$-$4f_{7/2}$	418 837 ±2	−3±0	2037±1	14	−40±2	1
$_{81}Tl$[e]	$5g_{7/2}$-$4f_{5/2}$	424 850 ±2	−9±1	2116±1	15	−42±2	1
	$5g_{9/2}$-$4f_{7/2}$	418 837 ±2	−3±0	2037±1	14	−40±2	1
$_{81}Tl$[b]	$5g_{9/2}$-$4f_{7/2}$	418 837 ±2	−3±0	2037±1	14	−40±2	1
$_{82}Pb$	$5g_{7/2}$-$4f_{5/2}$	435 664 ±2	−10±1	2189±1	16	−43±2	1
	$5g_{9/2}$-$4f_{7/2}$	429 343 ±2	−4±0	2105±1	15	−42±2	1
$_{82}Pb$[d]	$5g_{7/2}$-$4f_{5/2}$	435 664 ±2	−10±1	2189±1	16	−43±2	1
	$5g_{9/2}$-$4f_{7/2}$	429 343 ±2	−4±0	2105±1	15	−42±2	1
$_{82}Pb$[e]	$5g_{7/2}$-$4f_{5/2}$	435 664 ±2	−10±1	2189±1	16	−43±2	1
	$5g_{9/2}$-$4f_{7/2}$	429 343 ±2	−4±0	2105±1	15	−42±2	1

for this calibration error. As a result, the experimental energies increased somewhat and the discrepancy was reduced. The effect of this correction is indicated by the dashed line in Fig. 27. After a more complete data analysis and correction for the effect of the gold line, the experimental results of Vuilleumier *et al.* (1976) were almost in agreement with theory, even in the case of the $5g$-$4f$ transitions in Hg and Tl. Only the $5g$-$4f$ transitions in Pb and the $4f$-$3d$ transitions in Ba at around 430 keV still indicated any significant departure from the theoretical predictions.

At about the same time as these developments, new experimental contributions appeared and were in agreement with theory. The first came from CERN (Tauscher *et al.*, 1975); one advantage of this measurement was that the transitions in barium and lead were measured relative to each other, which provided a way of checking some systematic errors. Shortly thereafter, new results were also published by the Ottawa–Chicago group (Dixit *et al.*, 1975; Hargrove *et al.*, 1977) which also indicated agreement with theory and claimed smaller experimental errors. No reason for the difference between these new results and the previous experiment by this group (Dixit *et al.*, 1971) has been given.

Measurements to test QED in heavy muonic atoms have been continued at the meson factories. A group at Fribourg (Dubler *et al.*, 1978) remeasured the relevant transitions in Pb, Tl, and Ba, and also measured the $4f$-

TABLE VI. (*Continued*)

δE_{LS}	δE_R	δE_{NP}	δE_{ES}	E_{th}	E_{exp}	$E_{th}-E_{exp}$	$\frac{E_{th}-E_{exp}}{E_{th}}$(ppm)
0.24±0.00	0.18	0.03±0.00	−0.4±0.3	56 391.7±0.6	56 392.4± 0.9	−0.7± 1.1	−12± 20
−0.15±0.00	0.18	0.03±0.00	−0.4±0.3	56 216.4±0.6	56 216.2± 0.6	0.2± 0.8	4± 14
0.42±0.00	0.29	0.1 ±0.1	−0.5±0.4	76 942.3±0.6	76 942.9± 1.9	−0.6± 2.0	9± 26
−0.29±0.00	0.29	0.1 ±0.1	−0.5±0.4	76 617.6±0.6	76 617.2± 1.1	0.4± 1.2	5± 16
0.54±0.00	0.34	0.2 ±0.2	−0.5±0.4	88 443.2±0.6	88 425.5± 7.6	17.7± 7.6	200± 86
−0.51±0.00	0.34	0.2 ±0.2	−0.5±0.4	88 015.9±0.6	88 016.3± 2.5	−0.4± 2.6	−5± 30
1 ±0	1	3 ±2	−1 ±0.5	158 182 ±4	158 172 ± 7	10 ±8	63± 51
−1 ±0	1	2 ±1	−1 ±0.5	156 845 ±3	156 842 ± 5	3 ± 6	19± 38
4 ±0	1	4 ±2	−12 ±1	282 311 ±4	282 315 ±27	−4 ±28	14± 99
−3 ±0	1	4 ±2	−12 ±1	279 223 ±4	279 242 ±27	−19 ±28	−68±100
6 ±0	2	6 ±3	−13 ±1	349 980 ±5	349 975 ± 5	5 ± 7	14± 20
−4 ±0	2	5 ±3	−13 ±1	345 256 ±5	345 254 ± 7	2 ± 9	6± 26
9 ±1	4	10 ±2	−17 ±1	441 362 ±4	441 362 ± 5	0 ± 7	0± 16
−9 ±1	4	8 ±2	−17 ±1	433 909 ±4	433 905 ±10	4 ±11	9± 25
2 ±0	1	1 ±1	−31 ±1	201 274 ±3	201 275 ± 7	−1 ± 8	−4± 40
−1 ±0	1	1 ±1	−31 ±1	199 907 ±3	199 917 ± 5	−10 ± 6	−50± 30
9 ±1	4	10 ±2	−17 ±1	441 362 ±4	441 374 ± 9	−12 ±10	−27± 23
−9 ±1	4	8 ±2	−17 ±1	433 909 ±4	433 926 ± 8	−17 ± 9	−15± 21
9 ±1	4	10 ±2	−17 ±1	441 362 ±4	441 358 ± 8	4 ± 9	9± 20
−9 ±1	4	8 ±2	−17 ±1	433 909 ±4	433 897 ± 8	12 ± 9	27± 9
10 ±1	4	10 ±4	−18 ±1	474 329 ±6	474 330 ± 8	−1 ±10	−2± 21
−10 ±1	4	9 ±4	−18 ±1	465 748 ±6	465 754 ± 8	−6 ±10	−13± 21
7 ±0	2	6 ±3	−75 ±3	416 132 ±7	416 100 ±28	32 ±29	76± 70
−7 ±0	2	6 ±3	−77 ±3	410 331 ±7	410 292 ±28	39 ±29	95± 71
7 ±0	2	6 ±3	−79 ±3	426 868 ±6	426 851 ±29	17 ±30	39± 70
−7 ±0	2	6 ±3	−80 ±3	420 767 ±6	420 741 ±29	27 ±30	64± 71
7 ±0	2	6 ±3	−79 ±3	426 868 ±6	426 865 ± 8	3 ±10	7± 23
−7 ±0	2	6 ±3	−80 ±3	420 767 ±6	420 763 ± 8	4 ±10	10± 24
−7 ±0	2	6 ±3	−80 ±3	420 767 ±6	420 757 ± 4	10 ± 7	24± 17
7 ±0	2	5 ±2	−82 ±4	437 749 ±6	437 749 ±14	0 ±15	0± 34
−7 ±0	2	5 ±2	−82 ±4	431 336 ±6	431 328 ± 4	8 ± 7	19± 16
7 ±0	2	5 ±2	−82 ±4	437 749 ±6	437 748 ±12	1 ±14	2± 32
−7 ±0	2	5 ±2	−82 ±4	431 336 ±6	431 360 ±11	−24 ±13	−55± 30
7 ±0	2	5 ±2	−82 ±4	437 749 ±6	437 749 ± 8	0 ±10	0± 23
−7 ±0	2	5 ±2	−82 ±4	431 336 ±6	431 331 ± 8	5 ±10	12± 23

[a]Aas *et al.*, 1981.
[b]Hargrove *et al.*, 1977.
[c]Vuilleumier *et al.*, 1976.
[d]Tauscher *et al.*, 1978.
[e]Dubler *et al.*, 1978.

3*d* transitions in Ce. All of these transitions were measured relative to each other, providing a check on the internal consistency of the experimental results. Their work indicated good agreement between theory and experiment.

These results are summarized in Table VI. Here the various theoretical contributions to the transition energies are given for a number of elements in all regions of the periodic table, as well as the measured transition energies for all experiments analyzed since 1974. In general there is good agreement between theory and experiment, which indicates that QED has been verified at the level of 0.4%, even at large electric field strengths.

In comparison to the earlier work of 1971—72, all of the more recent experiments are characterized by a more careful treatment of possible systematic errors. In the case of the experiments discussed here, the measurement is, in principle, simple: muonic x-ray spectra are mea-

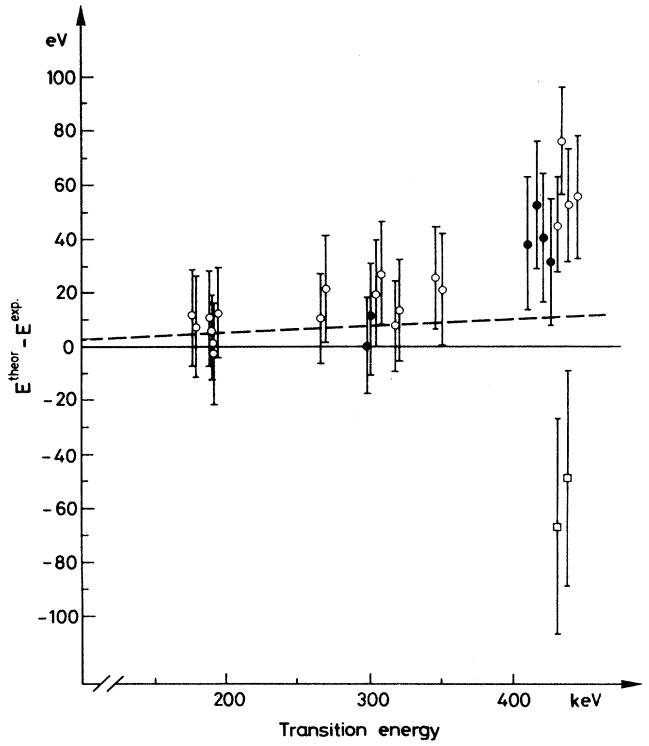

FIG. 27. Comparison between theory and experiment in several muonic atoms as a function of transition energy, at the end of 1973. Solid dots: Walter *et al.* (1972); open circles: Dixit *et al.* (1971); squares: Backenstoss *et al.* (1970). The dashed line shows the effect of the new gold standard (Deslattes *et al.*, 1975). See Aas *et al.* (1981) for a detailed explanation.

sured with high-resolution Ge(Li) detectors. Nuclear gamma rays from calibration sources are simultaneously measured. The x-ray energies for the interesting transitions lie in the range 100—450 keV. At a photon energy of 400 keV, even the best detectors have a resolution of 0.8—1.0 keV. In order to attain an accuracy of 20 eV, one must determine the center of the line to an accuracy of 0.5% of its natural width. At this level of precision, several possible sources of systematic error must be taken into account:

(i) Uncertainties in the energies of the calibration lines could have been underestimated. The most glaring example is, of course, the gold line, which has been used as a standard in determining the energies of other calibration lines. The most recent value (Kessler *et al.*, 1978) is 411 804.4±0.2 eV; before 1975, the accepted value was 411 796±7 eV (Murray *et al.*, 1963; Piller *et al.*, 1973), and the most successful recent reported value also represents a slight change as compared to the value of 411 806.2±1.4 eV reported in 1975 (Deslattes *et al.*, 1975). Since some other calibration lines have been measured relative to the gold line, these are affected also; uncertainties in the relative measurements are also present. The error in the gold line propagated as an error in the muonic transition energies which was, of course, not taken into account in the earlier experimental papers.

(ii) The fact that the configuration of the apparatus differs if muonic x rays or calibration events are recorded, could lead to an electronic shift between the corresponding spectra. The detector response typically depends upon the direction of the incoming photon. The size of this effect could be estimated using delayed gamma rays[4] following muon capture as calibration lines (Walter *et al.*, 1972; Vuilleumier *et al.*, 1976; Tauscher *et al.*, 1978; Dubler *et al.*, 1978). "Known" muonic transitions ($5g-4f$ in Ba, $4p-1s$ in C, etc.) were used for calibration by Tauscher *et al.* (1978). In addition, one must take care that the muonic spectra and calibration spectra are recorded as nearly simultaneously as possible in order to avoid effects of electronic instability.

(iii) The nonlinearity (which can be time dependent) of the detector response must be carefully measured.

(iv) The muonic x-ray peaks and the calibration gamma-ray peaks do not have the same shape. Weak, unresolved transitions will affect the muonic lines; their effect on the line shape must be estimated from a cascade calculation, whose reliability should be checked. The line shape must be well known in order to determine its position to within 0.5% of the linewidth.

(v) Even the process of generating a muon stop signal can produce electronic disturbances that will be correlated with the calibration event.

These effects have been considered in the more recent experiments or analyses, at least by those groups who have published detailed reports (Vuilleumier *et al.*, 1976; Tauscher *et al.*, 1978; Dubler *et al.*, 1978). The possible systematic errors were clearly underestimated in the earlier experimental work (Dixit *et al.*, 1971; Walter *et al.*, 1972). One can see this most clearly by comparing the results of a preliminary analysis of the data for Rh, Hg, and Tl (Walter *et al.*, 1972) with the results of the final analysis (Vuilleumier *et al.*, 1976), in which the above-mentioned problems were taken into account more carefully. For the $5g-4f$ transitions in Tl, the estimated error is 6-eV larger in the final results than in the preliminary results. Since the quoted uncertainty is 29 eV, this increase is significant. The problem of systematic errors is also clear from the fact that the Ottawa—Chicago group has measured the interesting transitions in Ba and Pb twice using essentially the same method (Dixit *et al.*, 1971, 1975), and can give no explanation for the two-standard-deviation discrepancy between the two measurements (Hargrove *et al.*, 1975).

---

[4]In addition to the previously mentioned reactions, the reaction

$^{138}\mathrm{Ba}(\mu,n\nu)^{137}\mathrm{Cs}^*$; $^{137}\mathrm{Cs}^*\rightarrow{}^{137}\mathrm{Cs}+\gamma(455.5\ \mathrm{keV})$

was used.

2. Experiments using crystal spectrometers

The calibration difficulties which are encountered when using Ge(Li) detectors can be reduced with a crystal spectrometer. The principal difficulty with Ge(Li) detectors is that the differential nonlinearity in the spectrum must be obtained empirically. With crystal spectrometers, however, this is calculated from geometrical considerations using Bragg's law. In addition, crystal spectrometers provide better resolution for x rays below a few hundred keV. This permits a rather precise measurement of the wavelength of the muonic x rays relative to a single standard wavelength.

Since a crystal spectrometer has a very small acceptance and solid angle, it is necessary to have a very-high-intensity muon beam in order to obtain sufficient statistics for a precision experiment. Up to now experimental tests of QED in muonic atoms have been performed with the bent-crystal spectrometer at the SIN superconducting muon channel. The experimental setup has been described by Piller *et al.* (1973); Beer and Kern (1974); Eichler *et al.* (1978); Aas, *et al.*, 1979; Leisi, 1977; and most recently in detail by Aas *et al.* (1981); Aas, Eichler, and Leisi, (1981); and Weber, *et al.* (1981). The Du Mond geometry of the spectrometer permits one to place a thin target directly inside the muon channel, thus obtaining a high muon stop rate. The Bragg angle is measured to high precision (± 0.02 arc sec) with a laser interferometer (Schwitz, 1978). The wavelength of muonic x rays is measured relative to the wavelength of the 84-keV gamma ray of ^{170}Tm (Borchert *et al.*, 1975; Kessler *et al.*, 1979),

$$\lambda_{\mathrm{Tm}}=(14.715\,430\pm 0.000\,013)\times 10^{-12}\ \mathrm{m}\ (0.9\ \mathrm{ppm})\ . \tag{187}$$

This setup permits the measurement of muonic x-ray transitions in an energy range between 40 and 100 keV with a precision of about 10 ppm. The $3d-2p$ transitions in muonic atoms having Z in the range $12-16$ lie in this energy range and can thus be measured with this precision. These transitions turn out to be particularly favorable for an experimental test of QED in that the contributions due to electron screening, nuclear finite size, and nuclear polarizability are very small relative to the VP contribution (see Table VII). The theoretical uncertainties can be further reduced if the $4f-3d$ transitions are also measured; this permits a better determination of the electron-screening correction to the $3d-2p$ transition energies (Ruckstuhl *et al.*, 1979). This measurement gives information as to the electron population, as discussed in Sec. II.I.

A typical angular spectrum (for ^{24}Mg) is shown in Fig. 28. The line-fit procedure is described by Aas *et al.* (1981). The measured transition energies are compared with the theoretical values in Tables VI and VII. The agreement is very good. Taking a weighted average of all the crystal spectrometer results we find (Aas *et al.*, 1981)

$$\left\langle \frac{E_{\mathrm{th}}-E_{\mathrm{exp}}}{E_{\mathrm{th}}} \right\rangle = (2\pm 8)\times 10^{-6}\ . \tag{188}$$

This result corresponds to a test of the vacuum polarization at the level of 0.2%.

The excellent agreement with theory found in these experiments leaves little room for a contribution from an anomalous interaction. We consider the contribution due to Higgs scalar exchange. As before,

$$V_\phi(r)=-g_\phi\frac{e^{-m_\phi r}}{r},\quad g_\phi=A\frac{g_\mu g_N}{4\pi}\ . \tag{189}$$

Then {with $\beta=Z\alpha m_r$ and $\gamma_n=[n^2-(Z\alpha)^2]^{1/2}$},

$$\delta E_\phi=\langle V_\phi\rangle_{2p_{3/2}}-\langle V_\phi\rangle_{3d_{5/2}} =\frac{\beta g_\phi}{2}\left[\frac{1}{\gamma_2(1+m_\phi/\beta)^{2\gamma_2}}-\frac{4}{3\gamma_3(2+3m_\phi/\beta)^{2\gamma_3}}\right]. \tag{190}$$

If, as in Jackiw and Weinberg (1972), we take $g_\phi=1.8\times 10^{-7}A\xi$, we obtain the values δE_ϕ shown in Table VIII as a function of the Higgs scalar mass.

If we require the energy shifts caused by Higgs exchange to be less than the experimental limits of the difference between experiment and current theory, we ob-

TABLE VII. Theoretical and experimental energies (in eV) for the $3d_{5/2}-2p_{3/2}$ transitions in muonic Mg, Si, and P. Also given are the contributions due to QED effects and non-QED effects. The experimental energies are taken from Aas *et al.* (1981).

	$_{12}$Mg	$_{14}$Si	$_{15}$P
QED contributions	178.7	274.9	332.2
Non-QED contributions	-1.2 ± 0.4	-2.8 ± 0.5	-4.5 ± 0.5
Total (theory)	$56\,216.4\pm 0.6$	$76\,617.6\pm 0.6$	$88\,015.9\pm 0.7$
Energy (experiment)	$56\,216.2\pm 0.6$	$76\,617.2\pm 1.1$	$88\,016.3\pm 2.5$
$E_{\mathrm{th}}-E_{\mathrm{exp}}$	0.2 ± 0.8	0.4 ± 1.2	-0.4 ± 2.5

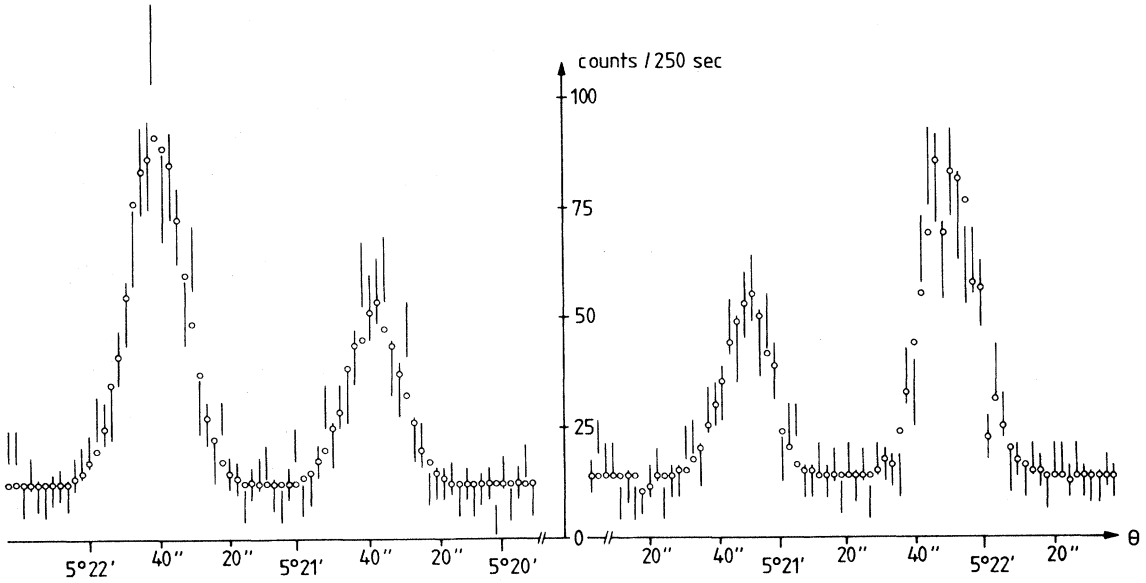

FIG. 28. Reflex pair (angular spectrum) from the $3d$-$2p$ transitions of muonic ^{24}Mg (Aas *et al.*, 1981a).

tain a limit on the value of g_ϕ (or equivalently g_ϕ/A) as a function of m_ϕ which is shown in Fig. 29. In either case, a very light Higgs scalar ($m_\phi \leq 9$ MeV) is practically ruled out.

3. Very light elements (Z = 1,2)

It is also possible to test QED using muonic atoms having a small atomic number. The most important QED corrections are due to the vacuum-polarization corrections of order $\alpha Z\alpha$ and $\alpha^2 Z\alpha$. In the cases of ^{1}H, ^{2}H, and ^{3}He the hyperfine structure is also important (Borie, 1980). However, the energies of muonic transitions have not yet been measured for these nuclei.

Since 1975 the results of a precision measurement of the $2s_{1/2}-2p_{3/2}$ splitting in the $(\mu\text{He})^+$ ion have been available (Bertin *et al.*, 1975). The experimental precision relative to the VP correction is, in fact, greater than in the case of other such measurements. The principle of the measurement is best understood by looking at the energy-level scheme as shown in Fig. 30. During the cascade, some muons reach the metastable $2s$ state. These are then pumped into the $2p$ state, using a tunable dye laser; the $2p$ state immediately decays to the ground state. When the laser is tuned to the proper frequency, the 8.2-keV K_α line is observed with higher probability (see Fig. 31) and the energy difference between the $2s$ and $2p$ states can be determined from the resonance curve. Experimental details are given by Carboni *et al.* (1976). The results of a still more careful determination of the $2s_{1/2}-2p_{3/2}$ splitting (Carboni *et al.*, 1977) and the $2s_{1/2}-2p_{1/2}$ splitting (Carboni *et al.*, 1978) are

$$S_{2\text{exp}} = E_{2p_{3/2}} - E_{2s_{1/2}} = 1527.5 \pm 0.3 \text{ meV}$$
$$S_{1\text{exp}} = E_{2p_{1/2}} - E_{2s_{1/2}} = 1381.3 \pm 0.5 \text{ meV} . \quad (191)$$

TABLE VIII. Values of $\delta E_\phi/\xi$ (in eV) as a function of the mass m_ϕ of a Higgs boson for the $3d_{5/2}-2p_{3/2}$ transitions which have been measured at the SIN crystal spectrometer (Aas *et al.*, 1981).

m_ϕ (MeV)	$^{24}_{12}$Mg	$^{28}_{14}$Si	$^{31}_{15}$P
1	4.8	6.8	8.1
10	0.5	1.0	1.3
20	0.2	0.2	0.3
50	0.01	0.01	0.02

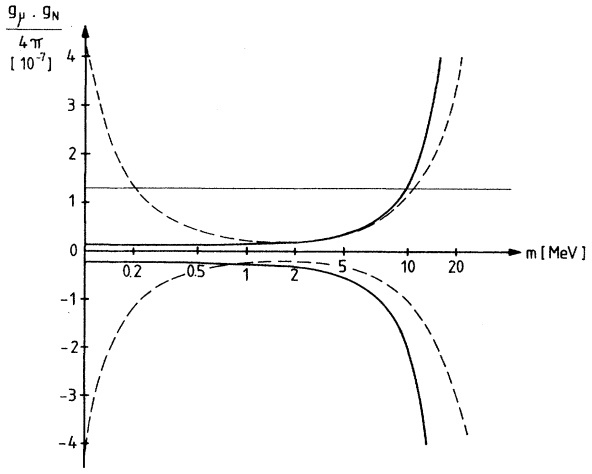

FIG. 29. Limits on the coupling constant g_ϕ for a muon-nucleon interaction mediated by a boson of mass m (Leisi, 1980). The solid curves are derived from crystal spectrometer experiments, and the dashed curves are derived from the muonic helium experiment. The straight line is the prediction of the Weinberg-Salam model.

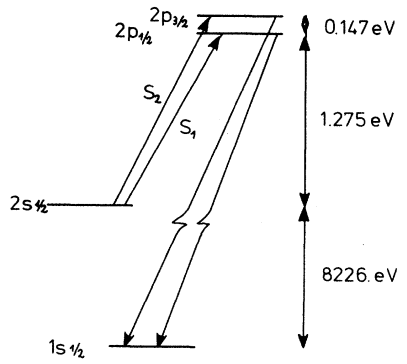

FIG. 30. Energy-level scheme for the low-lying states of muonic ^{4}He.

In order to reach an accuracy in the theoretical prediction which is comparable to the experimental uncertainties, it is necessary to take into account a number of small effects which are negligible in most of the other transitions which have been considered. For example, it is necessary to take into account the effect of finite nuclear size on the self-energy correction (and of course also the effect on the Uehling potential, recoil correction, etc.). The contribution of the Uehling potential cannot be calculated using perturbation theory. Even small effects such as hadronic vacuum polarization (Sundaresan and Watson, 1975b) and the two-photon recoil (Grotch and Yennie, 1969) contribute at the level of 0.1 meV. These contributions were summarized and compared with the results of previous calculations by Borie and Rinker (1978). This work represents an improvement over previous calculations (Borie, 1975a; Rinker, 1976) by these authors, and over the earlier work of Campani (1970). (See also Borie and Rinker, 1980.) The theoretical predictions are summarized in Table IX, which also includes some minor corrections to the results reported by Borie and Rinker (1978). The dependence of the various QED effects on the nuclear radius is explicitly displayed. Within the uncertainties, theory and experiment are in excellent agreement.

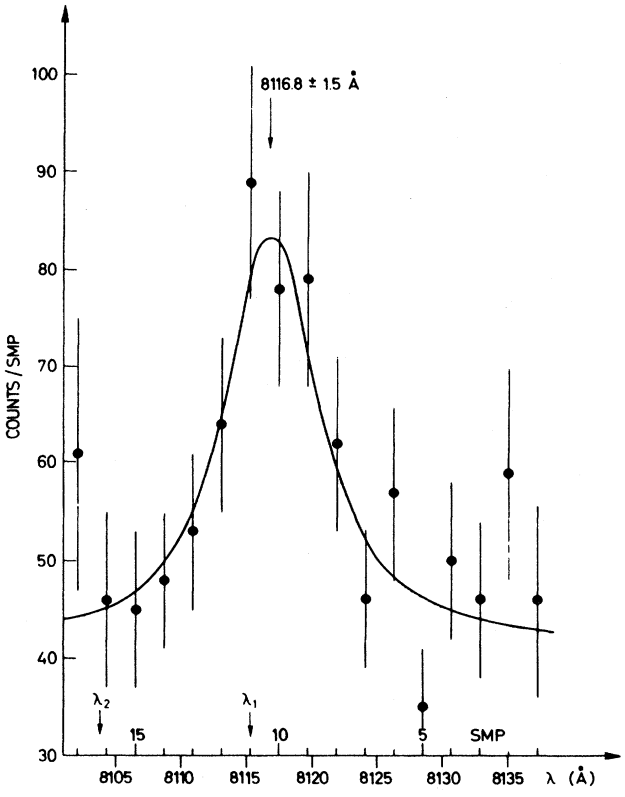

FIG. 31. The $2s_{1/2}-2p_{3/2}$ resonance signal in muonic ^{4}He as a function of laser frequency λ (Carboni *et al.*, 1976, 1977).

Unfortunately, the theoretical predictions are far less precise than the experiment, since the effects of nuclear physics on the binding energy of the $2s$ state are not sufficiently well known. The main source of uncertainty in the transition energy is the experimental uncertainty in the radius of ^{4}He as determined by electron scattering (Sick *et al.*, 1976). Using the radius given there,

$$\langle r^2\rangle^{1/2}=1.674\pm0.012 \text{ fm} , \tag{192}$$

the effect of finite nuclear size is -289.3 ± 4.2 meV, of which 0.4 meV is a result of the effect of finite nuclear size on the QED corrections.

In addition, determination of the nuclear-polarization correction is limited by uncertainties in the nuclear-excitation spectrum. As discussed in Sec. II.G.4.*b*, the contribution of 3.1 meV is probably correct to within the quoted uncertainty of 20%.

Since the nuclear physics parameters are the main source of theoretical uncertainty, it is possible to reverse the argument. If we assume that QED is correct, the measurement of the Zavattini group (Carboni *et al.*, 1977) can be regarded as an experimental determination of the charge radius of ^{4}He. In that case, we find (Borie and Rinker, 1978; see also Friar, 1979a, 1979b)

$$\langle r^2\rangle^{1/2}=1.673\pm0.001 \text{ fm} . \tag{193}$$

The error on the radius determined by this method is a factor of 10 less than the error estimated for electron scattering experiments.

The effect of Higgs scalar exchange on the transition energy is easily computed. We have

$$\Delta E_\phi=\langle V_\phi\rangle_{2s}-\langle V_\phi\rangle_{2p}=\frac{g_\phi(m_\phi/\beta)^2}{2(1+m_\phi/\beta)^4} , \tag{194}$$

where $\beta=Z\alpha m_r=1.50$ MeV. We require that this contribution be less than the uncertainty in the discrepancy between theory and experiment

$$\Delta E_\phi<0.004 \text{ eV} , \tag{195}$$

which implies

$$g_\phi<5.3\times10^{-9}\frac{(1+m_\phi/\beta)^4}{(m_\phi/\beta)^2} . \tag{196}$$

In Table X and Fig. 29 (Aas *et al.*, 1981) we show the

TABLE IX. Theoretical contributions to the splittings $S_1=E(2p_{3/2}-2s_{1/2})$, $S_2=E(2p_{1/2}-2s_{1/2})$ in muonic helium. The rms charge radii used are 1.674±0.012 fm for ^{4}He, and 1.844±0.045 fm for ^{3}He.

Splitting	^{4}He S_2	^{4}He S_1	^{3}He S_2	^{3}He S_1
Electron VP				
Uehling: first iteration	1664.44	1664.17	1640.2	1639.9
Higher iterations	1.70	1.70	1.4	1.4
Källen–Sabry $\alpha^2 Z\alpha$	11.55	11.55	11.4	11.4
$\alpha(Z\alpha)^{n\geq 3}$	−0.02	−0.02	−0.02	−0.02
$\alpha^2(Z\alpha)^2$	0.02	0.02	0.02	0.02
Muon VP	0.33	0.33	0.33	0.33
Muon-electron VP	0.02	0.02	0.02	0.02
Hadron VP	0.15	0.15	0.14	0.14
Total VP	1678.19	1677.92	1653.5	1653.2
Self-energy and $(g-2)$				
$\alpha Z\alpha$	−10.52	−10.85	−10.33	−10.65
$\alpha(Z\alpha)^{n\geq 2}$	−0.16	−0.16	−0.15	−0.15
$\alpha^2 Z\alpha$	−0.03	−0.03	−0.03	−0.03
Total self-energy	−10.71	−11.04	−10.5	−10.8
Recoil				
Breit	0.28	0.28	0.4	0.4
2-photon	−0.44	−0.44	−0.6	−0.6
Total recoil	−0.16	−0.16	−0.2	−0.2
Point Coulomb				
(Fine structure)	145.70	0	144.4	0
Total QED	1813.02	1666.72	1787.2	1642.2
Nuclear polarization	3.1±0.6	3.1±0.6	4.9±1.0	4.9±1.0
Finite nuclear size	−288.9±4.1	−288.9±4.1	−340.0±16.6	−340.0±16.6
Total	1527.2±4.2	1380.9±4.2	1452.1±16.6	1307.1±16.6
Experiment	1527.5±0.3	1381.3±0.5	. . .	. . .

TABLE X. Bounds for the muon-helium coupling constant g_ϕ(max) for scalar exchange, as a function of the ϕ boson mass m_ϕ.

m_ϕ (MeV)	g_ϕ (max)
0.15	7.8×10^{-7}
0.45	1.7×10^{-7}
1.5	0.85×10^{-7}
4.5	1.5×10^{-7}
15	7.8×10^{-7}
450	4.8×10^{-4}
600	8.6×10^{-4}
750	1.3×10^{-3}

maximum value of g_ϕ as a function of the ϕ mass m_ϕ. A comparison with the estimate of g_ϕ for ^{4}He by Jackiw and Weinberg (1972),

$$g_\phi \simeq 7.2\times10^{-7}\,, \tag{197}$$

indicates that a ϕ mass between 0.1 and 5 MeV is most unlikely. We have also considered a ϕ mass in the vicin-

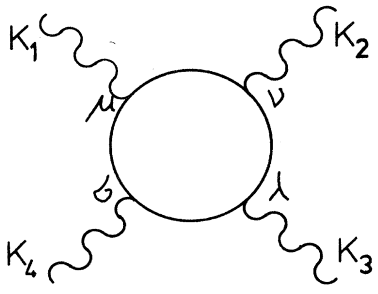

FIG. 32. Light-by-light scattering diagram.

ity of known hadronic resonances which play a role in NN scattering (e.g., the ε meson with mass $\simeq 600$ MeV). These limits are also shown in Table X.

The new limit on the coupling constant for the ϕ mass in the range 500–700 MeV is a factor of 10 smaller than was given in an earlier determination (Rinker and Wilets, 1973b).

IV. ACKNOWLEDGMENTS

One of us (G. R.) would particularly like to thank K. W. Ford, L. Wilets, R. M. Steffen, and R. B. Perkins for providing much appreciated interaction, stimulation, explanation, and opportunity during the long course of his learning about muonic atoms. Substantial portions of this work were begun in a series of lectures at the University of Fribourg. I am particularly grateful to L. Schaller for providing that opportunity. The other (E. B.) wishes to thank R. Engfer, H. Koch, W. W. Sapp, and L. Simons for stimulating and fruitful interaction and instruction about experimental methods. We are grateful to H. J. Leisi, L. Tauscher, and E. Zavattini for providing figures pertaining to their experimental work. The manuscript was prepared at the Los Alamos National Laboratory Central Computing Facility using the text editing–word processing program TEDI, written by C. W. Nielson, whom we should like to thank for making it available to us and for assisting our use of it. This work was supported in part by the U. S. Department of Energy.

APPENDIX

We present here some of the properties of the fourth-order vacuum-polarization tensor which were used in Borie's (1976a) calculation of the virtual Delbrück effect. The amplitude corresponding to the light-by-light scattering diagram (Fig. 32) is given by

$$T_{\mu\nu\lambda\sigma}(k_1,k_2,k_3,k_4)=\frac{1}{i\pi^2}\int d^4p\ \mathrm{Tr}\left[\gamma_\mu\frac{\not p+m_e}{p^2-m_e^2+i\varepsilon}\gamma_\nu\frac{\not p-\not k_2+m_e}{(p-k_2)^2-m_e^2+i\varepsilon}\gamma_\lambda\frac{\not p-\not k_2-\not k_3+m_e}{(p-k_2-k_3)^2-m_e^2+i\varepsilon}\right.$$
$$\left.\times\gamma_\sigma\frac{\not p+\not k_1+m_e}{(p+k_1)^2-m_e^2+i\varepsilon}\right], \tag{198}$$

where

$$k_1+k_2+k_3+k_4=0\ . \tag{199}$$

We then *define* the fourth-order vacuum polarization tensor by

$$G_{\mu\nu\lambda\sigma}(k_1,k_2,k_3,k_4)=T_{\mu\nu\lambda\sigma}(k_1,k_2,k_3,k_4)+T_{\nu\mu\lambda\sigma}(k_2,k_1,k_3,k_4)+T_{\mu\lambda\nu\sigma}(k_1,k_3,k_2,k_4)\ . \tag{200}$$

We observe that this definition differs from that of Papatzacos and Mork (1975) by a factor $i\pi^2$. We also use a different metric and conventions for the gamma matrices.

Since the trace is invariant under cyclic permutations of the gamma matrices, it follows that

$$T_{\nu\mu\lambda\sigma}(k_2,k_1,k_3,k_4)=T_{\mu\nu\sigma\lambda}(k_1,k_2,k_4,k_3),\quad T_{\mu\lambda\nu\sigma}(k_1,k_3,k_2,k_4)=T_{\lambda\mu\sigma\nu}(k_3,k_1,k_4,k_2)\ , \tag{201}$$

and so on. From this one can easily show that $G_{\mu\nu\lambda\sigma}(k_1,k_2,k_3,k_4)$ is symmetric under permutations of the variable pairs $(\mu k_1,\nu k_2,\lambda k_3,\sigma k_4)$ and under the transformation $k_i\rightarrow -k_i$. Furthermore, although each of the $T_{\mu\nu\lambda\sigma}$ contains an ultraviolet divergence, the full fourth-order vacuum-polarization tensor does not. The proof is well known and will not be given here. It can also be shown, using dimensional regularization (Khare, 1977), that $G_{\mu\nu\lambda\sigma}$ as given in Eq. (200) is gauge invariant and that it is therefore unnecessary to introduce subtraction constants.

Gauge invariance implies that

$$k_1^\mu G_{\mu\nu\lambda\sigma}(k_1,k_2,k_3,k_4)=k_2^\nu G_{\mu\nu\lambda\sigma}(k_1,k_2,k_3,k_4)=k_3^\lambda G_{\mu\nu\lambda\sigma}(k_1,k_2,k_3,k_4)=k_4^\sigma G_{\mu\nu\lambda\sigma}(k_1,k_2,k_3,k_4)=0\ . \tag{202}$$

This fact is used to express the divergent contributions to integrals like (198) in terms of convergent contributions, thus analytically eliminating them before any numerical calculations are performed.

Using relativistic invariance and Eq. (199) to eliminate k_4, we have (Karplus and Neumann, 1950; Costantini *et al.*, 1971; Papatzacos and Mork, 1975)

$$G_{\mu\nu\lambda\sigma}(k_1,k_2,k_3,k_4)=\sum_{ijlm=1}^{3}A^{ijlm}k_{i\mu}k_{j\nu}k_{l\lambda}k_{m\sigma}+\sum_{lm=1}^{3}[g_{\mu\nu}B_1^{lm}k_{l\lambda}k_{m\sigma}+g_{\mu\lambda}B_2^{lm}k_{l\nu}k_{m\sigma}+g_{\mu\sigma}B_3^{lm}k_{l\nu}k_{m\lambda}$$
$$+g_{\nu\lambda}B_4^{lm}k_{l\mu}k_{m\sigma}+g_{\nu\sigma}B_5^{lm}k_{l\mu}k_{m\lambda}+g_{\lambda\sigma}B_6^{lm}k_{l\mu}k_{m\nu}]+C_1g_{\mu\nu}g_{\sigma\lambda}+C_2g_{\mu\lambda}g_{\nu\sigma}+C_3g_{\mu\sigma}g_{\nu\lambda}\ . \tag{203}$$

The A^{ijlm} come from the most convergent contributions to the integral over p in (198) and they are not influenced by possible (but unnecessary) subtraction terms. It is therefore convenient from a computational standpoint to use Eq. (202) to express the B and C coefficients in terms of the A's. This method was used by Papatzacos and Mork (1975) for real Delbrück scattering. For example, we obtain

$$B_1^{jm}=-k_1^2A^{11jm}-k_1\cdot k_2A^{21jm}-k_1\cdot k_3A^{31jm}\ ,\quad j,m=2,3\ ,$$
$$B_1^{22}+B_4^{22}+B_5^{22}=-k_1\cdot k_2A^{2122}-k_2^2A^{2222}-k_2\cdot k_3A^{2322}\ ,\quad B_2^{3m}+B_4^{3m}=-k_1\cdot k_3A^{331m}-k_2\cdot k_3A^{332m}-k_3^2A^{333m}\ ,\quad m=1,2\ , \tag{204}$$

and so on, and hence also

$$C_1=\sum_{m=1}^{3}(k_1\cdot k_3k_1\cdot k_mA^{2m13}+k_2\cdot k_3k_1\cdot k_mA^{m123}+k_3^2k_1\cdot k_mA^{m133})\ , \tag{205}$$

and similarly for C_2 and C_3.

It remains to evaluate the A^{ijlm}. The integration over the electron loop momentum has been given by Papatzacos and Mork (1975). As in that calculation, we find that we can write

$$A^{ijlm}=\sum_{n=1}^{3}A_n^{ijlm}\ , \tag{206}$$

with

$$A_n^{ijlm}=\int_0^1dy\int_0^1dz\int_0^1dx\frac{x(1-x)a_n^{ijlm}}{(m^2+D_n^2)^2}\ . \tag{207}$$

The index n refers to the different topologies of the graphs of Fig. 16 or, equivalently, to the permutations in (200). The a_n^{ijlm} are real polynomials in x, y, and z [those needed for the virtual Delbrück effect were calculated using SCHOONSCHIP (Strubbe, 1974)], while the D_n are functions of the momenta k_1, k_2, and k_3, as well as of x, y, z. For future reference we remark that D_n can be written in the form [with $k'=k_2-q/2=(k_2-k_1)/2$]

$$D_n=\alpha_nk'^2+2\beta_nk'\cdot(q+k_3)+2\gamma_nk'\cdot q+\delta_n\ . \tag{208}$$

The α_n, β_n, and γ_n are also polynomials in x, y, and z, while δ_n depends also on the momenta q and k_3. They are given explicitly by

$$\alpha_1=\alpha_2=z(1-x)[1-z(1-x)],\quad \beta_1=-\beta_2=xyz(1-x),\quad \gamma_1=-\gamma_2=\alpha_1/2-xz(1-x)$$
$$\delta_1=\delta_2=q^2\left[\frac{\alpha_1}{4}+x(1-x)(1-z)\right]-xy(1-x)(2-z)q\cdot(q+k_3)+xy(1-xy)(q+k_3)^2$$
$$\alpha_3=x(1-x),\quad \beta_3=\alpha_3(y-z),\quad \gamma_3=\frac{\alpha_3}{2}(2z-1),$$
$$\delta_3=q^2\left[\frac{\alpha_3}{4}+z(1-z)(1-x)^2\right]-\{\beta_3+2z(1-x)[1-xy-z(1-x)]\}q\cdot(q+k_3)$$
$$+(q+k_3)^2[xy+z(1-z)][1-xy-z(1-x)]\ . \tag{209}$$

REFERENCES

Aas, B., W. Beer, I. Beltrami, K. Bongardt, P. Ebersold, R. Eichler, T. V. Ledebur, H. J. Leisi, W. W. Sapp, J. A. Pinston, J. Kern, R. Lanners, and W. Schwitz, 1979, Nucl. Phys. A **329**, 450.

Aas, B., W. Beer, I. Beltrami, P. Ebersold, R. Eichler, T. V. Ledebur, H. J. Leisi, W. Ruckstuhl, W. W. Sapp, A. Vacchi, J. Kern, J. A. Pinston, W. Schwitz, and R. Weber, 1981, submitted to Nuclear Physics.

Aas, B., R. Eichler, and H. J. Leisi, 1981, submitted to Nuclear Physics.

Abela, R., G. Backenstoss, I. Schwanner, P. Blüm, D. Gotta, L. M. Simons, and P. Zsoldos, 1977, Phys. Lett. B **71**, 290.

Abela, R., W. Kunold, L. M. Simons, and M. Schneider, 1980, Phys. Lett. B **94**, 331.

Abers, E. S., and B. W. Lee, 1973, Phys. Rep. **9**, 3.

Abramowitz, M., and I. Stegun, eds., 1965, *Handbook of Mathematical Functions* (Dover, New York), Chap. 11.

Adler, S. L., 1974, Phys. Rev. D **10**, 3714.

Adler, S. L., R. F. Dashen, and S. B. Treiman, 1974, Phys. Rev. D **10**, 3728.

Ahrens, J., H. Borchert, K. H. Czock, H. B. Eppler, H. Gimm, H. Gundrum, M. Kröning, P. Riehn, G. Sita Ram, A. Ziegler, and B. Ziegler, 1975, Nucl. Phys. A **251**, 479.
Ahrens, J., H. Gimm, A. Ziegler, and B. Ziegler, 1976, Nuovo Cimento A **32**, 364.
Akhiezer, A. I., and V. B. Berestetskii, 1965, *Quantum Electrodynamics* (Wiley Interscience, New York).
Anderhub, H., H. Hofer, F. Kottmann, P. Le Coultre, D. Makowiecki, O. Pitzurra, B. Sapp, P. G. Seiler, M. Wälchli, D. Taqqu, P. Truttmann, A. Zehnder, and C. Tschalär, 1977, Phys. Lett. B **71**, 443.
Anderson, H. L., C. K. Hargrove, E. P. Hincks, J. D. McAndrew, R. J. McKee, R. D. Barton, and D. Kessler, 1969, Phys. Rev. **187**, 1565.
Andrews, D. A., and G. Newton, 1976, Phys. Rev. Lett. **37**, 1254.
Appelquist, J. T., and S. J. Brodsky, 1970, Phys. Rev. A **2**, 2293.
Arafune, J., 1974, Phys. Rev. Lett. **32**, 560.
Backenstoss, G., S. Charalambus, H. Daniel, Ch. von der Malsburg, G. Poelz, H. P. Povel, H. Schmitt, and L. Tauscher, 1970, Phys. Lett. B **31**, 233.
Bailey, J., K. Borer, F. Combley, H. Drumm, C. Eck, F. J. M. Farley, J. H. Field, W. Flegel, P. M. Hattersly, F. Kreinen, F. Lange, G. Lebée, E. McMillan, G. Petrucci, E. Picasso, O. Rünolfsson, W. von Rüden, R. W. Williams, and S. Wojcicki, 1979, Nucl. Phys. B **150**, 1.
Bailey, J., and E. Picasso, 1970, Prog. Nucl. Phys. **12**, 43.
Barber, D. P., U. Becker, H. Benda, A. Boehm, J. G. Branson, J. Bron, D. Buikman, J. Burger, C. C. Chang, M. Chen, C. P. Cheng, Y. S. Chu, R. Clare, P. Duinker, H. Fesefeldt, D. Fong, M. Fukushima, M. C. Ho, T. T. Hsu, R. W. Kadel, D. Luckey, C. M. Ma, G. Massaro, T. Matsuda, H. Newman, J. Paradiso, J. P. Revol, M. Rhode, H. Rykaczewski, K. Sinram, H. W. Tang, S. C. C. Ting, K. L. Tung, F. Vannucci, M. White, T. W. Wu, P. C. Yang, and C. C. Yu, 1979a, Phys. Rev. Lett. **42**, 1110.
Barber, D. P., U. Becker, H. Benda, A. Boehm, J. G. Branson, J. Bron, D. Buikman, J. Burger, C. C. Chang, H. S. Chen, M. Chen, C. P. Cheng, Y. S. Chu, R. Clare, P. Duinker, G. Y. Fang, H. Fesefeldt, D. Fong, M. Fukushima, J. C. Guo, A. Hariri, G. Herten, M. C. Ho, H. K. Hsu, T. T. Hsu, R. W. Kadel, W. Krenz, J. Li, Q. Z. Li, M. Lu, D. Luckey, D. A. Ma, C. M. Ma, G. Massaro, T. Matsuda, H. Newman, J. Paradiso, F. P. Poschmann, J. P. Revol, M. Rhode, H. Rykaczewski, K. Sinram, H. W. Tang, L. G. Tang, S. C. C. Ting, K. L. Tung, F. Vannucci, X. R. Wang, P. S. Wei, M. White, G. H. Wu, T. W. Wu, J. P. Xi, P. C. Yang, X. H. Yu, N. L. Zhang, and R. Y. Zhu, 1979b, Phys. Rev. Lett. **43**, 1915.
Barbieri, R., M. Caffo, E. Remiddi, 1973, Nuovo Cimento Lett. **7**, 60.
Barbieri, R., J. A. Mignaco, and E. Remiddi, 1972a, Nuovo Cimento A **11**, 824.
Barbieri, R., J. A. Mignaco, and E. Remiddi, 1972b, Nuovo Cimento A **11**, 865.
Barbieri, R., and E. Remiddi, 1973, Nuovo Cimento A **13**, 99.
Barrett, R. C., 1968, Phys. Lett. B **28**, 93.
Barrett, R. C., 1970, Phys. Lett. B **33**, 388.
Barrett, R. C., 1974, Rep. Prog. Phys. **37**, 1.
Barrett, R. C., S. J. Brodsky, G. W. Erickson, and M. H. Goldhaber, 1968, Phys. Rev. **166**, 1589.
Barrett, R. C., D. Owen, J. Calmet, and H. Grotch, 1973, Phys. Lett. B **47**, 297.
Barshay, S., 1974, Phys. Rev. D **10**, 2313.
Beer, W., and J. Kern, 1974, Nucl. Instrum. Methods **117**, 183.
Bell, T. L., 1973, Phys. Rev. A **7**, 1480.
Bergmann, R., H. Daniel, T. von Egidy, F. J. Hartmann, J. J. Reidy, and W. Wilheim, 1979, Z. Phys. A **291**, 129.
Bergmann, R., H. Daniel, T. von Egidy, F. J. Hartmann, J. J. Reidy, and W. Wilhelm, 1981, "Measurement of Coulomb capture ratio and Lyman series intensities on solid solutions of Nb-V at five stoichiometric ratios," preprint, Physics Department, Technical University of Munich, Munich, Germany.
Bernabeu, J., and C. Jarlskog, 1974, Nucl. Phys. B **75**, 59.
Bernabeu, J., and C. Jarlskog, 1976, Phys. Lett. B **60**, 197.
Bernstein, J., 1974, Rev. Mod. Phys. **46**, 7.
Bertin, A., G. Carboni, J. Duclos, U. Gastaldi, G. Gorini, G. Neri, J. Picard, O. Pitzurra, A. Placci, E. Polacco, G. Torelli, A. Vitale, and E. Zavattini, 1975, Phys. Lett. B **55**, 411.
Bethe, H. A., 1947, Phys. Rev. **72**, 330.
Bethe, H. A., and J. W. Negele, 1968, Nucl. Phys. A **117**, 575.
Bjorken, J. D., and S. D. Drell, 1964, *Relativistic Quantum Mechanics* (McGraw-Hill, New York).
Blatt, J. M., 1967, J. Comput. Phys. **1**, 382.
Blomqvist, J., 1972, Nucl. Phys. B **48**, 95.
Borchert, G. L., W. Scheck, and K. P. Wieder, 1975, Z. Naturforsch. A **30**, 274.
Borie, E., 1975a, Z. Phys. A **275**, 347.
Borie, E., 1975b, Helv. Phys. Acta **48**, 671.
Borie, E., 1976a, Nucl. Phys. A **267**, 485.
Borie, E., 1976b, Z. Phys. A **278**, 127.
Borie, E., 1979, Habilitationschrift, University of Karlsruhe (unpublished).
Borie, E., 1980, Z. Phys. A **297**, 17.
Borie, E., 1981, Z. Phys. A **302** , 187.
Borie, E., and G. A. Rinker, 1978, Phys. Rev. A **18**, 324.
Borie, E., and G. A. Rinker, 1980, Z. Phys. A **296**, 111.
Borysowicz, J., and J. H. Hetherington, 1973, Phys. Rev. C **7**, 2293.
Bovet, E., F. Boehm, R. J. Powers, P. Vogel, K. C. Wang, and R. Kunselman, 1980, Phys. Lett. B **92**, 87.
Breit, G., 1937, Phys. Rev. **51**, 248.
Breit, G., and G. E. Brown, 1948, Phys. Rev. **74**, 1278.
Brodsky, S. J., and S. D. Drell, 1970, Annu. Rev. Nucl. Sci. **20**, 147.
Brown, G. E., J. S. Langer, and G. W. Schaefer, 1959, Proc. R. Soc. London A **251**, 92.
Brown, G. E., and D. G. Ravenhall, 1951, Proc. R. Soc. London A **208**, 552.
Brown, L. S., R. N. Cahn, and L. D. McLerran, 1974, Phys. Rev. Lett. **32**, 562.
Brown, L. S., R. N. Cahn, and L. D. McLerran, 1975a, Phys. Rev. D **12**, 581.
Brown, L. S., R. N. Cahn, and L. D. McLerran, 1975b, Phys. Rev. D **12**, 596.
Brown, L. S., R. N. Cahn, and L. D. McLerran, 1975c, Phys. Rev. D **12**, 609.
Calmet, J., and D. A. Owen, 1979, J. Phys. B **12**, 169.
Campani, E., 1970, Nuovo Cimento Lett. **4**, 982.
Carboni, G., U. Gastaldi, G. Neri, O. Pitzurra, E. Polacco, G. Torelli, A. Bertin, G. Gorini, A. Placci, E. Zavattini, A. Vitale, J. Duclos, and J. Picard, 1976, Nuovo Cimento A **34**, 493.
Carboni, G., G. Gorini, G. Torelli, L. Palffy, F. Palmonari, and E. Zavattini, 1977, Nucl. Phys. A **278**, 381.
Carboni, G., G. Gorini, E. Iacopini, L. Palffy, F. Palmonari,

G. Torelli, and E. Zavattini, 1978, Phys. Lett. B **73**, 229.
Chen, M.-Y., 1970a, Phys. Rev. C **1**, 1167.
Chen, M.-Y., 1970b, Phys. Rev. C **1**, 1176.
Chen, M.-Y., 1975, Phys. Rev. Lett. **34**, 341.
Cheng, K. T., and W. R. Johnson, 1976, Phys. Rev. A **14**, 1943.
Cheng, K. T., W. D. Sepp, W. R. Johnson, and B. Fricke, 1978, Phys. Rev. A **17**, 489.
Chlouber, C., and M. A. Samuel, 1978, Comput. Phys. Commun. **15**, 153.
Cole, R. K., 1969, Phys. Rev. **177**, 164.
Combley, F., F. J. M. Farley, and E. Picasso, 1981, Phys. Reps. **68**, C 93.
Cooper, L. N., and E. M. Henley, 1953, Phys. Rev. **92**, 801.
Costantini, V., B. de Tollis, and G. Pistoni, 1971, Nuovo Cimento A **2**, 733.
Dalgarno, A., and J. T. Lewis, 1955, Proc. R. Soc. London A **233**, 70.
Daniel, H., R. Bergmann, V. Dornow, F. J. Hartmann, J. J. Reidy, and W. Wilhelm, 1978, Hyperfine Interact. **5**, 215.
Daniel, H., W. Denk, F. J. Hartmann, J. J. Reidy, and W. Wilhelm, 1977, Phys. Lett. B **71**, 60.
Daniel, H., W. Denk, F. J. Hartmann, W. Wilhelm, and T. von Egidy, 1979, Phys. Rev. Lett. **41**, 853.
Daniel, H., 1979, Z. Phys. A **291**, 29.
Desiderio, A. M., and W. R. Johnson, 1971, Phys. Rev. A **3**, 1267.
Deslattes, R. D., E. G. Kessler, W. C. Sauder, and A. Henins, 1975, in *Proceedings of the 5th International Conference on Atomic Masses and Fundamental Constants, Paris,* edited by J. H. Sandars and A. H. Wapstra (Plenum, New York), p. 48.
Devons, S., and I. Deuerdoth, 1968, Adv. Nucl. Phys. **2**, 295.
Dey, W., P. Ebersold, H. J. Leisi, F. Scheck, H. K. Walter, and A. Zehnder, 1979, Nucl. Phys. A **326**, 418.
Dixit, M. S., H. L. Anderson, C. K. Hargrove, R. J. McKee, D. Kessler, H. Mes, and A. C. Thompson, 1971, Phys. Rev. Lett. **27**, 878.
Dixit, M. S., A. L. Carter, E. P. Hincks, D. Kessler, J. S. Wadden, C. K. Hargrove, R. J. McKee, H. Mes, and H. L. Anderson, 1975, Phys. Rev. Lett. **35**, 1633.
Drell, S., 1979, Physica A **96**, 3.
Dubler, T., 1978, Helv. Phys. Acta **51**, 743.
Dubler, T., K. Kaeser, B. Robert-Tissot, L. A. Schaller, L. Schellenberg, and H. Schneuwly, 1978, Nucl. Phys. A **294**, 397.
Dubler, T., K. Kaeser, B. Robert-Tissot, L. A. Schaller, L. Schellenberg, and H. Schneuwly, 1979, "Muonic X-ray intensities in phosphorous- and selenium modifications," contribution to the 8th International Conference on High Energy Physics and Nuclear Structure, Vancouver (unpublished).
Dubler, T., L. Schellenberg, H. Schneuwly, R. Engfer, J. L. Vuilleumier, H. K. Walter, A. Zehnder, and B. Fricke, 1974, Nucl. Phys. A **217**, 29.
Eichler, R., B. Aas, W. Beer, I. Beltrami, P. Ebersold, T. V. Ledebur, H. J. Leisi, W. W. Sapp, J. C. Dousse, J. Kern, and W. Schwitz, 1978, Phys. Lett. B **76**, 231.
Engfer, R., H. Schneuwly, J. L. Vuilleumier, H. K. Walter, and A. Zehnder, 1974, At. Data Nucl. Data Tables **14**, 509.
Engfer, R., J. L. Vuilleumier, and E. Borie, 1975, in Atomic Physics **4**, 141, edited by G. Zu Putlitz, E. W. Weber, and A. Winnacher (Plenum, New York).
Erickson, G. W., 1977, J. Phys. Chem. Ref. Data **6**, 831.
Erickson, G. W., and D. R. Yennie, 1965, Ann. Phys. (NY) **35**, 271.
Ericson, T. E. O., 1981, private communication.
Ericson, T. E. O., and J. Hüfner, 1972, Nucl. Phys. B **47**, 205.
Faessler, A., J. E. Galonska, K. Goeke, and S. A. Moszkowski, 1975, Nucl. Phys. A **239**, 477.
Fermi, E., and E. Teller, 1947, Phys. Rev. **72**, 399.
Fink, T., K. Kaeser, B. Robert-Tissot, A. Ruetschi, L. A. Schaller, L. Schellenberg, and H. Schneuwly, 1979, contribution to the 8th International Conference on High Energy Physics and Nuclear Structure, Vancouver (unpublished).
Fitch, V. L., and J. Rainwater, 1953, Phys. Rev. **92**, 789.
Ford, K. W., and G. A. Rinker, 1973, Phys. Rev. C **7**, 1206.
Ford, K. W., and G. A. Rinker, 1974, Phys. Rev. C **9**, 2444.
Ford, K. W., and J. G. Wills, 1969, Phys. Rev. **185**, 1429.
Friar, J. L., 1977, Phys. Rev. C **16**, 1540.
Friar, J. L., 1979a, Ann. Phys. (NY) **122**, 151.
Friar, J. L., 1979b, Phys. Lett. B **80**, 157.
Friar, J. L., and J. W. Negele, 1973a, Nucl. Phys. A **212**, 93.
Friar, J. L., and J. W. Negele, 1973b, Phys. Lett. B **46**, 5.
Friar, J. L., and J. W. Negele, 1975, Adv. Nucl. Phys. **8**, 219.
Fricke, B., 1969a, Nuovo Cimento Lett. **2**, 859.
Fricke, B., 1969b, Z. Phys. **218**, 495.
Fricke, B., 1973, Phys. Rev. Lett. **30**, 119.
Fricke, B., and V. L. Telegdi, 1975, Z. Naturforsch. **30a**, 1328.
Fujimoto, D. H., 1975, Phys. Rev. Lett. **35**, 341.
Fulcher, L., and A. Klein, 1973, Phys. Rev. D **8**, 2455.
Fullerton, L. W., 1981, private communication.
Fullerton, L. W., and G. A. Rinker, 1976, Phys. Rev. A **13**, 1283.
Fulton, T., and P. C. Martin, 1954, Phys. Rev. **95**, 811.
Furry, W. H., 1951, Phys. Rev. **81**, 115.
Furry, W. H., and J. R. Oppenheimer, 1934, Phys. Rev. **45**, 245.
Galonska, J. E., K. Goeke, and A. Faessler, 1973, Phys. Lett. B **45**, 414.
Gerdt, V. P., A. Karimkhodzaw, and R. N. Faustov, 1978, "Hadronic vacuum polarization and test of quantum electrodynamics at low energies," Joint Institute for Nuclear Research preprint PZ-11308.
Gerstein, S. S., and L. I. Ponomarev, 1977, in *Muon Physics,* edited by V. W. Hughes and C. S. Wu (Academic, New York), Vol. III.
Greiner, W., 1961, Z. Phys. **164**, 374.
Greiner, W., and L. Marschall, 1962, Z. Phys. **165**, 171.
Gröbner, W., and N. Hofreiter, 1966, *Integraltafel, II Teil* (Springer, Vienna).
Gross, F., 1969, Phys. Rev. **186**, 1448.
Grotch, H., and D. R. Yennie, 1969, Rev. Mod. Phys. **41**, 350.
Gyulassy, M., 1974, Phys. Rev. Lett. **32**, 1393.
Gyulassy, M., 1975, Nucl. Phys. A **244**, 497.
Hahn, A. A., J. P. Miller, R. J. Powers, A. Zehnder, A. M. Rushton, R. E. Welsh, A. R. Kunselmann, P. Roberson, and H. K. Walter, 1979, Nucl. Phys. A **314**, 361.
Hamming, R. W., 1959, J. Assoc. Comput. Mach. **6**, 37.
Hamming, R. W., 1962, *Numerical Methods for Scientists and Engineers* (McGraw-Hill, New York).
Hargrove, C. K., E. P. Hincks, H. Mes, R. J. McKee, M. S. Dixit, A. L. Carter, D. Kessler, J. S. Wadden, and H. L. Anderson, 1975, contribution to the 5th International Conference on High Energy Physics and Nuclear Structure, Santa Fe (unpublished).
Hargrove, C. K., E. P. Hincks, R. J. McKee, H. Mes, A. L. Carter, M. S. Dixit, D. Kessler, J. S. Wadden, H. L. Anderson, and A. Zehnder, 1977, Phys. Rev. Lett. **39**, 307.
Heisenberg, J., R. Hofstadter, J. S. McCarthy, I. Sick, B. C.

Clark, R. Herman, and D. G. Ravenhall, 1969, Phys. Rev. Lett. **23**, 1402.
Heisenberg, W., 1934, Z. Phys. **90**, 209.
Henley, E. M., F. R. Krejs, and L. Wilets, 1976, Nucl. Phys. A **256**, 349.
Hoehn, M. V., E. B. Shera, Y. Yamazaki, and R. M. Steffen, 1977, Phys. Rev. Lett. **39**, 1313.
Hoehn, M. V., E. B. Shera, and H. D. Wohlfahrt, 1980, Phys. Rev. C **22**, 678.
Hoehn, M. V., E. B. Shera, H. D. Wohlfahrt, Y. Yamazaki, R. M. Steffen, and R. K. Sheline, 1981, Phys. Rev. C (in press).
Huang, K. N., 1976, Phys. Rev. A **14**, 1311.
Hüfner, J., F. Scheck, and C. S. Wu, in *Muon Physics*, edited by V. W. Hughes and C. S. Wu (Academic, New York), Vol. I.
Hughes, V. M., and T. Kinoshita, 1977, in *Muon Physics,* edited by V. W. Hughes and C. S. Wu (Academic, New York), Vol. I.
Hughes, V. W., and C. S. Wu, Eds., *Muon Physics* (Academic, New York).
Jackiw, R., and S. Weinberg, 1972, Phys. Rev. D **5**, 2396.
Jacobsohn, B. A., 1954, Phys. Rev. **96**, 1637.
Jauch, J., and F. Rohrlich, 1955, *The Theory of Photons and Electrons* (Addison-Wesley, Reading, Mass.).
Jenkins, D. A., R. J. Powers, P. Martin, G. H. Miller, and R. E. Welsh, 1971, Nucl. Phys. A **175**, 73.
Joachain, C., 1961, Nucl. Phys. **25**, 317.
Kaeser, K., B. Robert-Tissot, L. A. Schaller, L. Schellenberg, and H. Schneuwly, "Muonic sodium x-ray intensities in different compounds," contribution to the 8th International Conference on High Energy Physics and Nuclear Structure, Vancouver (unpublished).
Källen, G., and A. Sabry, 1955, K. Dan. Vidensk. Selsk. Mat.-Fys. Medd. **29**, No. 17.
Karplus, R., and M. Neumann, 1950, Phys. Rev. **80**, 380.
Kelly, R. L., C. P. Horne, M. J. Losty, A. Rittenberg, T. Shimada, T. G. Trippe, C. G. Wohl, G. P. Yost, N. Barash-Schmidt, C. Bricman, C. Dionisi, M. Mazzucato, L. Montanet, R. L. Crawford, M. Ross, and B. Armstrong, 1980, Rev. Mod. Phys. **52**, S1.
Kessler, D., H. Mes, A. C. Thompson, H. L. Anderson, M. S. Dixit, C. K. Hargrove, and R. J. McKee, 1975, Phys. Rev. C **11**, 1719.
Kessler, E. G., R. D. Deslattes, A. Henins, and W. C. Sauder, 1978, Phys. Rev. Lett. **40**, 171.
Kessler, E. G., L. Jacobs, W. Schwitz, and R. D. Deslattes, 1979, Nucl. Instrum. Methods **160**, 435.
Khare, A., 1977, J. Phys. G **3**, 1019.
Kim, Y. N., 1971 *Mesic Atoms and Nuclear Structure* (North-Holland, Amsterdam).
Klarsfeld, S., 1977a, Nucl. Phys. A **285**, 493.
Klarsfeld, S., 1977b, Phys. Lett. B **66**, 86.
Klarsfeld, S., and A. Maquet, 1973, Phys. Lett. B **43**, 201.
Kunselman, R., J. Law, M. Leon, and J. Miller, 1976, Phys. Rev. Lett. **36**, 446.
Lakin, W., and W. Kohn, 1954, Phys. Rev. **94**, 787.
Lautrup, B. E., 1971, in *Proceedings of the 2nd Colloquium on Advanced Computing Methods in Theoretical Physics, Marseille,* edited by A. Visconti, p. I-58.
Lautrup, B. E., A. Peterman, and E. deRafael, 1972, Phys. Rep. **3** C, 193.
Leisi, H. J., 1977, in *Proceedings of the 1st course of the International School of Physics of Exotic Atoms, Erice, 24—30 April,* edited by G. Fiorentini and G. Torelli, p. 75.
Leisi, H. J., 1980, Nucl. Phys. A **335**, 3.
Lenz, F., 1969, Z. Phys. **222**, 491.
Lenz, F., and R. Rosenfelder, 1971, Nucl. Phys. A **176**, 513.
Leon, M., 1978, Phys. Rev. A **17**, 2112.
Leon, M., and J. H. Miller, 1977, Nucl. Phys. A **282**, 461.
Leon, M., and R. Seki, 1977, Nucl. Phys. A **282**, 445.
Lundeen, S. R., and F. M. Pipkin, 1975, Phys. Rev. Lett. **34**, 1368.
Mann, J. B., and G. A. Rinker, 1975, Phys. Rev. A **11**, 385.
Martin, P., G. H. Miller, R. E. Welsh, D. A. Jenkins, R. J. Powers, and A. R. Kunselman, 1973, Phys. Rev. C **8**, 2453.
Martorell, J., and F. Scheck, 1976, Nucl. Phys. A **274**, 413.
McKee, R. J., 1968, Enrico Fermi Institute for Nuclear Studies Report No. 68-39 (unpublished).
McKinley, J. M., 1969a, Phys. Rev. **183**, 106.
McKinley, J. M., 1969b, "Small Effects in the Theory of Muonic Atoms II," unpublished preprint, Oakland University, Rochester, Michigan.
McLoughlin, D., S. Raboy, E. Deci, D. Adler, R. Sutton, and A. Thompson, 1976, Phys. Rev. C **13**, 1644.
Merzbacher, E., 1970, *Quantum Mechanics,* 2nd ed. (Wiley, New York).
Missimer, J., and L. Simons, 1979, Nucl. Phys. A **316**, 413.
Mohr, P. J., 1974a, Ann. Phys. (NY) **88**, 26.
Mohr, P. J., 1974b, Ann. Phys. (NY) **88**, 52.
Mohr, P. J., 1975, Phys. Rev. Lett. **34**, 1050.
Mukhopadhyay, N. C., 1977, Phys. Rep. C **30**, 1.
Mukhopadhyay, N. C., 1980, Nucl. Phys. A **335**, 111.
Murray, G., R. L. Graham, and J. S. Geiger, 1963, Nucl. Phys. **45**, 177.
Naumann, R. A., and H. Daniel, 1981, Z. Phys. A, in press.
Nuding, E., 1957, Z. Naturforsch. A. **12**, 187.
Papatzacos, P., and K. Mork, 1975, Phys. Rev. D **12**, 206.
Pauli, W., and F. Villars, 1947, Rev. Mod. Phys. **21**, 434.
Pearson, J. M., 1963, Nucl. Phys. **45**, 401.
Pieper, W., and W. Greiner, 1969, Z. Phys. **218**, 327.
Pilkuhn, H., 1979, *Relativistic Particle Physics* (Springer, New York).
Piller, O., W. Beer, and J. Kern, 1973, Nucl. Instrum. Methods **107**, 61.
Ponomarev, L. I., 1973, Annu. Rev. Nucl. Sci. **23**, 395.
Popov, V. S., 1971, Sov. J. Nucl. Phys. **12**, 235 [Yad. Fiz. **12**, 429 (1970)].
Powers, R. J., P. Barreau, B. Bihoreau, J. Miller, J. Morgenstern, J. Picard, and L. Roussel, 1979, Nucl. Phys. A **316**, 295.
Powers, R. J., F. Boehm, A. A. Hahn, J. P. Miller, J. L. Vuillenmier, K. C. Wang, A. Zehnder, A. R. Kunselmann, and P. Roberson, 1977, Nucl. Phys. A **292**, 487.
Powers, R. J., P. Martin, G. H. Miller, R. E. Welsh, D. A. Jenkins, 1974, Nucl. Phys. A **230**, 413.
Rafelski, J., B. Müller, G. Soff, and W. Greiner, 1974a, Ann. Phys. (NY) **88**, 419.
Rafelski, J., B. Müller, and W. Greiner, 1974b, Nucl. Phys. B **68**, 585.
Reidy, J. J., H. Daniel, R. Bergmann, F. J. Hartmann, and W. Wilhelm, 1981, "Measurement and model of the hydrogen isotope effect on muonic x-ray intensities," preprint, Physics Department, Technical University of Munich, Munich, Germany.
Rein, D., 1969, Z. Phys. **221**, 423.
Rinker, G. A., 1976, Phys. Rev. A **14**, 18.
Rinker, G. A., 1979, Comput. Phys. Commun. **16**, 221.
Rinker, G. A., and J. Speth., 1978a, Nucl. Phys. A **306**, 360.

Rinker, G. A., and J. Speth., 1978b, Nucl. Phys. A **306**, 397.
Rinker, G. A., and R. M. Steffen, 1977, At. Data Nucl. Data Tables **20**, 143.
Rinker, G. A., and L. Wilets, 1973a, Phys. Rev. Lett. **31**, 1559.
Rinker, G. A., and L. Wilets, 1973b, Phys. Rev. D **7**, 2629.
Rinker, G. A., and L. Wilets, 1975, Phys. Rev. A **12**, 748.
Robert-Tissot, B., L. A. Schaller, L. Schellenberg, H. Schneuwly, G. Fricke, G. Glueckert, G. Mallot, M. V. Hoehn, and E. B. Shera, 1981, "Muonic isotope shifts in the stable molybdenum isotopes," contribution to the 8th International Conference on High Energy Physics and Nuclear Structure, Vancouver (unpublished).
Ruckstuhl, W., B. Aas, W. Beer, I. Beltranni, P. Ebersold, R. Eichler, M. Guanziroli, Th. v. Lederbur, H. J. Leisi, and W. W. Sapp, 1979, "Electron Screening Effect in Muonic ^{28}Si," contribution to the 8th International Conference on High Energy Physics and Nuclear Structure, Vancouver (unpublished).
Salpeter, E. E., 1952, Phys. Rev. **87**, 328.
Schaller, L. A., T. Dubler, K. Kaeser, G. A. Rinker, Jr., B. Robert-Tissot, L. Schellenberg, and H. Schneuwly, 1978, Nucl. Phys. A **300**, 225.
Schaller, L. A., L. Schellenberg, A. Ruetschi, and H. Schneuwly, 1980, Nucl. Phys. A **343**, 333.
Scheck, F., 1978, Phys. Rep. C **44**, 187.
Schellenberg, L., B. Robert-Tissot, K. Käser, L. A. Schaller, H. Schneuwly, G. Fricke, S. Glückert, G. Mallot, and E. B. Shera, 1980, Nucl. Phys. A **333**, 333.
Schiff, L. I., 1968, *Quantum Mechanics,* 3rd ed. (McGraw-Hill, New York).
Schneuwly, H., 1977, in *Proceedings of the first course of the international school of physics of exotic atoms,* edited by G. Fiorentini and G. Torelli, Erice.
Schneuwly, H., 1978, "Chemical effects in exotic atoms," paper delivered at Nordic Spring Symposium of Atomic Inner Shell Phenomena, Geilo, Norway (unpublished).
Schneuwly, H., T. Dubler, K. Kaeser, B. Robert-Tissot, L. A. Schaller, and L. Schellenberg, 1978a, Phys. Lett. A **66**, 188.
Schneuwly, H., V. I. Pokrovsky, and L. I. Ponomarev, 1978b, Nucl. Phys. A **312**, 419.
Schneuwly, H., and P. Vogel, 1980, Phys. Rev. A **22**, 2081.
Schwitz, W., 1978, Nucl. Instrum. Methods **154**, 95.
Serber, R., 1935, Phys. Rev. **48**, 49.
Shakin, C. M., and M. S. Weiss, 1973, Phys. Rev. C **8**, 411.
Shampine, L., 1973, Math. Comput. **27**, 91.
Shampine, L., and M. K. Gordon, 1975, *Computer Solution of Ordinary Differential Equations: the Initial Value Problem* (Freeman, San Francisco).
Shera, E. B., M. V. Hoehn, L. K. Wagner, Y. Yamazaki, R. M. Steffen, and K. S. Krane, 1977, Phys. Lett. B **67**, 26.
Sick, I., 1973, Phys. Lett. B **44**, 62.
Sick, I., 1974, Nucl. Phys. A **218**, 509.
Sick, I., J. S. McCarthy, and R. R. Whitney, 1976, Phys. Lett. B **64**, 33.
Skardhamar, H. F., 1970, Nucl. Phys. A **151**, 154.
Strubbe, H., 1974, Comput. Phys. Commun. **8**, 1.
Sundaresan, M. K., and P. J. S. Watson, 1972, Phys. Rev. Lett. **29**, 15.
Sundaresan, M. K., and P. J. S. Watson, 1975a, contribution to the 5th International Conference on High Energy Physics and Nuclear Structure, Santa Fe. (unpublished).
Sundaresan, M. K., and P. J. S. Watson, 1975b, Phys. Rev. D **11**, 230.
Tauscher, L., G. Backenstoss, K. Fransson, H. Koch, A. Nilsson, and J. DeRaedt, 1975, Phys. Rev. Lett. **35**, 410.
Tauscher, L., G. Backenstoss, K. Fransson, H. Koch, A. Nilsson, and J. DeRaedt, 1978, Z. Phys. A **285**, 139.
Todorov, I. T., 1973, in *Properties of Fundamental Interactions,* Part C, edited by A. Zichichi (Editrice Compositori, Bologna), Vol. 9, p. 953.
Uehling, E. A., 1935, Phys. Rev. **48**, 55.
VanDyck, R. S., P. B. Schwinberg, and H. G. Dehmelt, 1977, Phys. Rev. Lett. **38**, 310.
Vogel, P., 1973a, Phys. Rev. A **7**, 63.
Vogel, P., 1973b, Phys. Rev. A **8**, 2292.
Vogel, P., 1974, At. Data Nucl. Data Tables **14**, 599.
Vogel, P., and V. Akylas, 1977, Nucl. Phys. A **276**, 466.
Vogel, P., A. Winther, and V. Akylas, 1977, Phys. Lett. B **70**, 39.
Vogel, P., A. Zehnder, A. L. Carter, M. S. Dixit, E. P. Hincks, D. Kessler, J. S. Walden, C. K. Hargrove, R. J. McKee, H. Mes, and H. L. Anderson, 1977, Phys. Rev. A **15**, 76.
Von Egidy, T., and J. P. Desclaux, 1978, Z. Phys. A **288**, 23.
Vuilleumier, J. L., F. Boehm, A. A. Hahn, J. P. Miller, R. J. Powers, K. C. Wang, A. Zehnder, and A. R. Kunselman, 1978, Nucl. Phys. A **294**, 273.
Vuilleumier, J. L., W. Dey, R. Engfer, H. Schneuwly, H. K. Walter, and A. Zehnder, 1976, Z. Phys. A **278**, 109.
Wagner, L. K., E. B. Shera, G. A. Rinker, and R. K. Sheline, 1977, Phys. Rev. C **16**, 1549.
Walter, H. K., J. L. Vuilleumier, H. Backe, F. Boehm, R. Engfer, A. H. von Ganbon, R. Link, R. Michaelson, C. Petitjean, L. Schellenberg, H. Schneuwly, W. U. S. Schröder, and A. Zehnder, 1972, Phys. Lett. B **40**, 197.
Watson, P. J. S., and M. K. Sundaresan, 1974, Can. J. Phys. **52**, 2037.
Weber, R., J. Kern, U. Kiebele, J. A. Pinston, B. Aas, I. Beltrami, T. Bernold, K. Bongardt, T. v. Ledebur, H. J. Leisi, W. Ruckstuhl, G. Strassner, and A. Vacchi, 1981, Phys. Lett. B **98**, 343.
Weinberg, S., 1974, Rev. Mod. Phys. **46**, 255.
Wheeler, J. A., 1949, Rev. Mod. Phys. **21**, 133.
Wichmann, E. H., and N. M. Kroll, 1956, Phys. Rev. **101**, 843.
Wilets, L., 1954, K. Dan. Vidensk. Selsk. Mat.-Fys. Medd. **29**, No. 3.
Wilets, L., and G. A. Rinker, 1975, Phys. Rev. Lett. **34**, 339.
Wohlfahrt, H. D., E. B. Shera, M. V. Hoehn, Y. Yamazaki, G. Fricke, and R. M. Steffen, 1978, Phys. Lett. B **73**, 131.
Wu, C. S., and L. Wilets, 1969, Annu. Rev. Nucl. Sci. **19**, 527.
Yamazaki, Y., E. B. Shera, M. V. Hoehn, and R. M. Steffen, 1978, Phys. Rev. C **18**, 1474.
Yamazaki, Y., H. D. Wohlfahrt, E. B. Shera, M. V. Hoehn, and R. M. Steffen, 1979, Phys. Rev. Lett. **42**, 1470.
Zehnder, A., F. Boehm, W. Dey, R. Engfer, H. K. Walter, and J. L. Vuilleumier, 1975, Nucl. Phys. A 254, 315.